The Pennsylvania State University

The Graduate School

Graduate Program in Biology

THE ROLE OF BARREN INFLORESCENCE GENES, *barren inflorescence2 (bif2), barren stalk1 (ba1)* AND *suppressor of sessile spikelet1 (sos1)*, IN MAIZE INFLORESCENCE DEVELOPMENT

A Dissertation in

Biology

By

Xianting Wu

Submitted in Partially Fulfillment
of the Requirements
for the Degree of

Doctor of Philosophy

August 2008

The dissertation of Xianting Wu was reviewed and approved* by the following:

Paula McSteen
Assistant Professor of Biology
Dissertation Adviser
Chair of Committee

Hong Ma
Distinguish Professor of Biology
Graduate Program Chair

Zhi-chun Lai
Professor of Biology and BMB

Kathleen Brown
Professor of Postharvest Physiology

Douglas Cavener
Professor and Head of Biology

* Signatures are on file in the Graduate School

ABSTRACT

There are four types of axillary meristem initiated during maize inflorescence development. Thus, the structure of the maize inflorescence is quite different from Arabidopsis which has two types of axillary meristems. Other grass species such as rice, sorghum and wheat have similar inflorescence morphology. More importantly, as the inflorescence produces the seed, the increase in the complexity of the grass inflorescence has caused an increase in yield. Grass species are the main food source for human beings. Therefore, it is very important to understand the development of the grass inflorescence. In addition, the development of the grass inflorescence involves hormonal regulation. There are many advantages to choosing the maize inflorescence as a model system to study grass inflorescence development such as the large meristem size to perform hormone analysis, the multiple types of axillary meristem as well as the established genetic and genomic resources. Therefore, maize is a good system to perform research on inflorescence development and hormonal regulation.

In my work described in chapter 2, I provide support that polar auxin transport (PAT) is required for initiation of axillary meristems in the maize inflorescence such as the branch meristem (BM), spikelet pair meristem (SPM) and spikelet meristem (SM). In addition, RNA *in situ* hybridization analysis showed the interaction of two important *barren inflorescence* genes, *barren inflorescence2 (bif2)* and *barren stalk1 (ba1),* with PAT. *bif2* and *ba1* mutants have defects in the initiation of all axillary meristems. The role of *bif2* appears to be similar to *PINOID (PID)* in Arabidopsis which regulates auxin transport to initiate axillary meristems in the inflorescence. However, as *ba1* homologs are absent in Arabidopsis genome, *bif2* regulation of *ba1* may shed light in understanding the unique aspects of maize inflorescence development and signal transduction network.
My analysis of *bif2;ba1* double mutants in chapter 3 showed that the interaction between *bif2* and *ba1* is complex. My work together with others has shown that regulation occurs at both the transcription and post transcription level. This is consistent with the model we proposed in the chapter 2. In addition, we revise our model to account for all of the evidence from genetic and molecular analysis. This will provide information to further test the interaction between *bif2* and *ba1*.

In chapter 4, I characterized *Suppressor of sessile spikelet1 (Sos1)* and its interaction with *ramosa1 (ra1)* and *ramosa2 (ra2)*. Since these three genes are involved in determining SPM determinacy, their interaction determines the mature architecture of the maize inflorescence. We proposed a model based on all the molecular and genetic analysis which helps to understand how these three genes interact and function in maize meristem determinacy. Cloning of the *Sos1* gene will be very important to understand how the maize inflorescence produces paired spikelets instead of single spikelets. This is an important derived trait in grass inflorescence evolution. In addition, I showed in chapter 2 that blocking auxin transport in early development phenocopies the *Sos1* mutant phenotype. This indicates that *Sos1* may be involved in the auxin signal transduction pathway to regulate maize inflorescence development. The progress towards cloning *sos1* is shown in Appendix A.

Although our understanding of maize inflorescence development is ongoing, my research provides clues to understand some of the main players such as *bif2, ba1,* PAT, *Sos1, ra1* and *ra2*. In addition, my analysis primarily defines the positions of these genes in the network. By further analysis based on these models, we will understand more of the cross talk between these genes to control maize inflorescence development.

TABLE OF CONTENTS

Nomenclature

Arabidopsis nomenclature is used when describing genes in Arabidopsis and rice. For example, *PINOID (PID)* is used as the gene name, *pid* is used to describe the mutant. PID is used to describe the protein.

Maize nomenclature is applied when describing genes in maize. For example, *barren inflorescence2 (bif2)* refers to both the gene and the recessive mutant. When a dominant mutation is mentioned, the gene and the mutant are written as s*os1* and *Sos1*. Nomenclature for describing proteins is the same as in Arabidopsis.

LIST OF FIGURES

LIST OF TABLES

Acknowledgements

I sincerely thank my Ph.D adviser Paula McSteen for giving me wonderful instruction during my Ph.D work. I thank her for her patience and encouragement when things were not going smoothly and her kindness and understandness during my work. I must say it is an honor to be her first graduate student and I enjoyed our nice mentor-student relationship. I will cherish and take what I learnt from Paula and from the lab with me in my future work.

I'd like also to thank our postdoc Andrea Skirpan for her great comments and suggestions both in the experiments and the lab meetings. Her enthusiasm about science and her carefulness in doing experiments impressed me deeply. I learnt a lot from her.

My thanks also go to my graduate student labmate, Solmaz Barazesh, for her great company and help both in the field and the lab. We have been gone through a lot together during this work. I cherish the friendship we have built up.

I also need to thank several undergraduate students who helped in the lab and the field. They are Kim Phillips, Jason Hoar, Matt Davis, Chris Cook, Chris Hudson and Jeff Buterbaugh. Without their help in the field work and genotyping the plants for me, I would not be able to finish this work as efficiently as I did now.

I would also like to thank all my thesis committee members: Professor Hong Ma, Professor Zhi-chun Lai and Professor Kathleen Brown for their comments and suggestions for the experiments and my thesis writing.

I owe special thanks to the facility staff Missy Hazen and Ruth Haldeman and for their great instruction in how to use the SEM machine. I also thank Deb Grove in the Nucleic Acid Facility for her efficient support to get all the real time RT-PCR done.

Finally, I'd like to thank my family, my parents and my husband for always being there to help and support me. Without their love and support, I would not be what I am today.

CHAPTER ONE

Introduction

In plant development, the shoot organs and tissues initiate from the Shoot Apical Meristem (SAM). Meristem cells in the SAM are smaller and less vacuolated compared with the non-meristematic and differentiated cell types. Meristem cells must be able to self maintain as well as divide and differentiate new cells for organ initiation. Thus, the SAM is divided into two parts: the central zone (CZ) and the peripheral zone (PZ). The CZ is responsible for maintaining the meristem, therefore, cells in this region divide slowly and remain undifferentiated. On the other hand, cells in the PZ divide quickly and differentiate for organ initiation. Thus, the balance between division and differentiation rates in the CZ and the PZ determines SAM size and function.

Since the SAM regulates shoot morphology including stems, leaves, inflorescences and flowers, it is of interest to understand how the SAM is regulated. There are mainly three aspects to consider: meristem maintenance, meristem determinacy and meristem identity. First, meristem maintenance determines the ability of the meristem to maintain and renew itself. Second, determinacy specifies the ability of the meristem to generate new meristems (indeterminate) or produce differentiated organs (determinate). Finally, meristem identity controls the fate of the type of tissue or organ the meristem produces. The three aspects of the meristem are regulated by cross talk between the genes regulating each aspect to produce a network regulating plant development.

1.1 Shoot Development in *Arabidopsis*

The genes involved in meristem maintenance in Arabidopsis are *SHOOT MERISTEMLESS (STM), CLAVATA1, 2, 3 (CLV1, 2, 3)* and *WUSCHEL (WUS)*. *STM* encodes a homeodomain transcription factor required for SAM maintenance. In *stm* mutants, the SAM differentiates and loses its meristem characteristics (Long et al, 1996). The SAM is enlarged and more floral organs are produced in *clv1* mutants (Clark et al., 1993). *CLV1* is a receptor like kinase, *CLV2* stabilizes *CLV1* activity by forming a protein complex with *CLV1* and *CLV3* encodes a signal peptide ligand (Jeong et al., 1999; Trotochaud et al., 2000). Therefore, the *CLV* genes regulate SAM size by a protein kinase signaling pathway. *WUS* also maintains SAM size by limiting *CLV3* expression (Schoof et al., 2000). By such precise regulation, the meristem is maintained and able to initiate lateral organs during shoot development.

There are two developmental stages in the shoot: vegetative and reproductive stages. The vegetative SAM initiates stem, leaf primordia and axillary meristems in the axil of the leaf as the shoot elongates. At the end of vegetative development, the SAM transitions to become an inflorescence meristem (IM) and starts to initiate axillary meristems (AM) which give rise to floral meristems (FM). The identity of meristems is specified hierarchically from SAM, IM to FM. Thus, the FM is more determinate than SAM and IM. In the end, the FM is consumed as floral organs are made. *LEAFY* determines floral meristem identity in Arabidopsis (Huala, 1992). In *lfy* mutants, the axillary meristem generates indeterminate shoots instead of flowers. On the contrary, ectopic expression of *LFY* promotes early flowering. Additionally, *LFY* is responsible for the IM transition to FM. Thus, there is cross talk between meristem determinancy and identity.

1.2 Shoot Development in Maize

Axillary meristems in dicots initiate inflorescences and flowers. However, in monocots, inflorescence development is more complicated. For example, maize is a monoecious plant. This means it produces both a male and female inflorescence in one plant. The male inflorescence, the tassel is formed by the IM (Fig. 1A) while the female inflorescence, the ear is initiated by an AM set aside during vegetative development four to five leaf nodes below the tassel. When the SAM transitions to inflorescence identity, it becomes an IM which elongates and initiates several branch meristems (BMs) at the base which give rise to the long branches in the mature tassel (Fig. 1B). As the SAM and BMs elongate, they start to make regular protrusions called spikelet pair meristems (SPMs) (Fig. 1C). Each SPM produces two spikelet meristems (SMs) (Fig. 1D). One of the SM is called a pedicellate spikelet meristem (PSM) and the other one is a sessile spikelet meristem (SSM). Furthermore, each SM initiates two floral meristems (FMs) enclosed between bracts called the inner and outer glumes (Fig. 1E). According to their location along the longitudinal axis of the SAM, the two FMs are called the upper and lower floret. Each FM initiates a lemma and palea (like sepals in dicots), two lodicules (like petals in dicots), three stamens and one gynoecium (Fig. 1E). In the tassel, the gynoecium aborts and only male florets form. In the ear, there are no BMs. The lower FM and three stamens in the upper FM degenerate to produce each female floret in the ear. In conclusion, maize inflorescence development is hierarchical and there are four types of AM formation. Thus, the regulation of inflorescence development is more complicated in maize.

We can describe shoot development as the repeated formation of phytomers. Although shoot morphology differs between plants, the fundamental module can be found repeating in all plants. In each of the basic modules, called the phytomer, there is a node, an internode, a leaf and an axillary meristem. The plant produces phytomers during vegetative growth as well as reproductive growth. The difference is that either the leaf or the axillary meristem grows out. In vegetative development, the axillary meristem is arrested but the leaf grows out. However, during inflorescence development, the axillary meristems are dominant while the leaves are suppressed. For instance, the bract primordia is the suppressed leaf subtending the SPM and the lemma is the suppressed leaf of the

FM (Mcsteen and Leyser, 2005). The complexity of axillary meristem development in maize makes maize a unique model plant for inflorescence development research.

Based on the knowledge above, inflorescence development in maize is complex and genes involved in axillary meristem initiation, maintenance and differentiation are regulated hierarchically. I review genetic and molecular regulation of each meristem type in maize inflorescence development below. This information is summarized in Ttable I.

1.3 Genetic Regulation of Maize Inflorescence Development

1.3.1 Genes Involved in SAM Development in Maize

Genes involved in maize SAM development are conserved with Arabidopsis. The SAM is maintained by the homeodomain transcription factor *knotted1 (kn1)*, which is similar to *STM* in Arabidopsis. *kn1* is expressed in the SAM (Jackson et al., 1994). It is down regulated at the position where the lateral organs initiate and reappears in the axillary meristems. Therefore, *kn1* is used as a meristem marker in maize. *kn1* expression is also detected in veins. In the *kn1* loss-of-function mutants, vegetative development seems normal except that extra leaf-like structures are found on the leaf blade. This is possibly because loss of *kn1* expression causes the leaf initiation boundary to be unclear (Kerstetter et al., 1997). *kn1* also maintains the undifferentiated status of the meristem. Without *kn1*, the maintenance of the meristem is affected. Therefore, the inflorescence meristem (IM) is smaller in the mutants. As a result, in the recessive mutant, the tassel is shorter and sparse because fewer branches and spikelets are produced. In addition, ears often fail to be initiated or once initiated, they are shorter and skinnier (Kerstetter et al., 1994; Vollbrecht et al., 2000).

In maize, SAM size is maintained by the *CLAVATA* gene pathway as in Arabidopsis. The putative *CLV1* ortholog in maize is *thick tassel dwarf1 (td1).* The IM is larger in the *td1* mutant. Therefore, the spikelet density in the tassel is increased. Extra glumes are produced and additional stamens initiate in each floret. In the fasciated ear, SPMs and SMs are enlarged and more kernel rows and kernels are initiated (Bommert et al., 2005b). A leucine-rich repeat (LRR) receptor like protein, *fasciated ear2 (fea2),* in maize is the ortholog of *CLV2* in Arabidopsis. *fea2* also limits meristem cell proliferation. However, unlike Arabidopsis, *td1;fea2* double mutants display an additive phenotype suggesting that they do not function in the same pathway or that their pathways only partially overlap in regulation of apical and axillary IM size in maize (Taguchi-Shiobara et al., 2001; Bommert et al., 2005a). A *WUSCHEL* ortholog has not been identified in maize yet. However, maize *narrow sheath1, 2 (ns1, 2)* are homologous to the *WUS*-like gene *PRESSED FLOWER (PRS).* The phenotype of *ns1* and *ns2* is mainly in the leaf blade. The lateral leaf margins are absent in the lower leaf blades due to the failure to recruit the founder cells at the margin of the leaf primordia. However, expression of *ns1*

and *ns2* is also detected in the margins of all floral organs, suggesting that they may also play a role in the FM (Scanlon, 2000; Nardmann et al., 2004).

The gene *indeterminate1 (id1)* controls the transition of the vegetative SAM to the IM in maize. *id1* encodes a zinc-finger transcription factor. In *id1* mutants, extra leaves are produced and mini plants with roots appear in the tassel spikelet (Colasanti et al., 1998; Colasanti et al., 2006). Thus, axillary meristems can regenerate the whole plant when *id1* is mutated. Two orthologs of *LEAFY* exist in maize, *zea flo/lfy like1* and *2 (zfl1, zfl2)*. These two genes are redundant with each other. Double mutant analysis indicates that *zfl1* and *zfl2* function in the transition of SAM to IM in maize as in dicots. The IM transition is delayed in *zfl1;zfl2* double mutants. Therefore, several tassel ears surrounded by husk leaves initiate when the vegetative development ends. Although the tassel feminization in the double mutant is not understood yet, this suggests that *LFY* in maize has additional roles than in Arabidopsis. In addition, extra floret organs are produced and there are some floral organ identity defects in the double mutant plants. However, fewer BMs are produced in the *zfl1;zfl2* double mutant, which is different from the extra inflorescences produced in *lfy* mutants in Arabidopsis. This evidence further suggests that *ZFLs* may play a new role in inflorescence architecture in maize (Bomblies et al., 2003). Meanwhile, the expression of the rice *LEAFY* homolog, *RFL*, is not detected in the FMs (Kyozuka et al., 1998). Therefore, *LFY* function in FM development may differ between dicots and monocots.

1.3.2 Genes Involved in Vegetative Axillary Meristem Development

During vegetative phytomer development, the axillary meristems set aside by the SAM are usually inhibited by apical dominance. In maize *teosinte branched1 (tb1)* mutants, the lower vegetative axillary meristems (VAM) grow out and produce secondary branches called tillers (Doebley et al., 1997). The upper VAM produce male shoots instead of ears in the *tb1* mutant. Therefore, *tb1* may be essential to suppress VAM outgrowth in normal plants. *tb1* encodes a transcription factor similiar to *CYCLOIDEA* in *Antirrhinum.* An interesting discovery is that the expression of *tb1* in maize is two times higher than in its ancestor teosinte. Selection for increased expression of *tb1* may have shaped modern maize morphology. The selection on *tb1* expression during evolution

shows that regulation of axillary meristem branching can control the achitecture of the plant (Doebley et al., 1997; Hubbard et al., 2002). There are also other genes that control tiller formation in maize such as *Teopod1, 2, 3 (Tp1, 2, 3)* and *Tillered1 (Tlr1).* Dominant mutations in these genes increase the numbers of tillers (Veit et al., 1993). Overexpression of *Corngrass1*, which encodes two tandem *miR156* genes, also causes multiple tillers to form (Chuck et al., 2007a). Whether these genes interact with *tb1* in tiller formation is still unknown.

1.3.3 Genes Involved in Inflorescence Development

1.3.3.1 Genes Involved in All Axillary Meristems

In the maize inflorescence, genes which control the initiation of axillary meristems are called *barren* genes such as *barren inflorescence2 (bif2)* and *barren stalk1 (ba1).* In *bif2* and *ba1* mutants, VAMs, BMs, SPMs, SMs and FMs are affected. *bif2* is a co-ortholog of *PINOID* in Arabidopsis, encoding a serine/threonine protein kinase which regulates auxin transport (McSteen et al., 2007). In *bif2* mutants, fewer branches initiate in the tassel, few spikelets irregularly appear along the rachis of the tassel and there are fewer florets and floral organs. Mutant plants produce fewer ears and the ears initiated have fewer kernel rows and total kernel numbers (McSteen and Hake, 2001; McSteen et al., 2007). Similarly, there are fewer flowers and floral organs in *pid* mutants in Arabidopsis (Okada et al., 1991; Bennett, 1995). Expression of *bif2* is detected in all four types of inflorescence axillary meristem by RNA *in situ* hybridization analysis. These results indicate that normal auxin transport is required for axillary meristem and lateral organ initiation in both dicots and monocots (Benjamins et al., 2001a; Reinhardt et al., 2003a). In addition, *bif2;tb1* double mutants produce fewer tillers than the *tb1* single mutant, which suggests that *bif2* also plays a role in vegetative axillary meristem development (McSteen et al., 2007).

ba1 encodes a basis Helix Loop Helix (bHLH) transcription factor. Like *bif2*, branch and spikelet number is reduced in *ba1* mutants. However, there are regular protrusions along the main spike of the tassel which is a unique phenotype of *ba1* mutants. These regular bulges are bract primordia whose outgrowth is normally inhibited during normal tassel development (Ritter et al., 2002; Gallavotti et al., 2004). Ears are always absent in the *ba1* mutant. In addition, *ba1* is completely epistatic to *tb1*. There are no tillers produced in *ba1;tb1* double mutants. This result suggests that *ba1* plays an essential role in tiller formation during vegetative shoot development (Ritter et al., 2002). Based on the similar phenotype between *bif2* and *ba1*, it is of interest to understand the interactions between these two genes and their roles in maize inflorescence development.

1.3.3.2 Genes Involved in SPM Development

SPMs, SMs and FMs are determinate axillary meristems because they initiate a limited number of structures. In *ramosa1, 2, 3 (ra1, 2, 3)* mutants, the determinate SPMs become indeterminate. Extra branches, spikelet pairs and spikelets initiate in both the tassel and the ear. Therefore, unlike normal, there are mixed branches (branches with spikelet pairs and spikelets on the branches) and spikelet multimers (branches with single spikelets) in the tassel in *ra1* and *ra2* mutants and highly branched ears in *ra1* mutants. In *ra3* mutants, the branched phenotype is mainly apparent in the ear. All three *ramosa* genes are expressed only in the tassel and the ear but not in the other parts of the plant. This suggests that *ramosa* genes function specifically in inflorescence development (Vollbrecht et al., 2005; Bortiri et al., 2006; Satoh-Nagasawa et al., 2006; Bortiri and Hake, 2007). *ra1* encodes a Cys_2-His_2 zinc-finger of the EPF subclass of transcription factor with no orthologs in either Arabidopsis or rice. However, homologs of both *ra2* and *ra3* are found in other grass families. *ra2* encodes a lateral organ boundary (LOB) domain transcription factor and *ra3* encodes a trehalose-6-phosphate phosphatase.

Expression analysis shows that *ra2* is still expressed in both *ra1* and *ra3* mutants, *ra3* is expressed as normal in *ra1* and *ra2* mutants but *ra1* expression is reduced in *ra2* and *ra3* single mutants and even lower in the *ra2;ra3* double mutant by qRT-PCR analysis (Satoh-Nagasawa et al., 2006). Therefore, *ra2* and *ra3* could function upstream of *ra1*. *ra2* expression is detected in BMs, SPMs and SMs. The expression pattern of *ra2* is broader than both *ra1* and *ra3* suggesting that it may have additional functions in SPM and SM development. *ra1* is expressed only at the adaxial side of the SPM and then at the boundary between the two SMs later in development. The expression pattern of *ra3* in the SPM overlaps with *ra1* but is slightly wider. The interactions between these genes indicate that the determinacy of SPMs and SMs are regulated at the level of transcription.

Opposite to the *ramosa* mutant phenotype, the *Suppressor of sessile spikelets1 (Sos1)* mutant displays single instead of paired spikelets both in the tassel and the ear. Therefore, the SPMs in *Sos1* mutants are less determinate than normal. *Sos1* has been mapped to the short arm of chromosome 4 (Doebley et al, 1995). To understand the regulation of SPM determinacy, it is important to explore the interaction between the *ramosa* and *Sos1* genes.

1.3.3.3 Genes Involved in SM Development

Several genes are involved in SM determinacy. In the mutant *indeterminate spikelet1 (ids1),* SMs become indeterminate and extra flowers are produced (Chuck et al., 1998). Expression of *ids1* is detected in leaves, roots and the inflorescence, which suggests that *ids1* may play a broader role in plant development. In the inflorescence meristem, the earliest expression of *ids1* is in the adaxial side of SPMs and then in the SMs (Chuck et al., 1998). *ids1* belongs to a transcription factor family similar to *APETALA2 (AP2)* in Arabidopsis. *ids1* has been shown to be the target of *tasselseed4 (ts4)*, which is called *zm-MIR172e* and belongs to the *miR172* family known to regulate *AP2* transcription factors in Arabidopsis (Chen, 2004; Chuck et al., 2007b). *AP2* is known to affect many aspects in flower development in Arabidopsis. However, *ids1* functions differently in SPM determinacy in maize inflorescence development.

In the absence of the *indeterminate floral apex1 (ifa1)* gene, the SPMs become indeterminate and initiate extra SMs and the SMs produce more flowers. Although FM development is normal, the carpel becomes indeterminate. *kn1* is ectopically expressed in the center of the ovule, which suggests that *ifa1* is also required for FM determinacy (Laudencia-Chingcuanco and Hake, 2002). Interestingly, in *ids1;ifa1* double mutants, the SPMs become BMs and initiate more SPMs (Laudencia-Chingcuanco and Hake, 2002). The phenotype of *reversed germ orientation1 (rgo1)* is similar to *ids1* mutants, with an increased number of florets produced per SM both in the tassel and the ear. In the *ids1;rgo1* double mutants, the SMs adopt SPM identity to generate more SMs. Therefore, these three genes may play a role in specifying SM identity as well as SM determinancy (Kaplinsky and Freeling, 2003).

SM identity is determined by the gene *branched silkless1 (bd1)*. BM and SPM development is normal in the *bd1* mutant. However, the SMs fail to initiate the outer glumes but generate more SMs in a distichous manner, which indicates that the SM loses its identity and becomes an SPM. *bd1* encodes a putative ethylene-response element binding factor (ERF) protein. Northern blotting analysis shows that *bd1* is an inflorescence specific gene. RNA *in situ* hybridization analysis indicates that *bd1* is first expressed in a half circle between the SMs and the outer glumes, and later in a ring between the SMs and the inner glumes. So, it is possible that *bd1* expression sets the

boundary of the SM and regulates downstream factors to determine SM identity. Moreover, the expression pattern of *bd1* is similar both in rice and sorghum (Chuck et al., 2002). *frizzy panicle (fzp)*, the rice ortholog of *bd1*, has a similar phenotype as *bd1* in rice (Komatsu et al., 2003b). Therefore, the regulation of SM identity is conserved among the grasses.

To conclude, axillary meristem development is regulated in four ways. First, the AM is initiated from the SAM and IM at the right time and right place. Second, the axillary meristem must be maintained to allow a proper balance between meristem self renewal and the initiation of new organs. Third, the identity of each type of AM is specified. Last, determinacy of the AM is specified. However, maintenance, identity and determinacy of each type of AM may not be independent from each other. The genes involved are working in a complex network to precisely control these processes step by step. Hormonal and sugar signaling pathways may be involved in the cross talk between these pathways.

1.3.4 Models for SM and FM Initiation

There are two models to understand how determinate AMs such as SMs and FMs initiate. They are the conversion model and the lateral branching model. The conversion model was first proposed by Irish to explain the phenotypes of *tasselseed (ts)* mutants. These mutations cause feminization of the tassel florets. There are six *tasselseed* mutants identified so far. *ts1, ts2* and *ts4* are recessive mutations and *Ts3*, *Ts5* and *Ts6* are dominant mutations. Interestingly, in addition to the feminization phenotypes, *ts4* and *Ts6* mutants show some other phenotypes in AM development. In *ts4* mutants, the SPMs become indeterminate BMs and initiate several SPMs (Irish and Nilson, 1993). Additionally, the pedicellate SMs in *Ts6* mutants lose their determinacy and produce extra florets per spikelet (Irish, 1997). To explain these phenotypes, the conversion model proposes that the SPM initiates the sessile spikelet meristem (SSM) and all of the remaining cells of the SPM convert to become the pedicellate spikelet meristem (PSM). Thus, when two SMs form, there are no SPM cells left. The conversion of SPM identity is delayed in *ts4* mutants and more SMs initiate. Moreover, after the SM initiates the lower FM, the remaining SM converts to become the upper FM. Therefore, no SM cells remain when the two FMs form. SM development is delayed in *Ts6* mutants and thus more FMs are produced. According to this model, the cells of a lower order meristem would be completely converted into the next meristem type.

However, it is hard to apply this model to explain the phenotype of *ids1* mutants. *ids1* expression is in the boundary between the two SMs and between the two FMs. Since *ids1* specifies the determinacy of the SM, the residual *ids1* expression between the two FMs does not support the conversion model. Therefore, Chuck proposed the lateral branching model: Instead of complete conversion of the lower order meristem identity into the next meristem type, the SMs branch to form two lateral FMs and the residual SM remains between them (Chuck et al., 1998). Thus, in *ids1* mutants, the residual SM becomes indeterminate and many more flowers are produced.

Kaplinsky revised the interpretation of *ids1* in *rgo1;ids1* double mutant analysis. He proposed that when *ids1* is absent, SPMs initiate several SMs before converting completely into a SM. In *rgo1* mutants, the SMs could initiate two FMs before converting into a third FM. In the double mutants, the SPMs and SMs generate many

secondary meristems before converting into the next meristem type (Kaplinsky and Freeling, 2003). Both models can be used in explain the initiation of SMs and FMs in maize inflorescence development. The research in chapter 2 supports the conversion model.

Besides genetic regulation, other factors such as hormonal regulation are also very important in inflorescence development. Auxin, a plant hormone, plays an essential role in meristem initiation and lateral branching. The following section reviews the role of auxin in inflorescence and floral development in Arabidopsis.

1.4 The Role of Auxin in Inflorescence Development

Auxin, the first identified plant hormone, is known to play a role in meristem initiation, lateral organ and vasculature formation, phototropism and geotropism. Although auxin is detected in the root, the leaf primordia and the meristems, clues to the exact sites of auxin biosynthesis have only recently been discovered (Benjamins and Scheres, 2008).

1.4.1 Auxin Biosynthesis

The active form of auxin in plants is indole-3-acetic acid (IAA). IAA can form non-active conjugates to a variety of amino acids, peptides and sugars. The ratio between IAA biosynthesis and IAA conjugation is called auxin homeostasis. There are mainly two pathways for IAA biosynthesis: the tryptophan (TRP) dependant pathway and the TRP independent pathway. The TRP independent pathway is proposed by the evidence that auxin is made in TRP biosynthesis mutants such as *trp2-1* and *trp3-1*. Labeling studies indicates that this pathway may catalyze the precursor of TRP such as indole glucosinolate (IGP) or indole to IAA (Zhao et al., 2002; Benjamins and Scheres, 2008). The TRP dependant pathway is dominant in auxin biosynthesis. In this pathway, there are several pathways to turn TRP into IAA. One is from TRP through Indole-3-acetaldehyde (IAOx), indole-3-acetonitile (IAN) to form IAA. This pathway is catalyzed by the Arabidopsis cytochrome P450 enzymes such as *CYP79B2* and *CYP79B3*. Another pathway is catalyzed by *YUCCA* genes from trypamine (TAM) through N-hydroxyl

tryptamine (NHT) to form IAA (Zhao et al., 2002). The third pathway has been identified recently (Stepanova et al., 2008). TRYPTOPHAN AMINOTRANSFERASE IN ARABIDOPSIS1 (TAA1) catalyzes indole-3-pyruvate (IPA) formation from tryptophan.

The *YUCCA (YUC)* genes encode flavin monoxygenase enzymes (FMO) that have been shown to play a role in one of the most important enzymatic steps in IAA biosynthesis (Kendrew, 2001; Zhao et al., 2001). There are eleven predicted *YUC* genes in this FMO family in Arabidopsis. Among them, *YUC1, YUC2, YUC4, YUC6, YUC10* and *YUC11* have been shown to be essential for auxin biosynthesis (Cheng et al., 2006, 2007a). Ectopic expression of each gene causes more auxin to be produced. RNA *in situ* hybridization analysis shows that *YUC1* and *YUC4* are expressed mainly along the side of the inflorescence apex. In the floral organs, *YUC2::GUS* is expressed in the petals, stamens and gynoecium and *YUC6::GUS* is mainly detected in the stamens and pollen. *YUC1, 2, 4* and *6* have redundant functions with each other since single mutants do not display any developmental phenotypes. However, developmental defects are gradually more severe from double mutant *yuc1;yuc4* and *yuc2;yuc6* to triple mutants. Moreover, the most severe phenotype is in *yuc1;yuc2;yuc4;yuc6* quadruple mutants. Interestingly, exogenous application of auxin can not rescue *yuc* mutant phenotypes but transgenic expression of a bacterial auxin biosynthesis gene, *iaaM,* rescues the *yuc* phenotypes (Cheng et al., 2006). Therefore, de novo auxin biosynthesis in developing organs is important in plant development. Seven rice *YUCCA*-like gene *OsYUCCA1-7* have been identified and *OsYUCCA1* is involved in auxin biosynthesis in leaves, roots and vaculature (Yamamoto et al., 2007). Thus, *YUCCA* gene functions are conserved in eudicots and monocots.

1.4.2 Auxin and Polar Auxin Transport

Auxin is synthesized in the germinating seeds, leaf primordia, young leaves and initiating meristems. Besides the de novo auxin biosynthesis, recent research has shown that the direction of auxin transport (PAT) is also essential in the formation of the shoot and root axis during embryo development (Weijers and Jurgens, 2005), lateral root initiation (Benkova et al., 2003), lateral organ initiation in the shoot and floral organ

initiation (Reinhardt et al., 2003b; Friml et al., 2004). It has been proposed that auxin transport creates an auxin gradient that triggers signals for plant development.

There are two auxin transport pathways known so far. A fast path, together with other metabolites through the mature phloem, and a slower cell-to-cell path whereby auxin is transported from the shoot apex to the tip of the root and from the root apex back to the shoot (Muday and DeLong, 2001). In addition, the slower transport path in the shoot apex is from the newly initiated leaf primordia to the shoot apex to initiate the next leaf primordia or axillary meristem. After the leaf primordia and axillary meristem are initated, auxin is transported basipetally from the shoot. The cell-to-cell transport of auxin has polarity that is essential for organ initiation in plant development (Muday and DeLong, 2001; Reinhardt et al., 2003a; Blakeslee et al., 2005; Kepinski, 2005; Leyser, 2005)

How is PAT established and maintained in the plant? The Chemiosmotic model proposes that the pH is low (<7) in the apoplast and high (≥7) in the cytoplasm (Blakeslee et al., 2005). This pH difference is maintained by proton pump ATPases which are located on the plasma membrane (Li et al., 2005). IAA, which is the main form of auxin in the plant, exists as IAAH in the apoplast and is amphiphilic. IAAH can easily diffuse into the cytoplasm where it ionizes to form IAA^- in the higher pH cytoplasm. Since IAA^- is not amphiphilic, it is difficult for the molecule to cross the cell membrane to exit the cell. Therefore, further transportation of auxin out the cell requires protein carriers and energy. The protein carriers are called auxin efflux carriers. They are polarly localized in the cell membrane and specify the direction of PAT. In addition to uptake of auxin by diffusion, plants also have auxin influx carrier proteins to actively regulate auxin uptake.

1.4.3 Chemical Inhibitors of PAT

Early observations of PAT showed that certain types of chemicals inhibit tropic responses and auxin transport. These chemicals are called phytotropins. The typical structure of phytotropin is two connected aromatic rings. These chemicals are N-naphthlyphthalamic acid (NPA), 9-Hydroxy-9-fluorene-carboxylic acid (HFCA), Tri-idobenzoic acid (TIBA) and 2-carboxyphenyl-3-phenylpropane-1,2-dione (CPD). Among

these chemicals TIBA is an exception since it does not have the typical phytotropin structure (Katekar, 1980; Katekar, 1981).

Research results indicate that the auxin efflux protein complex is localized in the cell membrane to specify the direction of PAT. At least two kinds of proteins are members of this complex. They are the putative NPA-binding protein (NBP) and auxin efflux carriers such as PIN family proteins. NPA is one of the most popularly used auxin transport inhibitors as it effectively inhibits the transport of basipetal as well as acropetal auxin transport by targeting the putative NBP on the auxin efflux complex (Keitt and Baker, 1966; Murphy et al., 2002). Immunolocalization with a monoclonal antibody against a putative NBP from pea membrane, provided the first evidence of the basal localization of membrane proteins associated with the polar auxin transport complex (Jacobs, 1983). Except for one paper (Bernasconi et al., 1996), many other experiments suggest that the NBP is a peripheral protein associating with the cytoplasmic side of the membrane. Thus, NPA may target these membrane localized proteins to inhibit auxin transport. Since NPA is not targeted on PIN proteins, NBP may be part of the polar auxin efflux protein complex with PIN proteins.

1.4.4 Auxin Influx Carrier

AUXIN-RESISTANT1 (AUX1) is the main auxin influx carrier in Arabidopsis. It has similarity to a putative amino acid permease (AAP) family in plants (Bennett et al., 1996). Radio labeled IAA uptake experiments illustrate that AUX1 probably transports deprotonated IAA into the PM by pumping out two protons (Lomax et al., 1985; Sabater and Rubery, 1987). Moreover, in *aux1* mutants, root growth is normal on 1-naphthaleneacetic acid (1-NAA) plates but more defective on 2,4-dichlorophenoxyacetic acid (2,4-D) and IAA plates (1-NAA and 2,4-D are chemical homologs of IAA, but 1-NAA is membrane permeable). Thus, AUX1 is responsible for uptake of IAA and 2,4-D by the cell (Marchant et al., 1999). Further experiments of ^{3}H-IAA uptake affinity in a heterologous system, indicates that AUX1 facilitates the uptake of deprotonated IAA (Yang, 2006; Yang et al., 2006). AUX1 protein has been found in the lateral root cap (LRC) and protophloem. The asymmetric localization of AUX1 on the upper PM of the protophloem facilitates acropetal auxin transport to the root apex. However, AUX1

localization in the LRC is symmetric but overlaps with the asymmetrical localization of PIN2; therefore, AUX1 may also be involved in basipetal transport in the root. However, instead of directing auxin transport, it more likely that AUX1 facilitates auxin permeability in this region (Parry et al., 2001; Swarup et al., 2001). There are three *AUX1* like genes identified in Arabidopsis and named *Like AUX1 1, 2, and 3 (LAX1, 2, 3)*. But the single mutants do not have a visible phenotypes. Quadruple mutants, in addition to triple mutants with *aux1* and *lax1*, show defects in phyllotaxy in Arabidopsis development. The phenotypes in leaf primordia initiation patterning indicates that auxin influx transport may assist *PIN1* in determine phyllotaxy in Arabidopsis (Parry et al., 2001; Tanaka et al., 2006).

1.4.5 Auxin Efflux Complex

The putative auxin efflux carriers have been identified as PIN family membrane localized proteins (Friml and Palme, 2002b). There are eight genes in the *PIN* family in *Arabidopsis*. Within the *PIN* family, each of the genes has at least 10 transmembrane domains mainly distributed at the C- and N- terminus. *AtPIN1, 2, 3, 4,* and *7* share high homology and are clustered to one clade. *AtPIN5, 6* and *8* are grouped in a separate clade. The sequence similarity ranges from 32% to 85% between each combination of genes. These proteins are similar to a group of transporter proteins in bacteria. When the first member *AtPIN1* was cloned by transposon tagging, it was proposed to have auxin transport ability (Galweiler et al., 1998).

There is some convincing biochemical evidence that PIN proteins are essential to determine the direction of auxin transport (Benjamins and Scheres, 2008). Evidence for PIN proteins determining auxin transport direction are listed below: Firstly, the 5 characterized *PIN* proteins (1, 2, 3, 4, 7) are all polarly localized in the membrane. Secondly, *pin* mutant plants have phenotypes similar to plants treated with auxin transport inhibitors such as auxin accumulation, altered tropic responses and abnormal lateral organ development (Tanaka et al., 2006; Zazimalova et al., 2007). Thirdly, PAT chemical inhibitors treatment can phenocopy the *pin* inflorescence mutant phenotypes. Although the PAT chemical inhibitors are targeting proteins other than the PIN family, the similarity of the mutant phenotype suggests that the putative PAT inhibitor binding

protein and the auxin efflux carriers both regulate PAT (Muday and DeLong, 2001a). Fourthly, when PIN proteins were overexpressed in Arabidopsis suspension cells and tobacco BY-2 cells, there was an increase in auxin efflux out of the cell using radio labeled auxin (Petrasek et al., 2006). However, due to the lack of direct evidence that PIN proteins bind and transport auxin, detailed biochemical analysis are needed to confirm that PINs are the auxin efflux carrier.

AtPIN1 is basipetally localized in the xylem and cambial cells in the root and the stem (Galweiler et al., 1998). AtPIN1 is localized toward initiating primordia in the inflorescence meristem (Geldner et al., 2001; Friml and Palme, 2002a). AtPIN2 is distributed in the cortical and epidermal cells of the root tip and root elongation zone and is responsible for gravitropism (Muller et al., 1998). AtPIN3 protein is located on the lateral side of the membrane in cells of the hypocotyls (Friml et al., 2002a). AtPIN4 is basipetally and laterally distributed in the root tip and plays a role in generating an auxin sink below the quiescent centre which is essential for auxin distribution and patterning (Friml et al., 2002b). AtPIN7 is acropetally localized in the basal cell in early embryogenesis and redistributed basipetally in the globular embryo, therefore, regulating auxin distribution during embryogenesis (Friml et al., 2003). The function of *AtPIN5, 6* and *8* genes is still unclear (Paponov et al., 2005).

A recent study shows that PIN2 may guide auxin flow during the gravitropism response (Wisniewska et al., 2006). Using hemagglutinin (HA) tagged PIN1 and PIN2 expressed under the *PIN2* promoter, the researchers showed that the opposite asymmetric localization of PIN1 and PIN2 in the same epidermal cell in the root is determined not only by the cell type but also by the protein sequence of PIN1 and PIN2. In addition, *PIN2::PIN2-HA* could rescue the abnormal gravitropic response in *pin2* mutant roots since the location of PIN2-HA at the acropetal side of the cell may direct auxin flow. Therefore, the function of each PIN protein in directing auxin flow is tissue and cell specific.

1.4.6 Regulation of PAT

1.4.6.1 How Auxin Influx and Efflux Carrier Polarity is Maintained by Vesicle Trafficking

How is the polarized localization of auxin influx and efflux carriers maintained in the cell? Recent studies on endocytosis of carriers such as *AUX1, PIN1* and *PIN2* provide some clues.

Endocytosis and plasma membrane (PM) protein recycling have been intensely studied in yeast and animals (Mukherjee et al., 1997). The endocytosed vesicles formed from the PM move inward to form early endosomal compartments or sorting endosomes. These endosomal compartments could either move back to the PM for recycling or move to the Trans-Golgi Network (TGN) for modification or later recycling. Furthermore, the early endosomes could mature to become late endosomes or multivesicular body (MVB). MVBs could move into the TGN similar to the early endosome or they could be targeted to the lysosome for degradation. These endocytosis pathways are either clathrin mediated or clathrin involved receptor mediated (clathrin is a protein which coats vesicles for vesicle transport). There are also non clathrin mediated endocytosis types such as phagocytosis. Plant endocytosis is not as clearly understood as in animals. However, the early endosomes traffic similarly as clathrin mediated endosome travel either between the PM and the vesicle compartment or to the TGN for reuse. The mature endosomes are directed to the TGN for recycling or to the vacuole for protein degradation. The endosome compartment can be stained by FM4-64. A recent study shows that PIN1 and PIN2 internalization in the endosome may be clathrin mediated (Dhonukshe, 2007). Based on the knowledge above, genetic, molecular and cell biology methods have been used to explore the polar localization of auxin transport flux carriers.

The auxin transport efflux complex is not fixed on the membrane but is dynamically maintained because of the rapid turnover of the complex at the cell membrane (Steinmann et al., 1999; Geldner et al., 2001). Vesicle traffic inhibitors such as brefeldin A (BFA) can cause IAA and naphthaleneacetic acid (NAA) accumulation in the cell. However, 2,4-dichlorophenoxyacetic acid (2,4-D), an auxin mimic which is known to be taken up by the cell through the auxin influx carrier but not the efflux carrier, does not accumulate in BFA treated cells. In addition, PIN1 proteins accumulate in vesicle

bodies after BFA treatment, which indicates that auxin efflux carriers require vesicle trafficking to maintain their membrane localization. Furthermore, PIN1 localization can be restored by washing off BFA treatment and BFA effects are not influenced by cycloheximide (CHX), a protein synthesis inhibitor (Robinson et al., 1999), suggesting that protein localization rather than synthesis is influenced by BFA treatment. Therefore, localization of the auxin efflux complex cycles between vesicles and the cell membrane.

Genetic evidence also suggests that rapid *PIN1* turnover is regulated by the endosomal vesicle trafficking pathway (Geldner et al., 2003). *GNOM (GN)* encodes an ADP-ribosylation factor GDP/GTP exchange factor (ARF-GEF). ARF-GEF factors are known to be involved in vesicle budding through recruitment of proteins to the vesicle coat. In *gn* mutants, *PIN1* localization is affected and auxin transport is blocked by BFA. However, these effects are not sensitive to BFA in a modified BFA-resistant *GNOM* variant (Teh and Moore, 2007), indicating that the BFA sensitive vesicle transport is essential for *PIN1* localization on the membrane.

However, GNOM endosome trafficking is not the only endosome type implicated in regulating the *PIN* family. *SORTING NEXIN1* in Arabidopsis (*AtSNX1*) is involved in *PIN2* vesicle trafficking and PM localization (Jaillais et al., 2006). AtSNX1::GFP signal colocalizes with FM4-64 stain in vesicles after BFA treatment. However, AtSNX1::mRFP does not colocalize with GNOM::GFP. This indicates that the AtSNX1 endosome is different from the GNOM endosome although both endosomes are sensitive to BFA treatment. Furthermore, the AtSNX1 endosome but not the GNOM endosome is sensitive to a kinase inhibitor, wortmannin. As a result, the polar localization and vesicle transport of PIN1::GFP is not affected by wortmannin treatment. However, PIN2::GFP signal is retained in wortmannin induced endosomes although the polar localization is not changed.

The mature endosome vesicles, the multivesicular bodies (MVBs), are retromer complex proteins that are conserved between mammals and plants. MVBs are responsible for moving target protein cargos from the endosome to the TGN (Jaillais, 2007). *VACUOLAR PROTEIN SORTING29 (VPS29)* is one of three different proteins composing the plant retromer. The mutant *vps29* displays phenotypes such as abnormal cotyledons, defects in early embryo development and dwarf plant height. *VPS29* is

epistatic to *PIN1* since *vps29;pin1* double mutant phonocopies *vps29* single mutant. Homozygous *vps29;snx1* double mutants are embryo lethal and the *VPS29/vps29; snx1/snx1* double mutant phenotype is more severe than *snx1* single mutants. Therefore, VPS29 and SNX1 may partially interact with each other in regulating PIN1. However, GNOM-GFP, SNX1-GFP and AUX1-GFP localization are similar to wild type in *vps29* mutants. Hence, VPS29 may act downstream of the GNOM and the SNX1 endosomes to regulate PIN1 localization but not AUX1 localization.

The auxin influx carrier AUX1 may recycle using a different mechanism than the PIN proteins (Jaillais et al., 2006). AUX1::YFP has been shown to colocalize with the endosome compartment stain FM4-64, which suggests that AUX1 dynamically cycles between the PM and endosome compartments. The tagged AUX1 protein AUX1:HA partially colocalizes with PIN1:GFP, BRASSINOSTEROID-INSENSITIVE1:GFP (BRI1, a reported PM and endosome marker) and γ-COAT PROTEIN:GFP (γ-COP, Golgi marker) in the BFA endosome compartment. However, the localization of AUX1 on the upper surface of the PM in the protophloem is undisturbed by BFA treatment. Thus, AUX1 may use different BFA insensitive ARF-GEFs other than GNOM for endosome trafficking. Florescence recovery after photobleaching (FRAP) analysis with AUX1:YFP at the presence of BFA confirms that AUX1 polar localization still recovers in the presence of BFA (Kleine-Vehn et al., 2006). Interestingly, *AUXIN RESISTANT4 (AXR4)* has been identified to regulate AUX1 trafficking to the PM. In *axr4* mutants, AUX1 accumulates in the endoplasmic reticulum (ER). The similar phenotype of *axr4* and *aux1* can be rescued by exogenous application of the membrane permeable auxin mimic 1-NAA. Consequently, AXR4 is responsible for maintaining the PM localization of AUX1 so that auxin can be transported into the cell. Meanwhile, PIN1 and PIN2 localization are not changed in *axr4* mutants (Dharmasiri, 2006; Dharmasiri et al., 2006; Hobbie, 2006), which suggests that AXR4 may not affect auxin efflux. Thus, the mechanism of polar localization of auxin influx and efflux is different in Arabidopsis.

To conclude, vesicle trafficking regulates PINs and AUX1 localization on the PM, although the trafficking mechanisms differ from each other. The constitutive recycling of auxin influx and efflux carriers between the PM and endosome compartment may be

important for the plant to respond quickly to internal and external signaling cues for growth and development.

1.4.6.2 The Cytoskeleton is Involved in PAT Maintenance

As auxin efflux carriers cycle between the endosomal vesicles and the plasma membrane, how do they maintain their polar localization? Much evidence shows that the cytoskeleton is essential for polar localization (Geldner et al., 2001; Boutte et al., 2006). First, the vesicles traffic along cytoskeleton actin filaments; Second, it is known that NPA binding protein (NBP) is associated with actin filaments; Third, cytochalasin D, a chemical which interrupts actin filament polymerization, disrupts the polar localization of the auxin efflux complex (Geldner et al., 2001; Muday and DeLong, 2001b). Whether actin filaments act through the NBP to regulate the auxin efflux complex is still not clear, however, it is clear that actin filaments are involved in maintaining polar auxin localization (Davies, 2004). Latrunculin B is a commonly used reagent which alters the organization of actin filaments (Wakatsuki, 2001). However, Latrunculin B treatment in maize roots shows that actin is involved in the PIN1 internalization vesicle trafficking rather than polar localization on the PM. Less than three hours treatment with oryzalin, which is a chemical that interrupts microtubule depolymerization, shows no effects on the localization of PIN proteins both in Arabidopsis and maize. However, more than eight hours of oryzalin treatment disrupts the normal polarity of PIN proteins in the root of Arabidopsis (Boutte et al., 2006). Thus, microtubules may play a role in the polarity of PIN localization also.

1.4.6.3 PAT is Regulated by Phosphorylation and Dephosphorylation

Phosphorylation/dephosphorylation also plays a role in PAT regulation. For example, another NPA sensitive mutant, *ROOTS CURL ON NPA1 (RCN1),* encodes the A subunit of protein phosphatase 2A and is also called PP2AA1. In the *rcn1* mutant, polar auxin transport is interrupted (Garbers et al., 1996). There are two other *PP2AA* subunits in Arabidopsis genome, *PP2AA2* and *PP2AA3*. *PP2AA2* and *PP2AA3* are redundant with each other (Michniewicz et al., 2007). However, double mutants of *PP2AA2;3* combined with *PP2AA1* and the triple mutant show auxin related phenotypes

such as abnormal root development, fused or misshaped cotyledons and defects in the embryo. Reduced DR5:GFP signals in *pp2aa1;pp2aa2* and *pp2aa1;pp2aa3* double mutants suggest that auxin level is changed. In addition, in *pp2aa1;pp2aa2* and *pp2aa1;pp2aa3* double mutants, PIN1 basal localization is occasionally switched to the apical side of the cell in the embryo and PIN2 is relocalized from the basal to apical side of cortical cells in the root.

PINOID (PID), a Serine/Threonine kinase C gene, is expressed mainly in the lateral primordia both in the root and the shoot (Christensen et al., 2000b). The phenotype of *pid* in the shoot inflorescence mimics *pin1* mutants. This indicates that both *PID* and polar auxin transport are required for floral organ initiation and outgrowth. *35S::PID* causes phenotypes such as lateral root inhibition, dwarf plants, reduced apical dominance and curled leaf. These typical auxin insensitive phenotypes indicate that *PID* may negatively regulate the auxin signaling. However, *35S::PID* phenotypes could be rescued by NPA, the PAT inhibitor (Benjamins et al., 2001b). So, *PID* may positively regulate polar auxin transport. The most exciting results are the evidence which showed that *PID* acts as a regulator of *PIN1* polar localization (Friml et al., 2004). In *pid* mutants, apical localization of *PIN1* in the shoot switches to basal while in *35S::PID*, basal localization of *PIN1* in the root is changed to apical. Therefore, *PID* regulates auxin flow direction by maintaining *PIN1* polar localization in the cell.

Phosphorylation assays confirm that PIN1 is a direct phosphorylation target of PID and dephosphorylation target of PP2AA using tagged PIN1, PID and PP2AA protein extracts from the protoplasts of Arabidopsis (Michniewicz et al., 2007). Mass Spectrometry analysis indicates that the hydrophilic loop of the PIN1 protein is the site of phosphorylation. Thus, PID and PP2AA antagonistically interact with each other to regulate the polar localization of PIN1 protein and hence determine the direction of auxin flow.

An *ENHANCER OF PINOID (ENP)* has been identified recently in analysis of a cotyledon deficient mutant *laterne*. *ENP* works with *PID* to control *PIN1* polarity and specifically regulate cotyledon development (Treml et al., 2005). *ENP* is identical to *MACCHI-BOU4 (MAB4)* and *NPY1*, which encodes a novel protein similiar to the *NON-PHOTOTROPIC HYPOCOTYL3 (NPH3)* family. The cotyledon phenotype is more

severe in *mab4/enp;pid* double mutant than either single mutant (Cheng, 2007; Cheng et al., 2007b; Furutani et al., 2007). Also, the pin like inflorescence meristem phenotype is similar in *pin1, pid;pin* and *pid;mab4* mutants. In addition, MAB4/ENP partially colocalizes with PID but not PIN1 in internal vesicle compartments in cultured Arabidopsis cells. Therefore, *MAB4/ENP* and *PID* may partially interact to regulate PIN1 and this regulation may be involved in PIN1 recycling.

How is *PID* activated and regulated in the auxin signal transduction network? Yeast two hybridization analysis and immuno-pull down assay show that two proteins interact with PID in Arabidopsis (Benjamins, 2003; Benjamins et al., 2003). These two genes are *TOUCH3 (TCH3)* and *PID-BINDING PROTEIN1 (PBP1). TCH3* is a calmodulin related protein and *PBP1* is a putative calcium binding protein. Thus, calcium may be involved in the regulation of *PID*. However, in vitro protein kinase assay shows that PID can not phosphorylate TCH3 and PBP1. Therefore, *TCH3* and *PBP1* may function upstream of *PID* in auxin signal transduction (Benjamins et al., 2003). PID activates itself by autophosphorylation (Christensen et al., 2000a). This autophosphorylation is important for transphosphorylation of its the substrates in vitro. PID transphosphorylation of myelin basic protein (MBP) is negatively regulated by calcium but positively promoted by magnesium (Zegzouti et al., 2006a). Furthermore, 3-Phophoinositide-Dependant Kinase1 (*PDK1*) can bind to *PID* and promote *PID* autophosphorylation and transphosphorylation ability in vitro and in Arabidopsis protoplasts. Thus, *PDK1* is another factor that functions upstream of *PID*. However, whether PDK1 activated PID kinase activity is essential for PIN1 regulation is still not clear. Then, what are the downstream targets of PID in the network? PIN1 has been shown to be the first phosphorylation target of *PID* (Michniewicz et al., 2007). Also, *barren stalk1 (ba1)* in maize is a phosphorylation target of *PID* co-ortholog *bif2* in maize (Skirpan et al., 2007). *BA1* and its rice ortholog *LAX* are basic helix loop helix (bHLH) transcription factors, which are essential in inflorescence development (Ritter, 2002; Ritter et al., 2002; Komatsu et al., 2003a; Gallavotti et al., 2004).

Cloning of *PID* orthologs from other plant species show that *PID* belongs to the AGC-VIII protein kinase family (Zegzouti et al., 2006b). *PsPK2* is the PID ortholog in pea. The expression pattern of *PsPK2* is similar to *PID* in the young leaf, shoot apex and

floral organs (Chawla and and DeMason, 2004; Bai et al., 2005; Bai and and DeMason, 2006). Both *PsPK2* and *PsPIN1 (PIN1* otholog in pea) mRNA level is elevated by auxin (Bai and and DeMason, 2006). Thus, the function of *PID* appears to be conserved in dicots.

In monocots, both in rice and maize, there are two copies of *PID* due to the genome wide duplication event. *bif2*, which is the main interest of our lab, is a co-ortholog of *PID* in maize (McSteen et al., 2007). *bif2* is mainly expressed in the vegetative axillary meristem, the peripheral zone of the inflorescence meristem, the SPMs, SMs as well as FMs (McSteen et al., 2007). This is similar to the *PID* expression pattern in Arabidopsis and *OsPID* expression pattern in rice (Christensen et al., 2000b; Morita and Kyozuka, 2007). Expression of *kn1*, the meristem maintenance marker gene, is downregulated on the flanks of the *bif2* inflorescence, thus, *bif2* is required for BM, SPM, SM and FM initiation (McSteen and Hake, 2001b).

1.4.6.4 Other Factors in Regulation of Polar Auxin Transport (PAT)

Recent studies show that auxin itself inhibits PIN1 and PM H^+-ATPase endocytosis in the protophloem cells in the root (Paciorek et al., 2005). Application of IAA, 2,4-D and NAA all suppress internalization of PIN1:GFP signal in the endosome. Thus, increased levels of auxin accumulation in the cell stabilize PIN1 localization on the PM, facilitating auxin transport out the cell.

PAT is regulated by many factors in plants. Besides PIN proteins, recent characterization of Multidrug Resistance (MDR) class of p-glycoprotein (PGP) homologs in the plants such as *AtMDR1/PGP19* and *AtPGP1* indicates they may play a role in PAT regulation (Noh et al., 2003). It was shown that the auxin transport inhibitor NPA binds tightly and specifically to AtMDR1 and AtPGP1 proteins. In *mdr1* and *pgp1* mutant, PIN1 localization and auxin transport are interrupted. Yeast two hybrid analysis shows that PGP19 interacts with both PIN1 and PIN2 (Blakeslee et al., 2007). Florescence labeled fusion protein of PGP19 and PGP1 colocalize with labeled PIN1 and PIN2 in the root. The ortholog of *AtPGP1* in maize is *brachytic2 (br2)* and in sorghum is *dwarf3 (dw3)* (Multani et al., 2003). Auxin transport and growth defects in *br2* and *dw3* mutants

such as dwarf plants and short internodes indicate that MDR-mediated PAT regulation is conserved between dicots and monocots.

Flavonoids are naturally produced plant phenolic compounds and they play important roles in a broad range of plant physiological processes (Peer, 2004; Peer et al., 2004; Peer and Murphy, 2007; Peer, 2007). Some of the flavonoids are found to compete with NPA for binding to the NBP site on the membrane. So, flavonoids are in planta produced phytotropins that regulate auxin distribution patterns. Auxin transport is increased in the absence of flavonoids and reduced when extra flavonoids are produced. Flavonoid inhibition of auxin transport does not directly target PIN1 protein but the vesicles that maintained PIN localization.

PIN protein stability is regulated by *MODULATOR of PIN (MOP2* and *MOP3)* (Malenica et al., 2007). The phenotypes of *mop2* and *mop3* mimic auxin related mutants, for example, reduced root growth, irregular arrangement of columella cells, abnormal cotyledons and pin like inflorescence. Northern blot analysis shows that the transcription level of *PIN1, 2, 3, 4* and *7* are not very different between the wild type and *mop2-1* and *mop3-1* mutants. However, western blotting analysis indicates that PIN2 and PIN3 protein level are largely reduced in *mop2-1* and *mop3-1* mutant compared with the wild type. Thus, MOP2 and MOP3 regulate PIN proteins posttranslationally.

1.4.7 Auxin response and downstream signal transduction

Auxin biosynthesis, auxin conjugation and polar auxin transport determine auxin levels in the target cell and tissue. But, auxin itself can act as a signal to stimulate organogenesis. Therefore, downstream factors involved in auxin response must be important in plant organ differentiation and growth. Recent studies show that ubiquitin mediated protein degradation is essential for auxin response (Benjamins and Scheres, 2008). *TRANSPORT RESPONSE1 (TIR1),* which encodes an F-box protein, is one of the auxin receptors (Dharmasiri et al., 2005; Kepinski and Leyser, 2005). *TIR1* is one component of the SCF E3 ligase complex which mediates protein degradation (Hochstrasser, 1996; Leyser, 2002). In the complex, there are four types of protein: SKP1, F-box protein, RBX1 and CULLIN. CUL connects SKP1 and RBX1 and the F-box protein binds with SKP1. In addition, the F-box protein specifically recognizes and binds the target proteins of the SCF complex to promote degradation. Thus, there are many F-box proteins to determine SCF degradation specificity.

Auxin binds to TIR1 and AUX/IAA to mediate SCF^{TIR} complex degradation of AUX/IAA proteins (Dharmasiri et al., 2005; Kepinski and Leyser, 2005). These AUX/IAA proteins commonly contain four domains. Domain III and IV are essential for hetero- or homodimerization with other AUX/IAAs or with auxin response factor (ARF) proteins. Domain II is responsible for the stability of AUX/IAA proteins. Normally, AUX/IAA proteins repress ARFs. ARF proteins contain a DNA binding domain (DBD), which specifically recognizes TGTCTC repeats in the promoter region of auxin response genes. Therefore, auxin mediated degradation of AUX/IAA releases their repression of ARFs, enabling the ARFs to activate or repress the transcription of downstream auxin response genes (Leyser, 2002). For example, *BODENLOS(BDL)/IAA12* suppresses *MONOPTERS(MP)/ARF5* (Hamann et al., 1999; Hamann et al., 2002). In embryo development, abnormal phenotypes in the hypophysis and root meristem are similar in *bd1;mp* double mutant as in each single mutant. Yeast two hybridization also shows that these two proteins interact with each other. Therefore, auxin induced BDL degradation releases MP to activate downstream genes (Parry, 2006).

1.4.8 Other Factors and Conclusion

How does auxin biosynthesis and transport coordinate developmental and environmental stimuli with auxin responses? The *YUC* and *PID* pathway provides a clue to the answer. *NPY1* encodes a protein identical to ENH/MAB protein previously described. The double mutant *npy1;pid* phenocopies the *yuc1;yuc4;pid* triple mutant (Cheng et al., 2007b). In addition, the phenotype of no cotyledon formation in the *npy1;pid* double mutant is more severe than either single mutant. All these genetic interactions indicate that *NPY1* works with *PID* in the same pathway to connect developmental cues such as meristem initiation and differentiation to auxin response. This is a similar model to the blue light response coordinated by NPH3 and PHOT1 (PID kinase homolog). Interestingly, in *yuc1;yuc4;npy1* triple mutants, the mRNA level of *PIN, PID* and *ARF5/MP* is not changed. Therefore, regulation must be at the protein level. Thus, whether *NPY1* interacts with *PID* in a complex or other factors exist to activate *PID* other that *YUC* and *NPY1* will be interesting to explore.

To conclude, auxin biosynthesis, transport and auxin signaling response are tightly regulated networks in plant growth and development. Auxin can regulate its own biosynthesis and transport. De/phosphorylation regulates auxin transport and response. *PID* has an auxin-responsive element (AuxRE) in the promoter region and is induced by auxin. Vesicle trafficking of PIN proteins can quickly mediate auxin transport and accumulation in the target cells and organs. All these factors combine together to determine auxin level and transport in plant development. Therefore, auxin can promote plant growth and precisely regulate developmental events through multiple mechanisms.

1.5 Summary of Ph.D. research

Multiple axillary meristems are produced in the inflorescence of maize. How are these axillary meristems, such as BMs, SPMs, SMs and FMs initated? Is auxin and auxin transport involved in initiation of these meristems? To answer these questions, we designed the NPA treatment experiment which is presented in chapter 2 of this thesis.

Does *bif2*, the co-ortholog of *PID* in maize, have the same function as *PID* in inflorescence development? In addition, BA1 has been shown by yeast two hybridization analysis to interact with BIF2 in vitro. How do these two genes interact with each other genetically? To answer these questions, *bif2;ba1* double mutants have been constructed. Phenotype and genetic analysis were performed and are presented in chapter 3 of this thesis.

Furthermore, in the NPA treatment experiment, we found that the SPMs are converted to SMs when auxin transport is blocked. This phenotype is also observed in *Sos1* mutants. As I mentioned in the part III-4 of this chapter, *ramosa* mutants have opposite phenotypes to *Sos1* mutants as there are more SM initiated per SPM. Does *Sos1* interact with the *ramosa* pathway in determine SMs initiation? To address these questions, we analyzed the *Sos1* phenotype and *Sos1;ra1, Sos1;ra2* double mutant phenotype in detail. This is presented in chapter 4 of this thesis.

Since *Sos1* has a similar phenotype in NPA treated meristems, is *Sos1* involved in the auxin signaling pathway to regulate sessile spikelet initiation? Or is *Sos1* required for sessile spikelet initiation as a meristem identity gene in maize inflorescence development? These questions can only be understood after the gene is cloned and analyzed in detail. An attempt to clone this gene by transposon tagging was not successful as there were no *Mu* elements inserted in the mutant. Therefore, the cloning strategy was changed to map-based chromosome walking. This progress is presented in the appendix A of this thesis.

Finally, future work and experiments to test the remaining unanswered hypotheses on the role of *bif2, ba1* and *Sos1* in maize inflorescence development are discussed and presented in chapter 5 of this thesis.

Figure 1.1 Maize Tassel Inflorescence Development

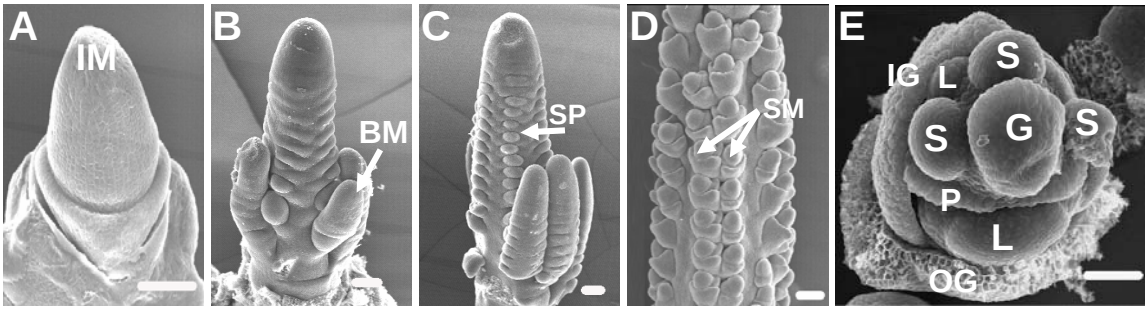

Figure 1.1 Maize Tassel Inflorescence Development

A) Shoot apical meristem transitions to become the inflorescence meristem (IM)
B) IM starts to initiate branch meristems (BM) at the bottom
C) Spikelet pair meristem (SPM) starts to initiate on both the main spike and branch
D) Spikelet meristem (SM) starts to initiate
E) One SM is disected out to show the inner glume (IG) and outter glume (OG), lower floret meristem (LFM). The upper floret has already developed three stamens (S), the gynoecium (G) and two lodicules (L). The palea (P) is between the upper floret meristem and the lower floret meristem

Table 1.1 Summary of Genes in Meristem Development in Maize

Meristem Type	Gene	Homolog	Phenotype in Maize
Shoot Apical Meristem (SAM)	*kn1*	*STM*	sparse tassel and ear
	td1	*CLV1*	bigger IM, fasciated ears, extra floral organs
	fea2	*CLV2*	fasciated ears, extra floral organs
	ns1,2	*WUS*-like *PRS*	narrow leaf blade
SAM to Inflorescence Meristem (IM)	*id1*	*PCP1* in potato	extra leaves, mini plantlets in the tassel, prolonged vegetative growth
	zfl1,2	*LFY*	tassel ears in the tassel, fewer branches
Vegetative Axillary Meristem (VAM)	*tb1*	*CYCLOIDEA* in *Antirrhinum*	extra tillers, shoots replace ears
	Cg1	*miR156*	increased tiller number
	Tp1,2,3	---	increased tiller number
	Tlr1	---	increased tiller number
All Axillary Meristems	*bif2*	*PID*	fewer BM, SPM, SM and FM, less floral organs in both ear and tassel
	ba1	*lax1* in rice	fewer BM, SPM, SM and FM in the tassel, no ears
Spikelet Pair Meristem (SPM)	*ra1*	---	indeterminate BM and SPM in both tassel and ear
	ra2	*ASL4*	Sparse, indeterminate BM and SPM in the tassel and some branches in the ear
	ra3	*T6P*	extra branches and spikelets in the tassel and ear
	Sos	---	fewer branches, single spikelets in both tassel and ear
Spikelet Meristem (SM)	*ids1*/*Ts6*	*AP2* like	extra florets/extra SMs and florets, feminized tassel florets
	ts4	*miR172*	extra SMs and florets, feminized tassel florets
	ifa1	---	extra spikelets and florets
	rgo1	---	extra florets and upside down kernels
	bd1	*fzp* in rice	extra spikelets

Notes: In homolog, the gene name is in *Arabidopsis* unless otherwise specified

References

Bai, F., and and DeMason, D.A. (2006). Hormone interactions and regulation of Unifoliata, PsPK2, PsPIN1 and LE gene expression in Pea (*Pisum sativum*) shoot tips. *Plant Cell Physiol* **47,** 935-948.

Bai, F., Watson, J.C., Walling, J., Weeden N., Santner, A.A., and D.A., a.D. (2005). Molecular characterization and expression of *PsPK2*, a *PINOID*-like gene from pea (*Psium sativum*). *Plant Sci* **168,** 1281-1291.

Benjamins, R., and Scheres, B. (2008). Auxin: the looping star in plant development. *Annu Rev Plant Biol* **59,** 443-465.

Benjamins, R., Ampudia, C.S., Hooykaas, P.J., and Offringa, R. (2003). PINOID-mediated signaling involves calcium-binding proteins. *Plant Physiol* **132,** 1623-1630.

Benjamins, R., Quint, A., Weijers, D., Hooykaas, P., and Offringa, R. (2001). The PINOID protein kinase regulates organ development in Arabidopsis by enhancing polar auxin transport. *Development* **128,** 4057-4067.

Benkova, E., Michniewicz, M., Sauer, M., Teichmann, T., Seifertova, D., Jurgens, G., and Friml, J. (2003). Local, efflux-dependent auxin gradients as a common module for plant organ formation. *Cell* **115,** 591-602.

Bennett, M.J., Green, H.G., May, S.T., Ward, S.P., Millner, P.A., Walker, A.R., Schulz, B., and and Feldmann, K.A. (1996). Arabidopsis *AUX1* genes: a permease-like regulator of root gravitropsim. *Science* **273,** 948-950.

Bennett, S.R.M., Alvarez, J., Bossinger, G. and Smyth, D. R. (1995). Morphogenesis in *pinoid* mutants of Arabidopsis thaliana. *Plant J.* **8,** 505–520.

Bernasconi, P.B., Reagan, J.D., and and Subramanian, M.V. (1996). The N-1-naphthylphthalamic acid-binding protein is an integral membrane protein. *Plant Physiol* **111,** 427-432.

Blakeslee, J.J., Peer, W.A., and Murphy, A.S. (2005). Auxin transport. *Curr Opin Plant Biol* **8,** 494-500.

Blakeslee, J.J., Bandyopadhyay, A., Lee, O.R., Mravec, J., Titapiwatanakun, B., Sauer, M., Makam, S.N., Cheng, Y., Bouchard, R., Adamec, J., Geisler, M., Nagashima, A., Sakai, T., Martinoia, E., Friml, J., Peer, W.A., and Murphy, A.S. (2007). Interactions among PIN-FORMED and P-glycoprotein auxin transporters in Arabidopsis. *Plant Cell* **19,** 131-147.

Bomblies, K., Wang, R.L., Ambrose, B.A., Schmidt, R.J., Meeley, R.B., and Doebley, J. (2003). Duplicate *FLORICAULA/LEAFY* homologs *zfl1* and *zfl2* control inflorescence architecture and flower patterning in maize. *Development* **130,** 2385-2395.

Bommert, P., Satoh-Nagasawa, N., Jackson, D., and Hirano, H.Y. (2005a). Genetics and evolution of inflorescence and flower development in grasses. *Plant Cell Physiol* **46,** 69-78.

Bommert, P., Lunde, C., Nardmann, J., Vollbrecht, E., Running, M., Jackson, D., Hake, S., and Werr, W. (2005b). *thick tassel dwarf1* encodes a putative maize ortholog of the Arabidopsis CLAVATA1 leucine-rich repeat receptor-like kinase. *Development* **132,** 1235-1245.

Bortiri, E., and Hake, S. (2007). Flowering and determinacy in maize. *J Exp Bot* **58,** 909-916.

Bortiri, E., Chuck, G., Vollbrecht, E., Rocheford, T., Martienssen, R., and Hake, S. (2006). *ramosa2* encodes a LATERAL ORGAN BOUNDARY domain protein that determines the fate of stem cells in branch meristems of maize. *Plant Cell* **18,** 574-585.

Boutte, Y., Crosnier, M.T., Carraro, N., Traas, J., and Satiat-Jeunemaitre, B. (2006). The plasma membrane recycling pathway and cell polarity in plants: studies on PIN proteins. *J Cell Sci* **119,** 1255-1265.

Chawla, R., and and DeMason, D.A. (2004). Molecular expression of *PsPIN1*, a putative auxin efflux carrier gene from pea (Pisum sativum L.). *Plant Growth Regul* **44,** 1-14.

Chen, X. (2004). A microRNA as a translational repressor of *APETALA2* in Arabidopsis flower development. *Science* **303,** 2022-2025.

Cheng, Y., Dai, X., and Zhao, Y. (2006). Auxin biosynthesis by the *YUCCA* flavin monooxygenases controls the formation of floral organs and vascular tissues in Arabidopsis. *Genes Dev* **20,** 1790-1799.

Cheng, Y., Dai, X., and Zhao, Y. (2007a). Auxin synthesized by the *YUCCA* flavin monooxygenases is essential for embryogenesis and leaf formation in Arabidopsis. *Plant Cell* **19,** 2430-2439.

Cheng, Y., Qin, G., Dai, X., and Zhao, Y. (2007b). *NPY1*, a BTB-NPH3-like protein, plays a critical role in auxin-regulated organogenesis in Arabidopsis. *Proc Natl Acad Sci U S A* **104,** 18825-18829.

Cheng, Y., Qin, G., Dai, X. and Zhao, Y. (2007). NPY1, a BTB-NPH3-like protein, plays a critical role in auxin-regulated organogenesis in Arabidopsis. *Proc Natl Acad Sci U S A* **104,** 18825-18829.

Christensen, S.K., Dagenais, N., Chory, J., and Weigel, D. (2000). Regulation of auxin response by the protein kinase PINOID. *Cell* **100,** 469-478.

Chuck, G., Meeley, R.B., and Hake, S. (1998). The control of maize spikelet meristem fate by the *APETALA2*-like gene *indeterminate spikelet1*. *Genes Dev* **12,** 1145-1154.

Chuck, G., Cigan, A.M., Saeteurn, K., and Hake, S. (2007a). The heterochronic maize mutant *Corngrass1* results from overexpression of a tandem microRNA. *Nat Genet* **39,** 544-549.

Chuck, G., Muszynski, M., Kellogg, E., Hake, S., and Schmidt, R.J. (2002). The control of spikelet meristem identity by the *branched silkless1* gene in maize. *Science* **298,** 1238-1241.

Chuck, G., Meeley, R., Irish, E., Sakai, H., and Hake, S. (2007b). The maize *tasselseed4* microRNA controls sex determination and meristem cell fate by targeting *Tasselseed6/indeterminate spikelet1*. *Nat Genet* **39,** 1517-1521.

Clark, S.E., Running, M.P., and Meyerowitz, E.M. (1993). *CLAVATA1*, a regulator of meristem and flower development in Arabidopsis. *Development* **119,** 397-418.

Colasanti, J., Yuan, Z., and Sundaresan, V. (1998). The *indeterminate* gene encodes a zinc finger protein and regulates a leaf-generated signal required for the transition to flowering in maize. *Cell* **93,** 593-603.

Colasanti, J., Tremblay, R., Wong, A.Y., Coneva, V., Kozaki, A., and Mable, B.K. (2006). The maize INDETERMINATE1 flowering time regulator defines a highly conserved zinc finger protein family in higher plants. *BMC Genomics* **7,** 158.

Davies, P.J. (2004). Plant hormones biosynthesis, signal transduction, action! (the Netherlands: Kluwer Academic Publishers).

Dharmasiri, N., Dharmasiri, S., and Estelle, M. (2005). The F-box protein TIR1 is an auxin receptor. *Nature* **435,** 441-445.

Dharmasiri, S., Swarup, R., Mockaitis, K., Dharmasiri, N., Singh, S.K., Kowalchyk, M., Marchant, A., Mills, S., Sandberg, G., Bennett, M.J., and Estelle, M. (2006). AXR4 is required for localization of the auxin influx facilitator AUX1. *Science* **312,** 1218-1220.

Dhonukshe, P., Aniento, F., Hwang, I., Robinson, D.G., Mravec, J. Stierhof, Y. and Friml, J. (2007). Clathrin-mediated constitutive endocytosis of PIN axuin efflux carriers in Arabidopsis. *Curr Biol* **17,** 520-527.

Doebley, J., Stec, A., and Hubbard, L. (1997). The evolution of apical dominance in maize. *Nature* **386,** 485-488.

Doebley, J., Adrian Stec, Beth Kent. (1995). *Suppressor of Sessile spikelets 1 (Sos1)*: a dominant mutant affecting inflorescence development in maize. *Am J Bot* **82,** 571-577.

Friml, J., and Palme, K. (2002). Polar auxin transport--old questions and new concepts? *Plant Mol Biol* **49,** 273-284.

Friml, J., Wisniewska, J., Benkova, E., Mendgen, K., and Palme, K. (2002a). Lateral relocation of auxin efflux regulator PIN3 mediates tropism in Arabidopsis. *Nature* **415,** 806-809.

Friml, J., Vieten, A., Sauer, M., Weijers, D., Schwarz, H., Hamann, T., Offringa, R., and Jurgens, G. (2003). Efflux-dependent auxin gradients establish the apical-basal axis of Arabidopsis. *Nature* **426,** 147-153.

Friml, J., Benkova, E., Blilou, I., Wisniewska, J., Hamann, T., Ljung, K., Woody, S., Sandberg, G., Scheres, B., Jurgens, G., and Palme, K. (2002b). AtPIN4 mediates sink-driven auxin gradients and root patterning in Arabidopsis. *Cell* **108,** 661-673.

Friml, J., Yang, X., Michniewicz, M., Weijers, D., Quint, A., Tietz, O., Benjamins, R., Ouwerkerk, P.B., Ljung, K., Sandberg, G., Hooykaas, P.J., Palme, K., and Offringa, R. (2004). A PINOID-dependent binary switch in apical-basal PIN polar targeting directs auxin efflux. *Science* **306,** 862-865.

Furutani, M., Kajiwara, T., Kato, T., Treml, B.S., Stockum, C., Torres-Ruiz, R.A., and Tasaka, M. (2007). The gene *MACCHI-BOU 4/ENHANCER OF PINOID* encodes a NPH3-like protein and reveals similarities between organogenesis and phototropism at the molecular level. *Development* **134,** 3849-3859.

Gallavotti, A., Zhao, Q., Kyozuka, J., Meeley, R.B., Ritter, M.K., Doebley, J.F., Pe, M.E., and Schmidt, R.J. (2004). The role of *barren stalk1* in the architecture of maize. *Nature* **432,** 630-635.

Galweiler, L., Guan, C., Muller, A., Wisman, E., Mendgen, K., Yephremov, A., and Palme, K. (1998). Regulation of polar auxin transport by AtPIN1 in Arabidopsis vascular tissue. *Science* **282,** 2226-2230.

Garbers, C., DeLong, A., Deruere, J., Bernasconi, P., and Soll, D. (1996). A mutation in *protein phosphatase 2A* regulatory subunit A affects auxin transport in Arabidopsis. *Embo Journal* **15,** 2115-2124.

Geldner, N., Friml, J., Stierhof, Y.D., Jurgens, G., and Palme, K. (2001). Auxin transport inhibitors block *PIN1* cycling and vesicle trafficking. *Nature* **413,** 425-428.

Geldner, N., Anders, N., Wolters, H., Keicher, J., Kornberger, W., Muller, P., Delbarre, A., Ueda, T., Nakano, A., and Jurgens, G. (2003). The Arabidopsis GNOM ARF-GEF mediates endosomal recycling, auxin transport, and auxin-dependent plant growth. *Cell* **112,** 219-230.

Hamann, T., Mayer, U., and Jurgens, G. (1999). The auxin-insensitive *bodenlos* mutation affects primary root formation and apical-basal patterning in the Arabidopsis embryo. *Development* **126,** 1387-1395.

Hamann, T., Benkova, E., Baurle, I., Kientz, M., and Jurgens, G. (2002). The Arabidopsis *BODENLOS* gene encodes an auxin response protein inhibiting *MONOPTEROS*-mediated embryo patterning. *Genes Dev* **16,** 1610-1615.

Hobbie, L.J. (2006). Auxin and cell polarity: the emergence of AXR4. *Trends Plant Sci* **11,** 517-518.

Hochstrasser, M. (1996). Ubiquitin-dependant protein degradation. *Annu Rev Genet.* **30,** 405-469.

Huala, E.S., I. M. (1992). *LEAFY* interacts with floral homeotic genes to regulate Arabidopsis floral development. *Plant Cell* **4,** 901-913.

Hubbard, L., McSteen, P., Doebley, J., and Hake, S. (2002). Expression patterns and mutant phenotype of *teosinte branched1* correlate with growth suppression in maize and teosinte. *Genetics* **162,** 1927-1935.

Irish, E.E. (1997). Experimental Analysis of Tassel Development in the Maize Mutant *Tassel Seed 6*. *Plant Physiol* **114,** 817-825.

Irish, E.E., and Nelson, T. M. (1993). Development of *tasselseed2* inflorescneces in maize. *Am J Bot* **80,** 292–299.

Jackson, D., Veit, B., and Hake, S. (1994). Expression of maize *KNOTTED1* related homeobox genes in the shoot apical meristem predicts patterns of morphogenesis in the vegetative shoot. *Development* **120,** 405–413.

Jacobs, M.G.S. (1983). Basal localization of the presumptive auxin transport carrier in pea stem cells. *Science* **220,** 1297-1300.

Jaillais, Y., Fobis-Loisy, I., Miege, C., Rollin, C., and Gaude, T. (2006). AtSNX1 defines an endosome for auxin-carrier trafficking in Arabidopsis. *Nature* **443,** 106-109.

Jaillais, Y., Santambrogio, M., Rozier F., Fobis-Loisy, I., Miege, C. adn Gaude T. (2007). the retromer protein VPS29 links cell polarity and organ initiation in plants. *Cell* **130,** 1057-1070.

Jeong, S., Trotochaud, A.E., and Clark, S.E. (1999). The Arabidopsis *CLAVATA2* gene encodes a receptor-like protein required for the stability of the *CLAVATA1* receptor-like kinase. *Plant Cell* **11,** 1925-1934.

Kaplinsky, N.J., and Freeling, M. (2003). Combinatorial control of meristem identity in maize inflorescences. *Development* **130,** 1149-1158.

Katekar, F. G. and Geissler, A.E. (1980). Auxin transport inhibitors. *Plant Physiol* **66,** 1190-1195.

Katekar, G. F., Nave, J.F. AND Geissler, A.E. (1981). Phytotropins. *Plant Physiol* **68,** 1460-1464.

Keitt, G.W., and Baker, R.A. (1966). Auxin Activity of Substituted Benzoic Acids and Their Effect on Polar Auxin Transport. *Plant Physiol* **41,** 1561-1569.

Kendrew, S.G. (2001). *YUCCA*: a flavin monooxygenase in auxin biosynthesis. *Trends Biochem Sci* **26,** 218.

Kepinski, S. and Leyser, O. (2005). The Arabidopsis F-box protein TIR1 is an auxin receptor. *Nature* **435,** 446-451.

Kepinski, S. and Leyser, O. (2005). Plant development: auxin in loops. *Curr Biol* **15,** R208-210.

Kerstetter, R., Vollbrecht, E., Lowe, B., Veit, B., Yamaguchi, J., and Hake, S. (1994). Sequence analysis and expression patterns divide the maize *knotted1*-like homeobox genes into two classes. *Plant Cell* **6,** 1877-1887.

Kerstetter, R.A., Laudencia-Chingcuanco, D., Smith, L.G., and Hake, S. (1997). Loss-of-function mutations in the maize homeobox gene, *knotted1*, are defective in shoot meristem maintenance. *Development* **124,** 3045-3054.

Kleine-Vehn, J., Dhonukshe, P., Swarup, R., Bennett, M., and Friml, J. (2006). Subcellular trafficking of the Arabidopsis auxin influx carrier AUX1 uses a novel pathway distinct from PIN1. *Plant Cell* **18,** 3171-3181.

Komatsu, K., Maekawa, M., Ujiie, S., Satake, Y., Furutani, I., Okamoto, H., Shimamoto, K., and Kyozuka, J. (2003a). *LAX* and *SPA*: major regulators of shoot branching in rice. *Proc Natl Acad Sci U S A* **100,** 11765-11770.

Komatsu, M., Chujo, A., Nagato, Y., Shimamoto, K., and Kyozuka, J. (2003b). *FRIZZY PANICLE* is required to prevent the formation of axillary meristems and to establish floral meristem identity in rice spikelets. *Development* **130,** 3841–3850.

Kyozuka, J., Konishi, S., Nemoto, K., Izawa, T., and Shimamoto, K. (1998). Down-regulation of *RFL*, the *FLO/LFY* homolog of rice, accompanied with panicle branch initiation. *Proc Natl Acad Sci U S A* **95,** 1979-1982.

Laudencia-Chingcuanco, D., and Hake, S. (2002). The *indeterminate floral apex1* gene regulates meristem determinacy and identity in the maize inflorescence. *Development* **129,** 2629-2638.

Leyser, O. (2002). Molecular genetics of auxin signaling. *Annu Rev Plant Biol* **53,** 377-398.

Leyser, O. (2005). Auxin distribution and plant pattern formation: how many angels can dance on the point of PIN? *Cell* **121,** 819-822.

Li, J., Yang, H., Ann Peer, W., Richter, G., Blakeslee, J., Bandyopadhyay, A., Titapiwantakun, B., Undurraga, S., Khodakovskaya, M., Richards, E.L., Krizek, B., Murphy, A.S., Gilroy, S., and Gaxiola, R. (2005). Arabidopsis H+-PPase AVP1 regulates auxin-mediated organ development. *Science* **310,** 121-125.

Lomax, T., Mehlhorn RJ, and WR., B. (1985). Active auxin uptake by zucchini vesicles: quantitation using ESR volume and pH determinations. *Proc Natl Acad Sci U S A* **82,** 6541-6545.

Long, J., Moan, E. I., Medford, J. I. and Barton, K. M. (1996). A member of the KNOTTED class of homeodomain proteins encoded by *STM* gene of Arabidopsis. *Nature* **379,** 66–69.

Malenica, N., Abas, L., Benjamins, R., Kitakura, S., Sigmund, H.F., Jun, K.S., Hauser, M.T., Friml, J., and Luschnig, C. (2007). *MODULATOR OF PIN* genes control steady-state levels of Arabidopsis PIN proteins. *Plant J* **51,** 537-550.

Marchant, A., Kargul J., May S., Muller P., Delbarre A., Perrot-Rechenmann C., and M., a.B. (1999). *AUX1* regulate root gravitropism in Arabidopsis by facilitating auxin uptake within root apical tissues. *Embo J* **18,** 2066-2073.

McSteen, P., and Hake, S. (2001). *barren inflorescence2* regulates axillary meristem development in the maize inflorescence. *Development* **128,** 2881-2891.

McSteen, P., Malcomber, S., Skirpan, A., Lunde, C., Wu, X., Kellogg, E., and Hake, S. (2007). *barren inflorescence2* Encodes a co-ortholog of the *PINOID* serine/threonine kinase and is required for organogenesis during inflorescence and vegetative development in maize. *Plant Physiol* **144,** 1000-1011.

McSteen, P. and Leyser, O. (2005). Shoot branching. *Annual review of plant biology* **56,** 353−374.

Michniewicz, M., Zago, M.K., Abas, L., Weijers, D., Schweighofer, A., Meskiene, I., Heisler, M.G., Ohno, C., Zhang, J., Huang, F., Schwab, R., Weigel, D., Meyerowitz, E.M., Luschnig, C., Offringa, R., and Friml, J. (2007). Antagonistic regulation of PIN phosphorylation by *PP2A* and *PINOID* directs auxin flux. *Cell* **130,** 1044-1056.

Mlotshwa, S., Yang, Z., Kim, Y., and Chen, X. (2006). Floral patterning defects induced by Arabidopsis *APETALA2* and microRNA172 expression in *Nicotiana benthamiana*. *Plant Mol Biol* **61,** 781-793.

Morita, Y., and Kyozuka, J. (2007). Characterization of *OsPID*, the rice ortholog of *PINOID*, and its possible involvement in the control of polar auxin transport. *Plant Cell Physiol* **48,** 540-549.

Muday, G.K., and DeLong, A. (2001). Polar auxin transport: controlling where and how much. *Trends Plant Sci* **6,** 535-542.

Mukherjee, S., Ghosh, R.N., and and Maxfield, F.R. (1997). Endocytosis. *Physiol Rev.* **77,** 759-803.

Muller, A., Guan, C., Galweiler, L., Tanzler, P., Huijser, P., Marchant, A., Parry, G., Bennett, M., Wisman, E., and Palme, K. (1998). *AtPIN2* defines a locus of Arabidopsis for root gravitropism control. *Embo J* **17,** 6903-6911.

Multani, D.S., Briggs, S.P., Chamberlin, M.A., Blakeslee, J.J., Murphy, A.S., and Johal, G.S. (2003). Loss of an MDR transporter in compact stalks of maize *br2* and sorghum *dw3* mutants. *Science* **302,** 81-84.

Murphy, A.S., Hoogner, K.R., Peer, W.A., and Taiz, L. (2002). Identification, purification, and molecular cloning of N-1-naphthylphthalmic acid-binding plasma membrane-associated aminopeptidases from Arabidopsis. *Plant Physiol* **128,** 935-950.

Nardmann, J., Ji, J., Werr, W., and Scanlon, M.J. (2004). The maize duplicate genes *narrow sheath1* and *narrow sheath2* encode a conserved homeobox gene function in a lateral domain of shoot apical meristems. *Development* **131,** 2827-2839.

Noh, B., Bandyopadhyay, A., Peer, W.A., Spalding, E.P., and Murphy, A.S. (2003). Enhanced gravi- and phototropism in plant *mdr* mutants mislocalizing the auxin efflux protein PIN1. *Nature* **423,** 999-1002.

Okada, K., Ueda, J., Komaki, M.K., Bell, C.J., and Shimura, Y. (1991). Requirement of the auxin polar transport system in early stages of arabidopsis floral bud formation. *Plant Cell* **3,** 677-684.

Paciorek, T., Zazimalova, E., Ruthardt, N., Petrasek, J., Tstierhof, Y., Kleine-Vehn, J., Morris, D.A., Emans, N., Jurgens, G., Geldner, N., and and Friml, J. (2005). Auxin inhibits endocytosis and promotes its own efflux from cells. *Nature* **435,** 1251-1256.

Paponov, I.A., Teale, W.D., Trebar, M., Blilou, I., and and Palme, K. (2005). The *PIN* auxin efflux facilitators: evolutionary and functional perspectives. *Trends Plant Sci* **10,** 170-177.

Parry, G., Marchant A, May S., Swarup R., Swarup K., James N., Granham N., Allen T., Martucci T., Yemm, A., Napier R., Manning K., King G., and M., a.B. (2001). Quick on the uptake: characterization of a family of plant auxin influx carriers. *J Plant Growth Regul* **20,** 217-225.

Parry, G. and Estelle, M. (2006). Auxin receptors: a new role for F-box proteins. *Curr Opin Cell Biol* **18,** 152-156.

Peer, W.A., Bandyopadhyay, A., Blakeslee, J.J., Makam, S.N., Chen, R.J., Masson, P.H., and Murphy, A.S. (2004). Variation in expression and protein localization of the *PIN* family of auxin efflux facilitator proteins in flavonoid mutants with altered auxin transport in Arabidopsis thaliana. *Plant Cell* **16,** 1898-1911.

Peer, W.A., and Murphy, A.S. (2007). Flavonoids and auxin transport: modulators or regulators? *Trends Plant Sci* **12,** 556-563.

Petrasek, J., Mravec, J., Bouchard, R., Blakeslee, J.J., Abas, M., Seifertova, D., Wisniewska, J., Tadele, Z., Kubes, M., Covanova, M., Dhonukshe, P., Skupa, P., Benkova, E., Perry, L., Krecek, P., Lee, O.R., Fink, G.R., Geisler, M., Murphy, A.S., Luschnig, C., Zazimalova, E., and Friml, J. (2006). PIN proteins perform a rate-limiting function in cellular auxin efflux. *Science* **312,** 914-918.

Reinhardt, D., Pesce, E.R., Stieger, P., Mandel, T., Baltensperger, K., Bennett, M., Traas, J., Friml, J., and Kuhlemeier, C. (2003). Regulation of phyllotaxis by polar auxin transport. *Nature* **426,** 255-260.

Ritter, M.K., Padilla, Christopher M. and Schmidt, Robert J. (2002). The maize mutant *barren stalk1* is defective in axillary meristem development. *Am J Bot* **89,** 203-210.

Robinson, J.S., Albert, A.C., and Morris, D.A. (1999). Differential effects of brefeldin A and cycloheximide on the activity of auxin efflux carriers in *Cucurbita pepo L.* *Journal of Plant Physiology* **155,** 678-684.

Sabater, M., and Rubery, P. (1987). Auxin carriers in cucurbita vesicles. imposed perturbations of transmembrane pH and electrical potential gradients cahracterized by radioactive probes. *Planta* **171,** 501-506.

Satoh-Nagasawa, N., Nagasawa, N., Malcomber, S., Sakai, H., and Jackson, D. (2006). A trehalose metabolic enzyme controls inflorescence architecture in maize. *Nature* **441,** 227-230.

Scanlon, M.J. (2000). *NARROW SHEATH1* functions from two meristematic foci during founder-cell recruitment in maize leaf development. *Development* **127,** 4573-4585.

Schoof, H., Lenhard, M., Haecker, A., Mayer, K.F., Jurgens, G., and Laux, T. (2000). The stem cell population of Arabidopsis shoot meristems in maintained by a regulatory loop between the *CLAVATA* and *WUSCHEL* genes. *Cell* **100,** 635-644.

Steinmann, T., Geldner, N., Grebe, M., Mangold, S., Jackson, C.L., Paris, S., Galweiler, L., Palme, K., and Jurgens, G. (1999). Coordinated polar localization of auxin efflux carrier PIN1 by GNOM ARF GEF. *Science* **286,** 316-318.

Stepanova, A.N., Robertson-Hoyt, J., Yun, J., Benavente, L.M., Xie, D.Y., Dolezal, K., Schlereth, A., Jurgens, G., and Alonso, J.M. (2008). TAA1-mediated auxin biosynthesis is essential for hormone crosstalk and plant development. *Cell* **133,** 177-191.

Swarup, R., Friml, J., Marchant, A., Ljung, K., Sandberg, G., Palme, K., and Bennett, M. (2001). Localization of the auxin permease AUX1 suggests two functionally distinct hormone transport pathways operate in the Arabidopsis root apex. *Genes Dev* **15,** 2648-2653.

Taguchi-Shiobara, F., Yuan, Z., Hake, S., and Jackson, D. (2001). The *fasciated ear2* gene encodes a leucine-rich repeat receptor-like protein that regulates shoot meristem proliferation in maize. *Genes Dev* **15,** 2755-2766.

Tanaka, H., Dhonukshe, P., Brewer, P.B., and Friml, J. (2006). Spatiotemporal asymmetric auxin distribution: a means to coordinate plant development. *Cell Mol Life Sci* **63,** 2738-2754.

Teh, O.K., and Moore, I. (2007). An ARF-GEF acting at the Golgi and in selective endocytosis in polarized plant cells. *Nature* **448,** 493-496.

Treml, B.S., Winderl, S., Radykewicz, R., Herz, M., Schweizer, G., Hutzler, P., Glawischnig, E., and Ruiz, R.A. (2005). The gene *ENHANCER OF PINOID* controls cotyledon development in the Arabidopsis embryo. *Development* **132,** 4063-4074.

Trotochaud, A.E., Jeong, S., and Clark, S.E. (2000). CLAVATA3, a multimeric ligand for the CLAVATA1 receptor-kinase. *Science* **289,** 613-617.

Veit, B., Schmidt, R.J., Hake, S., and Yanofsky, M.F. (1993). Maize floral development: new genes and old mutants. *Plant Cell* **5,** 1205-1215.

Vollbrecht, E., Reiser, L., and Hake, S. (2000). Shoot meristem size is dependent on inbred background and presence of the maize homeobox gene, *knotted1*. *Development* **127,** 3161-3172.

Vollbrecht, E., Springer, P.S., Goh, L., Buckler, E.S.t., and Martienssen, R. (2005). Architecture of floral branch systems in maize and related grasses. *Nature* **436,** 1119-1126.

Wakatsuki, T., Schwab, B., Thompson, NC. and Elson, EL. (2001). Effects of cytochalasin D adn latrunculin B on mechanical properties of cells. J Cell Sci **114,** 1025-1036.

Weijers, D., and Jurgens, G. (2005). Auxin and embryo axis formation: the ends in sight? *Curr Opin Plant Biol* **8,** 32-37.

Wisniewska, J., Xu, J., Seifertova, D., Brewer, P.B., Ruzicka, K., Blilou, I., Rouquie, D., Benkova, E., Scheres, B., and Friml, J. (2006). Polar PIN localization directs auxin flow in plants. *Science* **312,** 883.

Yamamoto, Y., Kamiya, N., Morinaka, Y., Matsuoka, M., and Sazuka, T. (2007). Auxin biosynthesis by the *YUCCA* genes in rice. *Plant Physiol* **143,** 1362-1371.

Yang, Y., Hammes, U.Z., Taylor, C.G., Schachtman, D.P., and Nielsen, E. (2006). High-affinity auxin transport by the AUX1 influx carrier protein. *Curr Biol* **16,** 1123-1127.

Yang, Y., Hammes U., Taylor C., Schachtman D., and Nielsen E. (2006). High-affinity auxin tansport by the AUX1 influx carrier protein. *Curr Biol* **16,** 1123-1127.

Zazimalova, E., Krecek, P., Skupa, P., Hoyerova, K., and Petrasek, J. (2007). Polar transport of the plant hormone auxin - the role of PIN-FORMED (PIN) proteins. *Cell Mol Life Sci* **64,** 1621-1637.

Zegzouti, H., Anthony, R.G., Jahchan, N., Bogre, L., and Christensen, S.K. (2006a). Phosphorylation and activation of PINOID by the phospholipid signaling kinase 3-phosphoinositide-dependent protein kinase 1 (PDK1) in Arabidopsis. *Proc Natl Acad Sci U S A* **103,** 6404-6409.

Zegzouti, H., Li, W., Lorenz, T.C., Xie, M., Payne, C.T., Smith, K., Glenny, S., Payne, G.S., and Christensen, S.K. (2006b). Structural and functional insights into the regulation of Arabidopsis AGC VIIIa kinases. *J Biol Chem* **281,** 35520-35530.

Zhao, Y., Christensen, S.K., Fankhauser, C., Cashman, J.R., Cohen, J.D., Weigel, D., and Chory, J. (2001). A role for flavin monooxygenase-like enzymes in auxin biosynthesis. *Science* **291,** 306-309.

Zhao, Y., Hull, A.K., Gupta, N.R., Goss, K.A., Alonso, J., Ecker, J.R., Normanly, J., Chory, J., and Celenza, J.L. (2002). Trp-dependent auxin biosynthesis in Arabidopsis: involvement of cytochrome P450s CYP79B2 and CYP79B3. *Genes Dev* **16,** 3100-3112.

CHAPTER TWO

The Role of Auxin Transport During Inflorescence Development in Maize, *ZEA MAYS* (*POACEAE*)

This chapter has been published in 2007.

Xianting Wu and Paula McSteen, (2007), The role of auxin transport during inflorescence development in maize (*ZEA MAYS, POACEAE*), *Am. J. B.* 94 (11): 1745-1755

2.1 Abstract

Axillary meristems play a fundamental role in inflorescence architecture. Maize (*Zea mays*) inflorescences are highly branched panicles due to the production of multiple types of axillary meristem. We use auxin transport inhibitors to show that auxin transport is required for axillary meristem initiation in the maize inflorescence. The phenotype of auxin transport inhibited plants is very similar to *barren inflorescence2* (*bif2*) and *barren stalk1* (*ba1*) mutants implying that they function in the same pathway. To dissect this pathway, we performed RNA in situ hybridization in auxin transport inhibited plants. We determined that *bif2* is expressed upstream and that *ba1* is expressed downstream of auxin transport enabling us to integrate the genetic and hormonal control of axillary meristem initiation. Furthermore, we found that treatment of maize inflorescences with auxin transport inhibitors, later in development, results in the production of single instead of paired spikelets. Paired spikelets are a key feature of the Andropogoneae, a group of over 1000 grasses that includes maize, sorghum and sugarcane. As all other grasses bear spikelets singly, these results implicate auxin transport in the evolution of inflorescence architecture. Furthermore, our results provide insights into mechanisms of inflorescence branching that are relevant to all plants.

Keywords

Auxin transport; axillary meristem; *barren inflorescence*; branch; maize; spikelet; *Zea mays*

2.2 Introduction

Development of higher plants is regulated by meristems (Steeves and Sussex, 1989). Meristems have two main functions; organogenesis, whereby organs are produced in the peripheral zone, and maintenance, whereby further growth is supported by the central zone (McSteen and Hake, 1998; Williams and Fletcher, 2005). The shoot apical meristem reiteratively produces modular units called phytomers, consisting of a leaf, axillary meristem, node and internode (Steeves and Sussex, 1989; McSteen and Leyser, 2005). During vegetative development in many plants such as Arabidopsis (*Arabidopsis thaliana*), the leaf is prominent while the axillary meristem either remains dormant or grows out to become a branch. After the transition to reproductive growth, the axillary meristem becomes prominent and produces flowers, while the subtending leaf, called a bract, is often reduced (Long and Barton, 2000; Grbic, 2005). The use of polar auxin transport inhibitors, such as N-1-naphthylphthalamic acid (NPA), has shown that auxin transport is required for initiation of leaves during vegetative development and flowers during reproductive development (Okada et al., 1991; Reinhardt et al., 2000; Reinhardt et al., 2003; Scanlon, 2003).

The role of auxin transport in organogenesis has also been shown by modeling and genetic studies. Auxin is transported towards primordia as they initiate, causing the primordia to become auxin sinks and preventing other organs from forming close by (Benkova et al., 2003; Reinhardt et al., 2003; Swarup et al., 2005; de Reuille et al., 2006; Jonsson et al., 2006; Smith et al., 2006). Mutations in the auxin efflux carrier, *PINFORMED1 (PIN1)* in Arabidopsis, fail to initiate floral meristems in the inflorescence (Okada et al., 1991; Galweiler et al., 1998; Petrasek et al., 2006). Mutations in *PINOID* (*PID*), a serine/ threonine protein kinase proposed to regulate auxin transport, have a very similar phenotype to *pin1* mutants (Bennett et al., 1995; Christensen et al., 2000; Benjamins et al., 2001; Friml et al., 2004; Lee and Cho, 2006). Therefore, regulated auxin transport is required for floral meristem initiation in Arabidopsis (Cheng and Zhao, 2007).

Unlike Arabidopsis, which has a raceme type of inflorescence, maize (*Zea mays*) inflorescences are branched panicles. Maize inflorescences are highly branched due to the production of multiple types of axillary meristem (Fig. 1) (Irish, 1997; McSteen et al.,

2000; Bommert et al., 2005; Kellogg, 2007). The male inflorescence, the tassel, forms at the apex of the plant and the female inflorescence, the ear, is produced from an axillary meristem a few nodes below the tassel. Long branches form at the base of the tassel and short branches called spikelet pairs cover the long branches and the main spike (Fig. 1A). Each spikelet consists of a pair of leaf-like glumes that enclose a pair of florets. The spikelet is the fundamental unit of all grass inflorescences (Clifford, 1987). Paired spikelets, however, are a defining character of the Andropogoneae, a group of 1000 grasses that includes maize, sorghum and sugarcane (Kellogg, 2000; G.P.W.G., 2001). Other grasses, outside the Andropogoneae, such as rice and barley have single spikelets (Shimamoto and Kyozuka, 2002; Bommert et al., 2005). Therefore, regulation of the determinacy of axillary meristems that give rise to branches and spikelets has played an important role in the evolution of inflorescence architecture in the grasses (McSteen, 2006; Kellogg, 2007). However, the production of multiple orders of axillary meristem before producing floral meristems is not restricted to the grasses, and is also found in eudicots with panicle or compound umbel inflorescence architecture (Borthwick et al., 1931; Manning, 1938; Tucker, 1989; Prusinkiewicz et al., 2007).

Four types of axillary meristem are initiated during inflorescence development in maize (Cheng et al., 1983; Irish, 1997; McSteen et al., 2000). In hierarchical order, they are branch meristem (BM), spikelet pair meristem (SPM), spikelet meristem (SM) and floral meristem (FM) (Fig. 1D). First, the inflorescence meristem produces a few primary axillary meristems, BMs, which become the long branches at the base of tassel (Fig. 1B). Then, the inflorescence meristem (and the branches) produce many additional primary axillary meristems called SPMs (Fig. 1B). Each of the SPMs gives rise to two secondary axillary meristems, the SMs (Fig. 1C). Each SM produces two leaf-like glumes enclosing two tertiary axillary meristems, the FMs (Fig. 1D). Finally, each FM initiates the floral organs. The early development of the tassel and ear are very similar except that ears do not produce BMs. The mechanism by which the SPMs produce the SMs and the SMs produce the FMs is unknown (McSteen and Leyser, 2005). Two alternative models for inflorescence branching have been proposed (Irish, 1997; Chuck et al., 1998; Irish, 1998). In the lateral branching model, it is proposed that the SPM gives rise to the two SMs by lateral branching leaving a residual SPM between the two SMs

(Chuck et al., 1998). In the conversion model, it is proposed that the SPM initiates the first SM by lateral branching and produces the second SM by a meristem conversion event (Irish, 1997, 1998). Despite the recent cloning of several meristem identity genes, this controversy remains unresolved (Chuck et al., 2002; Vollbrecht et al., 2005; Bortiri et al., 2006; Chuck et al., 2007).

A large class of mutants have been identified that fail to produce axillary meristems in maize (McSteen et al., 2000). Two of these mutants, *barren inflorescence2* (*bif2)* and *barren stalk1* (*ba1*), have been cloned and have been shown to be required for the initiation of axillary meristems in the inflorescence (Gallavotti et al., 2004; McSteen et al., 2007). Both mutants fail to produce ear shoots, branches, spikelets, florets and floral organs, all of which arise from axillary meristems (McSteen and Hake, 2001; Ritter et al., 2002). *bif2* encodes a co-ortholog of PID which regulates auxin transport in Arabidopsis (McSteen et al., 2007). There is evidence that BIF2 may regulate auxin transport in maize (Carraro et al., 2006; McSteen et al., 2007) and the rice ortholog, *OsPID,* may regulate auxin transport in rice (Morita and Kyozuka, 2007). *ba1* encodes an atypical bHLH transcription factor that is not present in Arabidopsis (Gallavotti et al., 2004). Overexpression of the rice ortholog of *ba1*, *lax panicle1*, causes defects indicative of a role in auxin action (Kyozuka et al., 2002; Komatsu et al., 2003). Therefore, auxin transport may also play a role in axillary meristem initiation in the inflorescence of maize and rice, though this has not yet been shown directly.

To determine if auxin transport is required for axillary meristem initiation during maize inflorescence development, we treated normal plants with different concentrations of NPA at multiple stages of inflorescence development. Scanning electron microscopy (SEM) analysis and RNA in situ hybridization using *kn1* as a marker for meristems showed that auxin transport is required for axillary meristem initiation, irrespective of meristem identity. We then utilized these auxin transport inhibited plants, to dissect the auxin transport pathway by testing the expression of *bif2* and *ba1* by RNA in situ hybridization. Although *bif2* mutants have a very similar phenotype as NPA treated plants, *bif2* is expressed in inflorescences of NPA treated plants. This suggest that *bif2* is expressed upstream of auxin transport. However, *ba1* was not expressed after NPA treatment indicating that *ba1* expression is dependent on polar auxin transport. This

analysis provided insight into the genetic and hormonal regulation of axillary meristem initiation in maize. Furthermore, the effects of NPA on spikelet initiation resolve the controversy over the mechanism of inflorescence branching in maize and provide insight into the mechanism of inflorescence branching in all plants.

2.3 Methods and Materials

2.3.1 Plant Growth Conditions

Maize (*Zea mays*) B73 seeds were planted in 4″ pots containing Scotts Metromix 360 soil (Griffin Greenhouse, Morgantown, PA, USA). Plants were grown in the greenhouse with supplemental lighting during winter/spring. Inflorescence meristems were dissected and observed with the stereomicroscope to determine the developmental stage. We used three developmental stages: (1) When the apical meristem was transitioning to inflorescence development (Fig. 2A) which occurred after about four weeks of growth when the inflorescences were about 1-2 mm tall, (2) When branch meristems were initiating (Fig. 2F) which occurred after about five weeks of growth when the inflorescences were 3-5 mm tall, and (3) when spikelet pair meristems were initiating which occurred after about six weeks of growth when the inflorescences were about 5-7 mm tall (Fig. 2K).

2.3.2 Polar Auxin Transport Inhibition

Plants were grown until the required developmental stages were visible when representative inflorescence meristems were dissected under the stereomicroscope. 15-20 plants were used for each stage and each concentration of treatment. Plants from each stage were watered for two weeks with NPA (ChemService, West Chester, PA. USA), dissolved in dimethyl sulfoxide (DMSO, Sigma-Aldrich, St. Louis, MO, USA) and then diluted with tap water to the appropriate concentration. Control plants were watered with tap water containing an equal amount of DMSO. All plants were watered with 150 ml solution every day at 10 a.m. This experiment was repeated three times for 100μM NPA, twice for 40μM, 80μM and 120μM NPA and once for 10μM and 20μM NPA. To test the effects of other auxin transport inhibitors, Hydroxyfluorene-9-carboxylic acid (HFCA, Sigma-Aldrich, St. Louis, MO, USA) and 2,3,5-Triiodobenzoic acid (TIBA, Sigma-Aldrich, St. Louis, MO, USA) were dissolved in DMSO and diluted with tapwater to 20μM, 40μM and 80μM. After two weeks treatment, inflorescence meristems were dissected, fixed in FAA (3.5% formalin, 50% ethanol, 5% acetic acid), dehydrated in a graded ethanol series and stored in 100% ethanol at 4^{o}C.

Cautionary note: A trace amount of β - NPA contaminates NPA during commercial production (A. Murphy, personal communication). β - NPA is potentially hydrolyzed by aminopeptidases within the plant to β - naphthylamine which is a carcinogen (Reznikoff et al., 1993; Murphy and Taiz, 1999). Therefore, plant tissues treated with NPA must be treated as potentially hazardous.

2.3.3 Scanning Electron Microscopy (SEM)

Meristems from each treatment were critical point dried with liquid CO_2 (BAL-TEC CPD 030), sputter coated with Au-Pd (BAL-TEC SCD 050) and viewed at 20 kV accelerating voltage by SEM (JEOL JSM5400).

2.3.4 RNA *in situ* Hybridization

After fixing and dehydration, inflorescence meristems were embedded in paraffin wax (Paraplast, Oxford Labware, St. Louis, MO, USA). 8 μm thick sections were cut with a Finesse Paraffin Microtome and mounted on slides (Probe-on plus, Thermo Fisher, Waltham, MA, USA). The *kn1* and *bif2* probes were previously described (Jackson et al., 1994; McSteen et al., 2007). The *ba1* probe was generated by PCR from genomic DNA (primer 1: 5′ - GAT GCA GCA CGA GGA AGG ATG CCA T - 3′, primer 2: 5′ - ATA CGG TGT ATC ATC TGC GAT CAG CGG A - 3′). This 524 bp sequence from the 3' end of *ba1*, not including the bHLH domain, was sub cloned into the pGEM-TEasy vector (Promega, Madison, WI, USA). The plasmid was digested with *NdeI* to generate antisense probe with T7 RNA polymerase. RNA *in situ* hybridization was performed according to Jackson et al., (1994).

2.3.5 Histology

For histological analysis, 8 μm sections were treated with Histoclear (National Diagnostics, Atlanta, GA, USA) to remove wax, and hydrated through an ethanol series. Sections were then stained in 0.05% Toluidine Blue O (TBO) for 30 seconds, dehydrated through an ethanol series, mounted using Histosolve and Histomount (Thermo Shandon, Waltham, MA, USA) and observed on the light microscope. The number of vascular bundles was counted and the data pooled from 40μM, 80μM, 100μM and 120μM NPA

treated meristems as there was no statistical difference in vascular bundle number between samples treated with different concentrations of NPA. Statistical analysis was performed using Minitab software (Minitab, State College, PA, USA).

2.4 Results

2.4.1 NPA Inhibits the Initiation of Axillary Meristems in the Inflorescence

To determine that auxin transport was required for axillary meristem initiation in maize we treated normal plants with NPA by watering them every day for two weeks. Control plants were mock treated with water containing a small amount of the solvent used to dissolve NPA (Fig. 2B,G,L). Three days after treatment the roots became agravitropic indicating that the NPA was effective and had similar effects on root development as seen in other species (Rashotte et al., 2000) (Supplemental Fig. S1). Two weeks of treatment was required for sufficient growth and development to have occurred to see the effect in the inflorescence. After two weeks, inflorescences were dissected, fixed and viewed by SEM. As development proceeds in a defined spatial and temporal order, the effect of NPA on different axillary meristems types could be investigated by starting the treatment at different times and hence different stages of development (Fig. 2A,F,K). As development proceeds, younger meristems are located closer to the tip of the inflorescence and older meristems towards the base.

Upon the transition to reproductive development, the shoot apical meristem stops initiating leaves and elongates to form the transition stage inflorescence meristem (Fig. 2A) (Cheng et al., 1983; McSteen et al., 2000). This transition occurred after four weeks of growth in our greenhouse conditions. A few days later, branch meristems (BMs) became visible at the base of the inflorescence (Fig. 2F). As the main rachis and branches elongated, bract primordia became visible (Fig. 2K). After more than five weeks of growth, spikelet pair meristems (SPMs) arose in the axils of bract primordia which were suppressed (Fig. 2B,G,K).

To determine that auxin transport was required for primary axillary meristem initiation (BM and SPM), plants that were at the transition stage of inflorescence development (Fig. 2A, four weeks old) were treated with NPA for two weeks. In contrast to untreated controls (Fig. 2B), BMs and SPMs did not develop on the flanks of the inflorescence after NPA treatment (Fig. 2C-E). However, the apical inflorescence meristem appeared to be unaffected by the treatment and continued to elongate. Inhibition of SPM initiation was also seen when plants that had already begun to initiate BMs (Fig. 2F, five weeks of age) were treated. In this case, inhibition of SPM initiation

was seen in the apical region of the inflorescence, where the youngest meristems would have initiated (Fig. 2H-J). If BMs had already initiated before the treatment took effect, then they continued to elongate but did not produce SPMs on their flanks (arrows in Fig. 2I,N,O). Occasionally, secondary branches formed at the base of the primary branches and similarly, they elongated without producing SPMs (Fig. 3C). Additionally, the surface of the inflorescence rachis was not completely smooth as ridges were visible (Fig. 2H-J). These ridges formed rings surrounding the inflorescence stem (close up shown in Fig. 3C,D). In conclusion, NPA inhibited the production of the first axillary meristems (BM or SPM) to be produced by the inflorescence but did not affect the elongation of the apical inflorescence meristem.

To determine the sensitivity of the inflorescence to NPA, plants were treated with different concentrations of NPA. Plants at the transition stage of inflorescence development (Fig. 2A), showed a threshold effect. NPA at 10μM concentration had no effect on axillary meristem initiation while 20μM had a weak effect (not shown). However, NPA at 40, 80 and 120μM had similar effects (Fig. 2C-E). A dose response was apparent when inflorescences that had already begun to initiate BMs (Fig. 2F), were treated with NPA (Fig. 2H-J). Approximately half of the apical region of the inflorescence had no SPMs in plants treated with 40μM NPA, (Fig. 2H); however, 80μM and 120μM NPA caused inhibition of SPM initiation in over two thirds of the apical region of the inflorescence (Fig. 2I,J). As NPA blocked the formation of BMs and SPMs in a concentration dependent manner we conclude that auxin transport is required for the formation of BMs and SPMs.

To determine if NPA blocked the initiation of BMs and SPMs or whether these meristems initiated and then aborted, we performed RNA in situ hybridization using *kn1* as a marker for meristems. In normal plants, *kn1* is expressed in the inflorescence meristem and all axillary meristems (Fig. 4A) (Jackson et al., 1994). The first indication of bract leaf initiation is the absence of *kn1* expression on the flanks of the inflorescence meristem (Fig. 4A, arrow). The first indication of BM and SPM initiation is in a few cells in the axil of the bract primordia that express *kn1* before a protrusion is visible (Fig. 4A). The expression of *kn1* then expands as the axillary meristem grows out (Fig. 4A). In the inflorescences of NPA treated plants, *kn1* was expressed in the apical inflorescence

meristem and in the stem and vasculature as normal (Fig. 4B). However, *kn1* was not expressed on the flanks of the inflorescence (Fig. 4B, arrow). These results indicate that NPA treatment does not inhibit the initiation of bract primordia and that the ridges visible after NPA treatment likely correspond to bract primordia. Furthermore, as no expression of *kn1* was visible on the flanks of the inflorescence meristem, we infer that BMs and SPMs do not initiate after NPA treatment and that auxin transport is required for the initiation of BMs and SPMs. These results are similar to the expression of *kn1* in *bif2* and *ba1* mutants in maize (McSteen and Hake, 2001; Ritter et al., 2002).

2.4.2 NPA Effects on Spikelet Initiation Provide Support for the Conversion Model of Inflorescence Branching

The effects of NPA on primary axillary meristems might have been predicted from results in Arabidopsis (Okada et al., 1991). However, the effects of NPA on secondary axillary meristems (SMs) depended on which of the models for inflorescence branching in maize was correct, and in fact afforded an opportunity to distinguish between these models. If the lateral branching model for inflorescence branching was correct, NPA treatment should inhibit SPMs from initiating both SMs leading to the production of arrested SPMs. However, if the conversion model was correct, then NPA treatment should inhibit the initiation of the first SM but might not inhibit the conversion from SPM to SM identity leading to the production of single spikelets. The identity of the meristem as an SM rather than SPM can be determined by its ability to produce glumes (Fig. 3A).

To distinguish between these models for inflorescence branching and to determine the effects of NPA on spikelet meristem (SM) initiation, plants in which SPMs had already begun to initiate (Fig. 2F,K) were treated with NPA. In control plants, the SPM produced two SMs, which give rise to the larger pedicellate spikelet and the smaller sessile spikelet (Fig. 3A). In support of the conversion model for inflorescence branching, NPA treated plants produced inflorescences with single instead of paired spikelets (Figs. 2H-J, 2M-O, 3B). If plants were treated at five weeks of age, single spikelets were found at the base of the inflorescence (Fig. 2H-J). If plants were treated at six weeks of age, single spikelets were produced towards the apex while the older spikelets at the base of

the inflorescence, which had presumably initiated before the treatment took effect, were still paired (Fig. 2M-O). Similarly, single spikelets were also observed near the tips of branches (Fig. 2M arrow). A dose response was apparent with increasing concentrations of NPA causing more SPMs to produce single SMs. Only the SMs near the tip of the apex were inhibited by 40µm NPA treatment (Fig. 2M). With 80µm NPA treatment, usually a third of the apical part of the inflorescence was affected, producing single spikelets (Fig. 2N). The most severe phenotype was seen when plants were treated with 120µM NPA, in some cases the entire inflorescence produced single spikelets (Fig. 2O). The production of single spikelets shows that although NPA inhibits the ability of the SPM to initiate an SM it does not inhibit the ability of the SPM to convert to SM identity as evidenced by the production of glumes.

In NPA treated inflorescences, spikelets that formed were borne on elongated pedicels similar to pedicellate spikelets (Fig. 3B). However, the SMs that formed were more elongated than normal (Fig. 3D). This was clearly evident in RNA in situ hybridization experiments using *kn1*. In control inflorescences, *kn1* was strongly expressed in SPMs and SMs (Fig. 4C). However, in the inflorescences of NPA treated plants, *kn1* expression was seen in SMs that were more elongated relative to normal (Fig. 4D). Therefore, although NPA inhibits the initiation of axillary meristems, it does not inhibit the growth of axillary meristems that have already formed.

2.4.3 NPA Causes Defects in Lateral Organ Development in the Inflorescence

In normal inflorescences, the first lateral organs to be produced by the SMs are the glumes (Cheng et al., 1983). First, an outer glume becomes visible on the pedicellate spikelet followed by the appearance of an outer glume on the sessile spikelet (Figs. 1C,3A). Then, an inner glume becomes visible on both the pedicellate and sessile spikelet (Fig. 3A). When spikelets formed in inflorescences treated with NPA (at 5 or 6 weeks old), they had several defects in glume development dependent on when NPA took effect. Occasionally, glumes did not appear to initiate when viewed by SEM (Fig. 3E,F arrows). Absence of glumes was visible on both single spikelets (Fig. 3E) and on the sessile SM of paired spikelets (Fig. 3F). However, as down regulation of *kn1* is visible on the flanks of elongated SMs (Fig. 4D), glumes may actually initiate but fail to grow

out. This inhibition of glume outgrowth was more apparent at increasing NPA concentrations (compare glume size on spikelets at the base of Fig. 2H-J). Commonly, glumes that formed had defects in organ separation. Frequently, the glumes formed a ring surrounding the SM as if there were defects in separation of the inner and outer glumes (Fig. 3D,H). Occasionally, the glumes of neighboring spikelets fused together (Fig. 3G). In older inflorescences, NPA treatment usually had no effect on floral organ development (Fig. 3I). In a few cases, however, there were defects in floral organ development, such as inhibition and fusion of organ primordia, similar to the effects of NPA on glume development (Fig. 3J). These results imply that continued auxin transport is required for the normal development of lateral organs in the inflorescence, similar to the role of auxin transport in lateral organs during leaf development (Scanlon, 2003).

2.4.4 NPA Causes a Reduction in Vascular Ddevelopment in the Inflorescence Stem

Auxin plays a fundamental role in vascular development (Aloni, 2004). In Arabidopsis, NPA treatment causes an increase in vasculature in the inflorescence stem (Galweiler et al., 1998). However, in *bif2* mutants in maize, where there is a reduction in auxin transport, there is a reduction in vasculature (McSteen et al., 2007). To determine if this was a difference between monocots and eudicots, the effects of NPA on vascular development in the maize inflorescence was determined. Plants at the transition stage of development were treated with NPA for two weeks. Inflorescences were sectioned in the transverse dimension and stained with Toluidine Blue O (TBO). Vascular bundles were visible as oval shaped, darkly staining groups of cells (Fig. 5A). The number of vascular bundles near the base of the inflorescence stem was counted in NPA treated plants compared to untreated controls (Fig. 5A,B). The number of vascular bundles was then divided by the area of the cross section of the stem to account for the fact that NPA treated inflorescences were slightly narrower than control inflorescences. This analysis showed that NPA treated inflorescences had significantly fewer vascular bundles compared to the controls (T-value = 2.71, DF = 10, P-value = 0.01, Fig. 5C). Therefore, NPA treatment led to a reduction in vascular bundle number in the inflorescence stem, which is similar to the phenotype of *bif2* mutants in maize.

2.4.5 Effects of Other Auxin Transport Inhibitors

To determine if other auxin transport inhibitors had similar effects on axillary meristem initiation as NPA, we treated plants with Hydroxyfluorene-9-carboxylic acid (HFCA) and 2,3,5-Triiodobenzoic acid (TIBA). Plants were grown for four weeks until they had just transitioned to inflorescence development and were then treated for two weeks with different concentrations of HFCA and TIBA. The lowest concentration of HFCA that effectively inhibited BM and SPM initiation was 80μM HFCA (Fig. 6B). 20μM HFCA had no effect on BM or SPM initiation (not shown). 40μM HFCA usually had little effect on BM or SPM initiation (Fig. 6A) but occasionally, if the plants were particularly small, BM and SPM were inhibited (Fig. 6C). Furthermore, RNA in situ hybridization using *kn1* showed that HFCA inhibited the initiation of BMs and SPMs (Fig. 6C). Therefore, NPA and HFCA have similar effects on development though they differ in their effectiveness. On the other hand, TIBA had no observable effect on maize inflorescence development either at 20μM (not shown), 40 or 80μM TIBA (Fig. 6D-F).

2.4.6 *bif2* Is Expressed in NPA Treated Meristems

In *bif2* mutants, the inflorescence meristem fails to initiate BMs and SPMs (McSteen and Hake, 2001). As NPA treatment of normal maize plants phenocopies the *bif2* mutant phenotype, we tested if *bif2* was expressed in the inflorescences of NPA treated plants. In normal plants, *bif2* is expressed on the flanks of the inflorescence before SPMs arise and is subsequently expressed in all axillary meristems (McSteen et al., 2007). In TIBA treated plants which look normal, *bif2* was expressed as normal in SPMs as they arose (Fig. 7A). Surprisingly *bif2* was expressed in NPA treated plants (Fig. 7B). The expression of *bif2* was in a ring surrounding the inflorescence meristem (Fig. 7B, arrow). However, *bif2* was not expressed at the base of the inflorescence indicating that *bif2* expression failed to be maintained (Fig. 7B). Similar results were seen in inflorescences of HFCA treated plants (not shown). Therefore, early expression of *bif2* does not depend on active auxin transport.

2.4.7 *ba1* Is Not Expressed in NPA Treated Meristems

ba1 mutants also fail to initiate BMs and SPMs in maize (Ritter et al., 2002; Gallavotti et al., 2004). To test if the early expression of *ba1* was dependent on polar auxin transport, we performed RNA in situ hybridization of *ba1* in the inflorescences of NPA treated plants. In normal plants, *ba1* is expressed on the flanks of the inflorescence meristem on the adaxial side of initiating BMs and SPMs (Gallavotti et al., 2004). In TIBA treated plants, *ba1* was expressed as normal (Fig. 7C). However, no *ba1* transcript was detected in the inflorescences of NPA (not shown) or HFCA treated plants (Fig. 7D). These results suggest that, unlike *bif2*, polar auxin transport is required for the initial expression of *ba1* during BM and SPM initiation. Therefore, NPA treatment allows us to dissect the pathway for axillary meristem initiation in maize.

2.5 Discussion

We show that treatment with auxin transport inhibitors prevents axillary meristem initiation in the maize inflorescence. In Arabidopsis, treatment with auxin transport inhibitors prevents the initiation of floral meristems (FMs), which are the primary axillary meristems produced by the inflorescence (Okada et al., 1991; Long and Barton, 2000). In maize, the BM and SPM are the primary axillary meristems produced by the inflorescence meristem (McSteen et al., 2000). Therefore, polar auxin transport inhibitors prevent the initiation of axillary meristems, irrespective of meristem identity. Furthermore, polar auxin transport inhibitors also inhibit the initiation of secondary axillary meristems, resulting in the production of single instead of paired spikelets in maize. These results provide insight into the mechanism of inflorescence branching in grasses and have significance for the regulation of inflorescence architecture in all plants with branched inflorescences. In addition, analysis of the expression of *bif2* and *ba1* in the inflorescence of auxin transport inhibited plants enabled us to dissect the pathway for axillary meristem initiation in maize.

2.5.1 Implications for Models of Inflorescence Branching

A striking effect of NPA treatment of maize is the production of single instead of paired spikelets in the inflorescence. These results strongly support the conversion model for spikelet initiation. We propose that in NPA treated inflorescences, inhibition of auxin transport prevents the SPM from initiating an SM, but does not affect the ability of the SPM to convert to SM identity as evidenced by its ability to produce glumes. If the lateral branching model for spikelet initiation was correct then auxin transport inhibition would have resulted in the production of aborted spikelet pair meristems which was rarely seen. These results imply that although auxin transport is required for the initiation of axillary meristems, auxin transport is not required for the meristem to convert to a new meristem identity.

Paired spikelets are a defining character of the Andropogoneae, while other grasses outside the Andropogoneae, such as rice and barley have single spikelets (Clifford, 1987; Kellogg, 2000; G.P.W.G., 2001). The presence of single spikelets is also characteristic of *bif2* and *ba1* mutants in maize (McSteen and Hake, 2001; Gallavotti et

al., 2004). This suggests that auxin transport or response is required for the formation of paired spikelets in maize. Therefore, the regulation of auxin transport may have played a role in the evolution of inflorescence architecture in the grasses. Furthermore, as branched inflorescence architecture in all plants can be explained by a similar mechanism (Prusinkiewicz et al., 2007), our results support the idea that meristem conversion events also occur in other plants in which the inflorescence produces multiple orders of axillary meristem.

2.5.2 NPA Does Not Inhibit the Elongation of Apical or Axillary Meristems

A notable feature of the NPA experiments is that the apical inflorescence meristem is unaffected by NPA treatment. The inflorescence meristem continues to elongate even though it cannot initiate axillary meristems or lateral primordia. This effect on the apical inflorescence meristem is also seen in other plants treated with NPA (Okada et al., 1991; Reinhardt et al., 2000) as well as auxin transport mutants in Arabidopsis and maize (Christensen et al., 2000; Vernoux et al., 2000; McSteen and Hake, 2001). We suggest that NPA fails to affect the inflorescence meristem because the inflorescence meristem, or more correctly, the central zone at the tip of the inflorescence meristem, is auxin insensitive as proposed by de Reuille et al., (2006). This difference in the effects of NPA on apical versus axillary meristems, could be due to the identity of the meristem as apical rather than axillary. However, our results show that axillary meristems also continue to elongate, if they had initiated before NPA treatment. In maize inflorescences treated with NPA, BMs that had initiated continue to elongate without initiating lateral organs. BMs normally elongate so the more significant result is that SPMs or SMs which normally do not elongate also continue to grow without producing lateral primordia. Hence, once a meristem has initiated, whether it is apical or axillary, its ability to elongate is not inhibited and in fact may be promoted by NPA treatment. We suggest that this is because active auxin transport is only required in the peripheral zone of the meristem and that the central (and rib) zones of the meristem do not require active auxin transport for growth.

2.5.3 Polar Auxin Transport Inhibitors Differ in Their Effectiveness

Both NPA and HFCA were effective at inhibiting axillary meristem initiation. However, unlike results in eudicots, an additional auxin transport inhibitor, TIBA, was not effective at inhibiting axillary meristem initiation (Okada et al., 1991; Mattsson et al., 1999; Sieburth, 1999) though it did cause effects on root gravitropism. We suggest that this is due to the difference in the mechanism of action of TIBA (Thomson et al., 1973; Petrasek et al., 2003). TIBA is less effective at inhibiting auxin transport than NPA (Thomson et al., 1973; Katekar and Geissler, 1977). Moreover, TIBA has a different chemical structure than NPA and has similarities with the structure of the most common auxin, indole-3-acetic acid (Katekar and Geissler, 1977, 1980). Therefore, TIBA is proposed to act as an auxin antagonist (Katekar and Geissler, 1980) while NPA is proposed to act as an inhibitor of the auxin efflux carrier (Lomax et al., 1995; Muday, 2000; Muday and Murphy, 2002). HFCA is proposed to have a similar mechanism of action as NPA (Thomson and Leopold, 1974; Katekar and Geissler, 1980).

Differences in the effects of TIBA were not seen in Arabidopsis (Okada et al., 1991; Mattsson et al., 1999; Sieburth, 1999). One possibility is that there may be a difference in how monocots and eudicots respond to TIBA. Support for this assertion is that while NPA and TIBA have similar effects on leaf development in eudicots (Mattsson et al., 1999; Sieburth, 1999), NPA and TIBA have different effects on leaf development in maize (Tsiantis et al., 1999; Scanlon, 2003).

2.5.4 Model for Axillary Meristem Initiation in Maize

As *bif2* mutants have the same phenotype as the NPA treated meristems, we propose that *bif2* and polar auxin transport are both required for axillary meristem initiation (Fig. 8). The similarity of the phenotype of NPA treated plants to *bif2* mutants includes the failure to initiate axillary meristems, the production of single spikelets, the reduction in vasculature and the lack of an effect on the apical inflorescence meristem (McSteen and Hake, 2001; McSteen et al., 2007). Similar to *bif2* mutants, circular ridges which do not express *kn1* are produced in NPA treated plants (McSteen and Hake, 2001). It is proposed that these are bract primordia that do not separate showing that phyllotaxy is abolished in *bif2* mutants and in NPA treated inflorescence meristems. There is

evidence that *bif2* and its co-orthologs in other species, regulate auxin transport (Benjamins et al., 2001; Friml et al., 2004; Lee and Cho, 2006; McSteen et al., 2007; Morita and Kyozuka, 2007). The expression of *bif2* in NPA treated meristems, shows that *bif2* is expressed independently of polar auxin transport.

ba1 mutants also fail to initiate axillary meristems in the tassel. However, the *ba1* mutant phenotype differs from *bif2* and NPA treated meristems in that bract primordia are visible in a regular pattern on the barren rachis (Ritter et al., 2002). The regular pattern of bract primordia initiation suggests that auxin transport is normal in *ba1* mutants and that *ba1* acts downstream of polar auxin transport. In support of this, RNA *in situ* hybridization shows that *ba1* is not expressed in NPA treated meristems early in development. This suggests the polar auxin transport is required for the initial expression of *ba1* (Fig. 8). Hence, we propose a model in which *bif2* acts upstream and *ba1* acts downstream of polar auxin transport in the regulation of axillary meristem initiation in the maize inflorescence. Future work on the genetic and biochemical interaction between *bif2* and *ba1* will further resolve this model.

Fig. 2.1 Maize inflorescence development

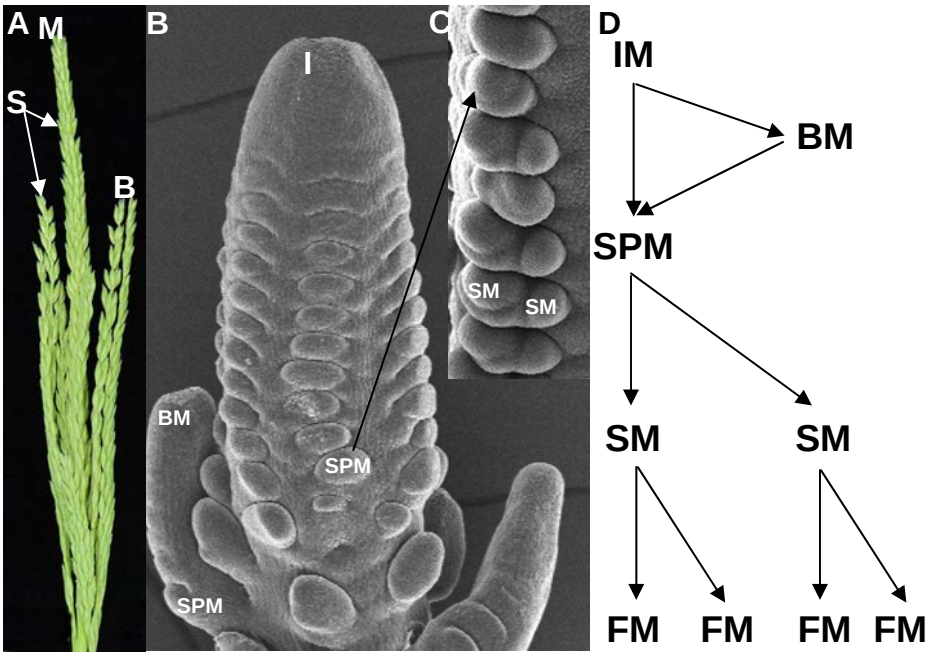

Fig. 2.1 Maize inflorescence development.

(A)Mature tassel has several branches with spikelet pairs on the branches and the main spike.

(B) SEM of early stage of tassel development, showing that the inflorescence meristem produces branch meristems (at the base) and spikelet pair meristems.

(C) Close up of a later developmental stage showing that spikelet pair meristems produce spikelet meristems.

(D) Schematic of the order of meristem initiation. BM, branch meristem; Br, branch; FM, floral meristem; IM, inflorescence meristem; MS, main spike; SM, spikelet meristem; SP, Spikelet pair; SPM, spikelet pair meristem.

Fig. 2.2 SEM analysis shows that NPA inhibits axillary meristem initiation in the inflorescence

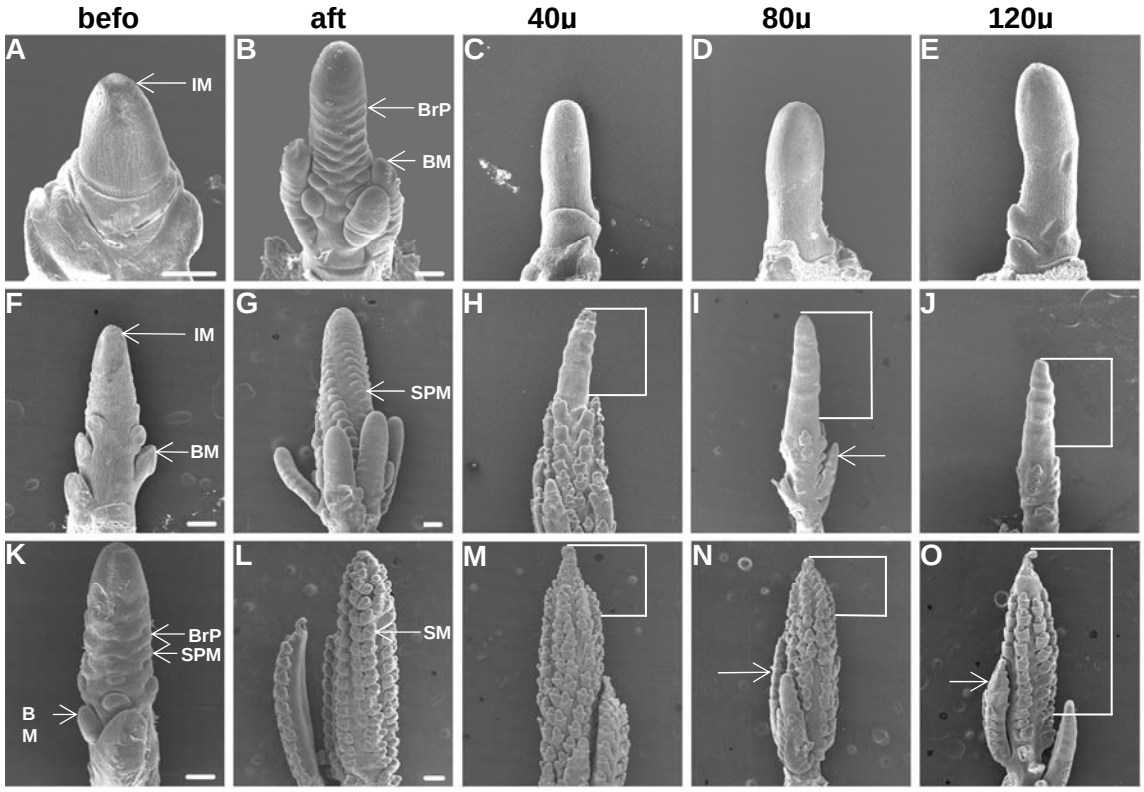

Fig. 2.2 SEM analysis shows that NPA inhibits axillary meristem initiation in the inflorescence.

Plants were grown until the tassel inflorescence meristem had reached the appropriate development stage, (A) transition stage (4 weeks old), (F) branch meristem initiation stage (5 weeks old) or (K) spikelet pair meristem initiation stage (6 weeks old), and were then treated with different concentrations of NPA for two weeks, (C, H, M) 40 μM NPA; (D, I, N) 80 μM NPA and (E, J, O) 120 μM NPA. For each time point, there were two controls: (A, F, K) Inflorescence before NPA treatment; (B, G, L) Inflorescence of plant grown for two weeks without NPA treatment. Bracketed regions in H, I & J show inhibition of SPM initiation, and in M, N & O show inhibition of SM initiation.
BM, branch meristem; BrP, bract primordia; IM, inflorescence meristem;
SM, spikelet meristem; SPM, spikelet pair meristem.
Scale bar = 100μm (A-K), 200μm (L-O)

Fig. 2.3 NPA causes defects in spikelet and floret development

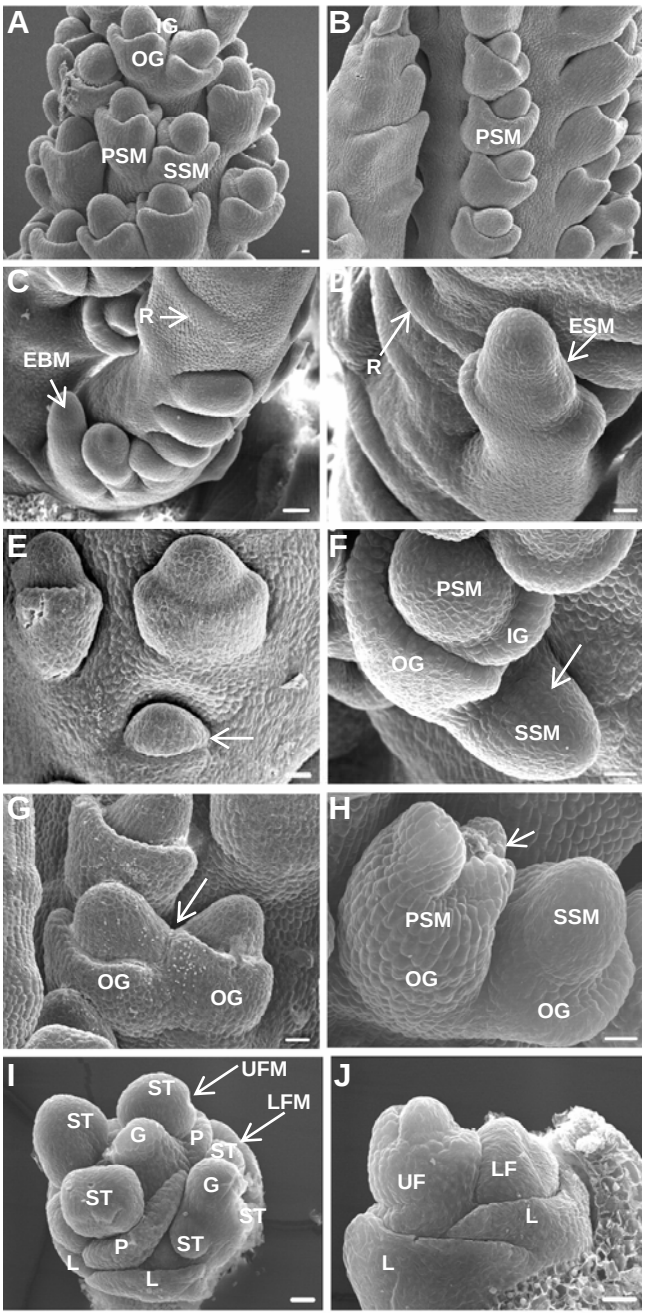

Fig. 2.3 NPA causes defects in spikelet and floret development.
SEM analysis of (A) Control inflorescence and (B-J) Representative meristems from inflorescences of NPA treated plants.
(A)Control inflorescence produces paired spikelets, one pedicellate and the other sessile. The outer and inner glumes are the first lateral organs to be produced by the SMs.
(B) Inflorescence from NPA treated plant producing single spikelets.
(C) Elongated branch meristem at the base of a branch.
(D) Elongated spikelet meristem with a glume primordium forming a ring around the meristem.
(E) Spikelet meristem with no visible glumes (arrow).
(F) Sessile spikelet meristem with no visible glumes (arrow).
(G) The outer glumes of two adjacent spikelets are fused together.
(H) In the pedicellate spikelet, the outer glume and inner glume are fused together. In the sessile spikelet, the glumes form a circular primordium.
(I) When older plants are treated with NPA, floral organs usually form normally (glumes have been removed).
(J) Occasionally, defects in floral organ initiation and separation were detected after NPA treatment (glumes have been removed). EBM, elongated branch meristem; ESM, elongated spikelet meristem;
G, gynoecium; IG, inner glume; L, lemma; LF, lower floret; LFM, lower floral meristem; OG, outer glume; P, palea; PSM, pedicellate spikelet meristem; R, ridge; SM, spikelet meristem; SSM, sessile spikelet meristem; ST, stamen; UF, upper floret; UFM, upper floral meristem. Scale bar = 25 μm.

Fig. 2.4 RNA *in situ* hybridization with *kn1*

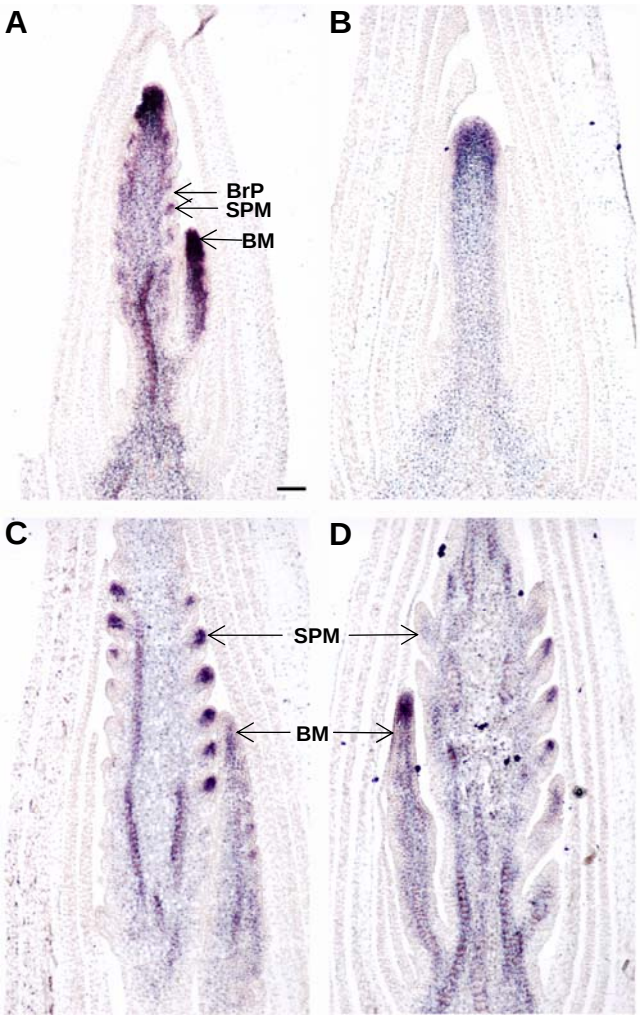

Fig. 2.4 RNA *in situ* hybridization with *kn1*.
(A) Control inflorescence, (B) Inflorescence of plant treated with 40 µM NPA, shows that *kn1* is not expressed on the flanks of the inflorescence meristem (arrow).
(C) Control inflorescence, (D) Inflorescence of plant treated with 40µM NPA, shows that spikelet meristems are elongated. BrP, bract primordia; BM, branch meristem; IM, inflorescence meristem; SM, spikelet meristem; SPM, spikelet pair meristem. Scale bar = 100µm.

Fig. 2.5 Vasculature defects in NPA treated inflorescences

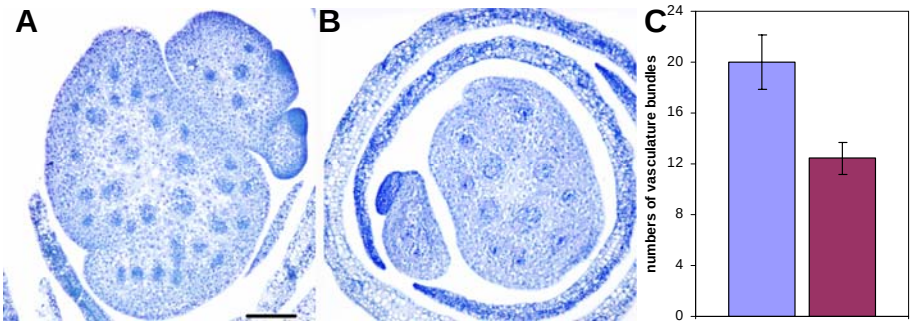

Fig. 2.5 Vasculature defects in NPA treated inflorescences.
(A) TBO staining of a cross section at the base of an untreated inflorescence shows scattered vascular bundles in the inflorescence stem. (B) Cross section at the base of an inflorescence treated with 80 μM NPA shows a reduced number of vascular bundles. (C) Mean +/- standard error of the number of vascular bundles/mm2 in control (n=4) versus NPA treated inflorescences (n=8). The inflorescences of NPA treated plants show a statistically significant reduction in the number of vascular bundles. Scale bar = 100μm.

Fig. 2.6 Effect of other auxin transport inhibitors.

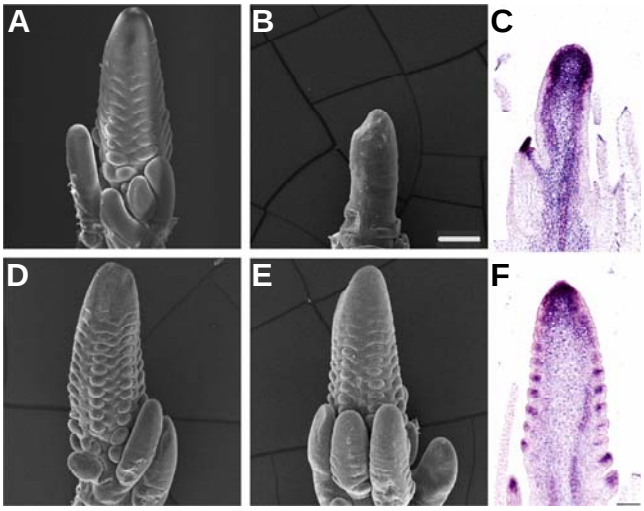

Fig. 2.6 Effect of other auxin transport inhibitors.
Plants at the transition stage (4 weeks) were treated for two weeks with two other auxin transport inhibitors, HFCA and TIBA. SEM analysis of inflorescences, (A) 40 µM HFCA, (B) 80 µM HFCA, (D) 40 µM TIBA and (E) 80 µM TIBA. RNA *in situ* hybridization with *kn1*, (C) 40 µM HFCA and (F) 80 µM TIBA. Scale bar = 100µm.

Fig. 2.7 RNA *in situ* hybridization with *bif2* and *ba1*.

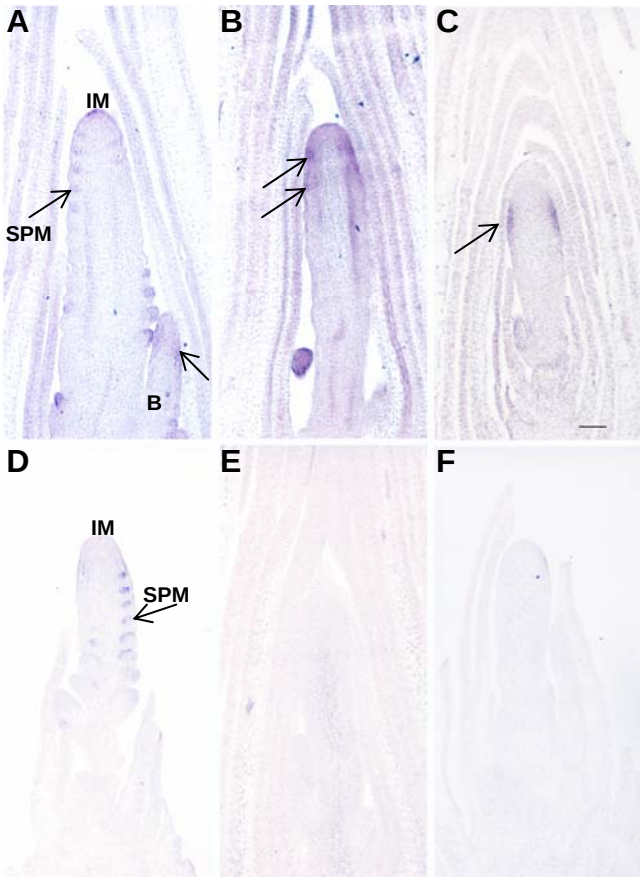

Fig. 2.7 RNA *in situ* hybridization with *bif2* and *ba1*.
(A) *bif2* is expressed in SPMs on the flanks of the inflorescence meristems in 20 μM TIBA treated plants which have normal inflorescence development. (B) *bif2* is expressed in a ring around the inflorescence meristem (arrow) in plants treated with 40 μM NPA. (C) *ba1* is expressed as normal in SPMs of plants treated with 40 μM TIBA. (D) Expression of *ba1* is not detected in plants treated with 80 μM HFCA. SPM, spikelet pair meristem. Scale bar = 100 μm.

Fig. 2.8 Model for axillary meristem initiation in maize.

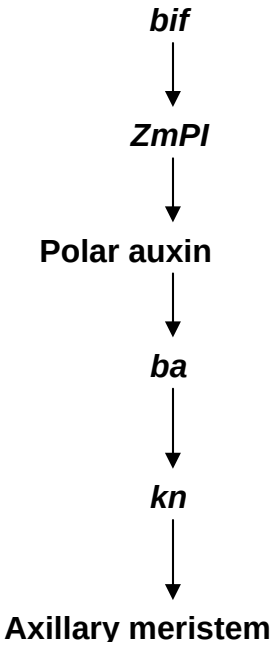

Fig. 2.8 Model for axillary meristem initiation in maize.
NPA treatment inhibits axillary meristem initiation, which indicates that polar auxin transport is required to initiate axillary meristems. RNA *in situ* hybridization analysis in NPA treated meristems indicates that *bif2* is expressed upstream and *ba1* is expressed downstream of auxin transport. These genes together with *ZmPIN1* (Carraro et al., 2006) and *kn1* (Jackson et al., 1994; McSteen and Hake, 2001; Ritter et al., 2002) are required for axillary meristem initiation in maize

Fig. 2.S1 Auxin transport inhibitors cause root agravitropism in maize.

.

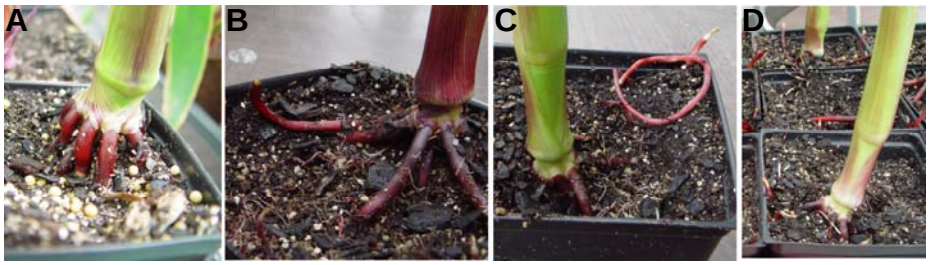

Fig. 2.S1 Auxin transport inhibitors cause root agravitropism in maize.
(A) Roots in control plants show normal gravitropism. (B) 40 μM NPA,
(C) 80 μM HFCA and (D) 80 μM TIBA cause roots to grow agravitropically.

References

Aloni, R. (2004). The induction of vascular tissues by auxin. *In* P. J. Davies [ed.], Plant hormones: Biosynthesis, Signal transduction, Action!, 471-492. Kluwer Academic Publishers, The Netherlands.

Benjamins, R., Quint,A., Weijers, D., Hooykaas, P. and Offringa, R. (2001). The PINOID protein kinase regulates organ development in Arabidopsis by enhancing polar auxin transport. *Development* **128,** 4057-4067.

Benkova, E., M. Michniewicz, M. Sauer, T. Teichmann, D. Seifertova, G. Jergens, and J. Friml. (2003). Local, efflux-dependent auxin gradients as a common module for plant organ formation. *Cell* **115,** 591-602.

Bennett, S. R. M., Alvarez, J. Bossinger, G. and Smyth, D. R. (1995). Morphogenesis in *pinoid* mutants of *Arabidopsis thaliana*. *Plant Journal* **8,** 505-520.

Bommert, P., Satoh-Nagasawa, N., Jackson, D. and Hirano, H. Y. (2005). Genetics and evolution of inflorescence and flower development in grasses. *Plant and Cell Physiology* **46,** 69-78.

Borthwick, H. A., Phillips, M. and Robbins, W. W. (1931). Floral development in *Daucus carota*. *American Journal of Botany* **18,** 784-U711.

Bortiri, E., Chuck, G., Vollbrecht, E., Rocheford, T., Martienssen, R. and Hake, S. (2006). *ramosa2* encodes a LOB domain protein that determines the fate of stem cells in branch meristems of maize. *Plant Cell* **18,** 574-585.

Carraro, N., Forestan, C., Canova, S., Traas, J. And Varotto, S. (2006). *ZmPIN1a* and *ZmPIN1b* encode two novel putative candidates for polar auxin transport and plant architecture determination of maize. *Plant Physiology* **142,** 254-264.

Cheng, P.C., Greyson, R. I. and Walden, D. B. (1983). Organ initiation and the development of unisexual flowers in the tassel and ear of *Zea mays*. *American Journal of Botany* **70,** 450-462.

Cheng, Y. F. and Zhao, Y. D. (2007). A role for auxin in flower development. *Journal of Integrative Plant Biology* **49,** 99-104.

Christensen, S. K., Dagenais, N., Chory, J. and Weigel, D. (2000). Regulation of auxin response by the protein kinase PINOID. *Cell* **100,** 469-478.

Chuck, G., Meeley, R. B. and Hake, S. (1998). The control of maize spikelet meristem fate by the *APETALA2*- like gene *indeterminate spikelet1*. *Genes & Development* **12,** 1145-1154.

Chuck, G., Cigan, A. M., Saeteurn, K. and Hake, S. (2007). The heterochronic maize mutant *Corngrass1* results from overexpression of a tandem microRNA. *Nature Genetics* **39,** 544-549.

Chuck, G., Muszynski, M. Kellogg, E., Hake, S. and Schmidt. R. J. (2002). The control of spikelet meristem identity by the *branched silkless1* gene in maize. *Science* **298,** 1238-1241.

Clifford, H. T. (1987). Spikelet and floral morphology. *In* T. R. Soderstrom, K. W. Hilu, C. S. Campbell, and M. E. Barkworth [eds.], Grass Systematics and Evolution, 21-30. Smithsonion Institution Press, Washington, D.C.

De Reuille, P. B., Bohn-Courseau, I., Ljung, K., Morin, H., Carraro, N., Godin, C. and Traas, J. (2006). Computer simulations reveal properties of the cell-cell signaling network at the shoot apex in Arabidopsis. *Proceedings of the National Academy of Sciences USA* **103,** 1627-1632.

Friml, J., Yang, X., Michniewicz, M., Weijers, D., Quint, A., Tietz, O., Benjamins, R., Ouwerkerk, P.B. F., Ljung, K., Sandberg, G., Hooykaas, P. J. J., Palme, K. and Offringa, R. (2004). A PINOID-dependent binary switch in apical-basal PIN polar targeting directs auxin efflux. *Science* **306,** 862-865.

G.P.W.G. (2001). Phylogeny and subfamilial classification of the grasses (*Poaceae*). *Annals of the Missouri Botanical Garden* **88,** 373-457.

Gallavotti, A., Zhao, Q., Kyozuka, J., Meeley, R. B., Ritter, M., Doebley, J. F., Pe, M. E. and Schmidt, R. J. (2004). The role of *barren stalk1* in the architecture of maize. *Nature* **432,** 630-635.

Galweiler, L., Guan, C. H., Muller, A., Wisman, E., Mendgen, K., Yephremov, A. and Palme, K. (1998). Regulation of polar auxin transport by AtPIN1 in Arabidopsis vascular tissue. *Science* **282,** 2226-2230.

Grbic, V. (2005). Comparative analysis of axillary and floral meristem development. *Canadian Journal of Botany* **83,** 343-349.

Irish, E. E. (1997). Class II *tassel seed* mutations provide evidence for multiple types of inflorescence meristems in maize (*Poaceae*). *American Journal of Botany* **84,** 1502-1515.

Irish, E. E. (1998). Grass spikelets: a thorny problem. *Bioessays* **20,** 789-793.

Jackson, D., Veit, B. and Hake, S. (1994). Expression of maize *knotted1* related homeobox genes in the shoot apical meristem predicts patterns of morphogenesis in the vegetative shoot. *Development* **120,** 405-413.

Honsson, H., Heisler, M.G., Shapiro, B. E., Meyerowitz, E. M. and Mjolsness, E. (2006). An auxin-driven polarized transport model for phyllotaxis. *Proceedings of the National Academy of Sciences USA* **103,** 1633-1638.

Katekar, G. F. and Geissler, A. E. (1977). Auxin Transport Inhibitors III Chemical requirements of a class of auxin transport inhibitors. *Plant Physiology* **60,** 826-829.

Katekar, G. F. and Geissler, A. E. (1980). Auxin Transport Inhibitors IV Evidence of a common mode of action for a proposed class of auxin transport inhibitors - the Phytotropins. *Plant Physiology* **66,** 1190-1195.

Kellogg, E. A. (2000). The grasses: A case study in macroevolution. *Annual Review of Ecology and Systematics* **31,** 217-238.

Kellogg, E. A. (2007). Floral displays: genetic control of grass inflorescences. *Current Opinion in Plant Biology* **10,** 26-31.

Komatsu, K., Maekawa, M., Ujiie, S., Satake, Y., Furutani, I., Okamoto, H., Shimamoto, K. And Kyozuka, J. (2003). *LAX* and *SPA*: Major regulators of shoot branching in rice.*Proceedings of the National Academy of SciencesUSA***100,**11765-70

Kyozuka, J., Komatsu, K., Okamoto, N., Maekawa, M. and Shimamoto, K. (2002). The *LAX PANICLE (LAX)* gene of rice is required for axillary meristem initiation in the inflorescence. *Plant and Cell Physiology* **43,** S8-S8.

Lee, S.H. and Cho, H. T. (2006). PINOID positively regulates auxin efflux in Arabidopsis root hair cells and tobacco cells. *Plant Cell* **18,** 1604-1616.

Lomax, T. L., Muday, G. K. and Rubery, P.H. (1995). Auxin transport. *In* P. J. Davies [ed.], Plant hormones: Physiology, Biochemistry and Molecular Biology, 509-530. Kluwer Academic Publishers, The Netherlands.

Long, J. and Barton, M. K. (2000). Initiation of axillary and floral meristems in Arabidopsis. *Developmental Biology* **218,** 341-353.

Manning, W. E. (1938). The morphology of the flowers of the *Juglandaceae* I The inflorescence. *American Journal of Botany* **25,** 407-419.

Mattsson, J., Sung, Z. R. and Berleth, T. (1999). Responses of plant vascular systems to auxin transport inhibition. *Development* **126,** 2979-2991.

McSteen, P. (2006). Branching out: The *ramosa* pathway and the evolution of grass inflorescence morphology. *Plant Cell* **18,** 518-522.

McSteen, P. and Hake, S. (1998). Genetic control of plant development. *Current Opinion in Biotechnology* **9,** 189-195.

McSteen, P. and Hake, S. (2001). *barren inflorescence2* regulates axillary meristem development in the maize inflorescence. *Development* **128,** 2881-2891.

McSteen, P. and Leyser, O. (2005). Shoot branching. *Annual Review of Plant Biology* **56,** 353-374.

McSteen, P., Laudencia-Chingcuanco, D. and Colasanti, J. (2000). A floret by any other name: control of meristem identity in maize. *Trends in Plant Science* **5,** 61-66.

McSteen, P., Malcomber, S., Skirpan, A., Lunde, C., Wu, X., Kellogg, E. and Hake, S. (2007). *barren inflorescence2* encodes a co-ortholog of the *PINOID* serine/threonine kinase and is required for organogenesis during inflorescence and vegetative development in maize. *Plant Physiology* **144,** 1000-1011.

Morita, Y. and Kyozuka, J. (2007). Characterization of *OsPID*, the rice ortholog of *PINOID*, and its possible involvement in the control of polar auxin transport. *Plant and Cell Physiology* **48,** 540-549.

MUDAY, G. K. (2000). Maintenance of asymmetric cellular localization of an auxin transport protein through interaction with the actin cytoskeleton. *Journal of Plant Growth Regulation* **19,** 385-396.

Muday, G. K. and Murphy, A. S. (2002). An emerging model of auxin transport regulation. *Plant Cell* **14:** 293-299.

Murphy, A. and Taiz, L. (1999). Naphthylphthalamic acid is enzymatically hydrolyzed at the hypocotyl-root transition zone and other tissues of *Arabidopsis thaliana* seedlings. *Plant Physiology and Biochemistry* **37,** 413-430.

Okada, K., Ueda, J., Komaki, M. K., Bell, C. J. and Shimura, Y. (1991). Requirement of the auxin polar transport system in early stages of Arabidopsis floral bud formation. *Plant Cell* **3,** 677-684.

Petrasek, J., Cerna, A., Schwarzerova, K., Elckner, M., Morris, D. A. And Zazimalova, E. (2003). Do phytotropins inhibit auxin efflux by impairing vesicle traffic? *Plant Physiology* **131,** 254-263.

Petrasek, J., Mravec, J. Boouchard, R., Blakeslee, J. J., Abas, M., Seifertova, D., Wisniewska, J., Tadele, Z., Kubes, M., Covanova, M., Dhonukshe, P., Skupa, P., Benkova, E., Perry, L., Krecek, P., Lee, O. R., Fink, G. R., Geisler, M., Murphy, A. S., Luschnig, C., Zazimalova, E. and Friml, J. (2006). PIN proteins perform a rate-limiting function in cellular auxin efflux. *Science* **312,** 914-918.

Prusinkiewicz, P., Erasmus, Y., Lane, B., Harder, L. D. and Coen, E. (2007). Evolution and development of inflorescence architectures. *Science* **316,** 1452-1456.

Rashotte, A. M., Brady, S. R., Reed, R. C., Ante, S. J. and Muday, G. K. (2000). Basipetal auxin transport is required for gravitropism in roots of arabidopsis. *Plant Physiology* **122,** 481-490.

Reinhardt, D., Mandel, T. and Kuhlemeier, C. (2000). Auxin regulates the initiation and radial position of plant lateral organs. *Plant Cell* **12,** 507-518.

Reinhardt, D., Pesce, E. R., Stieger, P., Mandel, T., Baltensperger, K., Bennett, M., Traas, J., Friml, J. And Kuhlemeier, C. (2003). Regulation of phyllotaxis by polar auxin transport. *Nature* **426,** 255-260.

Reznikoff, C. A., Kao, C., Messing, E. M., Newton, M. and Swaminathan, S. (1993). A molecular genetic model of human bladder carcinogenesis. *Seminars in Cancer Biology* **4,** 143-152.

Ritter, M. K., Padilla, C. M. And Schmidt, R. J. (2002). The maize mutant *barren stalk1* is defective in axillary meristem development. *American Journal of Botany* **89,** 203-210.

Scanlon, M. J. (2003). The polar auxin transport inhibitor N-1-naphthylphthalamic acid disrupts leaf initiation, KNOX protein regulation, and formation of leaf margins in maize. *Plant Physiology* **133,** 597-605.

Shimamoto, K. and Kyozuka, J. (2002). Rice as a model for comparative genomics of plants. *Annual Review of Plant Biology* **53,** 399-419.

Sieburth, L. E. (1999). Auxin is required for leaf vein pattern in Arabidopsis. *Plant Physiology* **121,** 1179-1190.

Smith, R. S., Guyomarc'h, S., Madel, T., Reinhardt, D., Kuhlemeier, C. and Prusinkiewicz, P. (2006). A plausible model of phyllotaxis. *Proceedings of the National Academy of Sciences USA* **103,** 1301-1306.

Steeves, T. and Sussex, I. (1989). Patterns in plant development. Cambridge University Press, Cambridge, UK.

Swarup, R., Kramer, E. M., Perry, P., Knox, K., Leyser, H. M. O., Haseloff, J., Beemster, G. T. S., Bhalerao, R. and Bennett, M. J. (2005). Root gravitropism requires lateral root cap and epidermal cells for transport and response to a mobile auxin signal. *Nature Cell Biology* **7,** 1057-1065.

Thomson, K. S. and Leopold, A. C. (1974). In-vitro binding of morphactins and 1-N-Naphthylphthalamic acid in corn coleoptiles and their effects on auxin transport. *Planta* **115,** 259-270.

Thomson, K. S., Hertel, R., Muller, S. and Tavares, J. E. (1973). 1-N-Naphthylphthalamic acid and 2,3,5-Triiodobenzoic acid - In-vitro binding to particulate cell fractions and action on auxin transport in corn coleoptiles. *Planta* **109,** 337-352.

Tslantis, M., Brown, M. I. N., Skibinski, G. and Langdale, J. A. (1999). Disruption of auxin transport is associated with aberrant leaf development in maize. *Plant Physiology* **121,** 1163-1168.

Tucker, S. C. (1989). Overlapping organ initiation and common primordia in flowers of *Pisum Sativum* (*Leguminosae, Papilionoideae*). *American Journal of Botany* **76,** 714-729.

Vernoux, T., Kronenberger, J., Grandjean, O., Laufs, P. and Traas, J. (2000). *PIN-FORMED 1* regulates cell fate at the periphery of the shoot apical meristem. *Development* **127,** 5157-5165.

Vollbrecht, E., Springer, P. S., Goh, L., Buckler IV, E. S. and Martienssen, R. (2005). Architecture of floral branch systems in maize and related grasses. *Nature* **436,** 1119-1126.

Williams, L. and Fletcher, J. C. (2005). Stem cell regulation in the Arabidopsis shoot apical meristem. *Current Opinion in Plant Biology* **8,** 582-586.

CHAPTER THREE

Genetic Analysis of the Interaction Between *barren inflorescence 2 (bif2)* and *barren stalk1 (ba1)*

Part of this chapter has been published

Skirpan, A., Wu, X., and McSteen, P. (2008). Genetic and physical interaction suggest that BARREN STALK1 is a target of BARREN INFLORESCENCE2 in maize inflorescence development. *Plant J*. in press.

Note: in the published paper, my part of the work is the genetic interaction between *bif2* and *ba1*. The physical interaction part was done by Andrea Skirpan. In this chapter, I only present my work including some data which has not yet been published.

3.1 Abstract

In maize inflorescence development, some of the genes are identified to control the initiation of axillary meristems. *barren inflorescence2 (bif2)* and *barren stalk1 (ba1)* are such genes. *bif2* encodes a serine/threonine protein kinase which involves in auxin signaling. *ba1* is a bHLH transcription factor. Double mutant analysis was performed to test how *bif2* and *ba1* interact with each other to initiate axillary meristems. We propose that *bif2* is epistatic and upstream of *ba1* in spikelet initiation. In supporting this epistasis, molecular analysis shows that *bif2* is still expressed in the *ba1* mutants but *ba1* expression is suppressed in *bif2* mutants. In addition, the somewhat additive aspects of the interaction show that *bif2* and *ba1* have their own unique roles in axillary meristem initiation and ear formation. The interaction of each of these genes with *kn1* in maize inflorescence development was also tested. This analysis showed that both *bif2* and *ba1* are epistatic to *kn1*. A genetic interaction model is proposed based on this data.

3.2 Introduction

In normal maize inflorescence development, the inflorescence meristem initiates four types of axillary meristems after transitioning from the vegetatitive shoot apical meristem to form the tassel. These four types of axillary meristems are branch meristem (BM), spikelet pair meristem (SPM), spikelet meristem (SM) and floral meristem (FM). In both *bif2* and *ba1* mutants, the tassel has difficulties initiating all four types of meristem and has a barren inflorescence phenotype. To genetically determine the interaction of these genes in maize inflorescence development, we analyze double mutants between *bif2*, *ba1* and *kn1*.

The tassel phenotype of each single mutant is shown in Figure 1a. *bif2* is required for axillary meristem initiation. In *bif2* mutants, the number of SPMs on the main rachis of the tassel is reduced and their arrangement on the axis is irregular. Mostly, only pedicellate spikelets form. Sometimes, SMs initiate incomplete sessile spikelets. In the florets, only 25% of the upper florets and 95% of the lower florets are normal, with various organs absent in the other florets (McSteen and Hake, 2001). Ears are usually produced in the *bif2* mutant but few kernels are initiated. *bif2* encodes a serine/threonine protein kinase. RNA gel blotting shows that *bif2* is specifically expressed in the ear and tassel. RNA *in situ* hybridization analysis shows that *bif2* is detected in BMs, SPMs, SMs and FMs (McSteen et al., 2007).

kn1 is a homeobox gene expressed in the shoot apical meristem as well as lateral axillary meristems (Jackson et al., 1994). *kn1* is down regulated in differentiated organs. Thus, *kn1* is an ideal molecular marker for labeling meristem cells. The *kn1-R1* allele we used for analysis is a recessive allele of *kn1*, which has a stop codon in the homeodomain at the C terminus (Kerstetter et al., 1997). In *kn1* mutants, there are fewer branch meristems and spikelet pair meristems, thus, a sparse tassel appears. Also, no ear is produced usually. However, if an ear is produced, it is shorter and smaller than normal.

ba1 encodes a bHLH transcription factor (Gallavotti et al., 2004). In *ba1* loss of function mutants, the tassel phenotype is barren (Ritter, 2002). In severe *ba1* mutants, no branch meristems form and few or no spikelets initiate. The main rachis, instead of being smooth, initiates many regular “bumps” densely distributed in the basal and middle part of the tassel. These “bumps” has been shown not to be axillary meristems because *kn1*

expression is down regulated in these bumps. Instead, these bumps are proposed to be subtending bract primordia which are usually inhibited during normal tassel development. However, in *ba1* mutants, the bract primordia grow larger than normal as the axillary meristems do not form. Usually, the apical part of the tassel is smaller and thinner compared with the rest of the tassel. Ears are not produced in *ba1* mutants. RNA *in situ* hybridization analysis shows that *ba1* is expressed both in the vegetative axillary meristems and inflorescence axillary meristems. In the inflorescence meristem, *ba1* is detected in a small region in BMs, SPMs, SMs and FMs at the boundary where new axillary meristems are going to initiate (Gallavotti et al., 2004).

To understand how bract primordia are produced, it is important to know that they are aborted leaf like structures and part of the phytomer. In shoot development, the "phytomer" refers to the repeating structure generated by the SAM during vegetative development. The phytomer contains a node, an internode, a leaf and an axillary meristem in the axil of the leaf (Mcsteen and Leyser, 2005). The entire shoot is established by reiterative production of phytomers. Axillary meristem activity varies during vegetative development. During leaf development, many axillary buds remain dormant while the leaf blades grow out. However, in flower phytomer development, the axillary meristem is responsible for floral organ formation while the leaf primordia are inhibited. Therefore, all axillary meristems are subtended by leaves even if they are not visible. In inflorescence development, these leaves are called bracts. The "bract" leaf primordia subtend the BMs and SPMs. The subtending leaf primordia of SMs are glumes which grow out as a sheath like structures whose function is to protect the florets. The leaf primordia of FMs are the lemmas, a leaf like structure subtending the florets.

In order to understand the role of *bif2* and *ba1* as well as their interaction in maize inflorescence development, we performed several genetic analysis in this chapter. We made *bif2;ba1* double mutants, analyzed the vegetative phenotype including leaf number and plant height measurements. In addition, we analyzed *bif2;ba1* double mutants at an early development stage by SEM and counted spikelet formation in the mature tassel in each of the genotype categories. Moreover, real time RT-PCR analysis was used to quantify the expression of *bif2* in *ba1* mutants and *ba1* expression in *bif2*

mutants. Based on all the genetic analysis plus the molecular data, a model has been proposed to explain the interaction between *bif2* and *ba1*.

3.3 Methods and Materials

3.3.1 Plant Growth Condition

Around 500 plants of the *bif2;ba1* double mutant population were planted separately in two fields, in 2005 and 2006 and around 300 plants were planted in 2007 in Rocksprings, PA. Around 300 plants of *bif2;kn1* and *ba1;kn1* double mutant populations were planted in two fields in 2005 in Rockspring, PA. Generally, plants in the first field were planted two weeks earlier than in the second field. The *bif2-77* allele was used, *ba1-ref* allele was used (Gallavotti et al., 2004) and kn1-R1 allele was used (Kerstetter et al., 1997).

Seeds were generated both in State College (summer) and in Puerto Rico (winter) by crossing *bif2* and *ba1* heterozygous parents to generate *bif2/+;ba1/+* heterozygous F1 seeds in B73 inbred background. The F1 was selfed to determine the segregation ratio of the F2 seeds. In addition, the parental lines were selfed to determine which families were heterozygous. Once the segregation within each family was determined, these families were used for further analysis. Leaf number was counted by cutting every fifth leaf with scissors throughout the field season. Plant height was measured after anthesis from the soil surface to the top of the tassel.

3.3.2 Genotype Information

Four or five double mutants families of *ba1;bif2* were genotyped by PCR with primers designed from *ba1*, *bif2* and transposon insertion sequences. Plants were genotyped for wild type *bif2* (bif2-57-F: 5'-CAG CCT GCC GCG CTG CTC CAG-3' and bif2-250-R: 5'-CGG CGC AGC AGC CTG AAG TCC-3'), mutant *bif2* (bif2-77-F: 5'-CAG TGG CGG TAG AAA TTT G-3' and bif2-250-R: 5'-GGC GCA GCA GCC TGA AAG TCC-3', wild type ba1 (ba1-07-F: 5'-GCT AAG CTA CTG TAA GCG GGA TGG ACA-3' and ba1-04-R: 5'-TGG CAT TGC ATG GAA GCG TGT ATG AGC-3') and mutant ba1 (ba1-05-F: 5'-TCC TAG ACA TGC ATA TCT GAA CCA GAG CT-3' and ba1-04-R: 5'-TGG CAT TGC ATG GAA GCG TGT ATG AGC-3'). 5-10 tassels from genotyped homozygous double mutant plants, single mutant, heterozygous and wild type plants were collected separately to do further analysis.

3.3.3 Tassel Scoring and Phenotyping Method

Tassel phenotypes were scored in all the families and chi-square analysis was performed on the segregation ratios. The tassels of the genotyped 2007 population were collected and branches and spikelets were counted. The tassel height was measured from the ridges of the first branch to the tip of the tassel. (In the *bif2* mutants which have no branches, the tassel height was measured from the tip to the residual branch line at the base of the tassel above the flag leaf. Spikelets were counted in the following categories: branches, triple spikelets, paired spikelets, single spikelets, aborted paired spikelets and aborted single spikelets. The aborted paired spikelets were the spikelet pairs in which the sessile spikelets only contain a glume like organ but no other floral organs. The aborted single spikelets were spikelets formed with no floral organs but some glume like organ remained attached to the pedicel.

3.3.4 Real Time RT-PCR

2-3 tassel meristems around 3-6mm long were pooled to extract total RNA from each category of normal, *ba1/+*, *ba1/ba1* and *bif2/bif2*. 3-4 samples from each category were tested as biological replicates. Furthermore, three technical replicates of each biological replicate were performed. Internal controls of ubiquitin amplification for each RT-PCR run were used. Total RNA was extracted with the NucleoSpin RNA Plant kit (Macherey-Nagel GmbH & Co. KG, Germany). To detect *bif2* expression, the Taqman® probe was (FAM-5’-CTC CGC CAC CGC ATG CCC 3’-BHQ) and the RT-PCR primers were bif2F (5’-CTG CGT CGT CAC GGA GTT C-3’) and bif2R (5’-TGC CCA TCA TGT GCA GGT ACT-3’). To detect *ba1* expression, the Taqman® probe was (FAM-5’-ACG CGG CTT CCC CAT CAT CCA 3’-BHQ) and the RT-PCR primers were ba1F (5’-TGG ATC CAT ATC ACT ACC AAA CCA-3’) and ba1R (5’-ACC GGG TGC TGG AGG TAA G-3’). To detect *ubi* expression, the Taqman® probe was (5' FAM-AAA TCC ACC CGT CGG CAC CTC C-3' BHQ) and the RT-PCR primers were ubqF (5’-CTC TTT CCC CAA CCT CGT GTT-3’) and ubqR (5’-ACG AGC GGC GTA CCT TGA-3’). The real time RT-PCR experiments were performed in the Nucleic Acid Facility in Pennsylvania State University by Deborah S. Grove as described (Barazesh and McSteen, 2008).

3.4 Results

3.4.1 Chi-square Analysis Shows That *bif2* and *ba1* Segregate as Expected in a 9:3:3:1 Ratio

Since *bif2* and *ba1* are recessive alleles, the segregation ratio of their double mutants in the F3 generation would be normal*: bif2: ba1: bif2;ba1*=9:3:3:1 for additive interactions and normal*:bif2/ba1: bif2;ba1* = 9:4:3 for epistatic interactions. The chi-square analysis is shown in Table 1.

The P value was higher than 0.5 for all families tested which indicates the failure to reject the segregation ratio listed as 9:3:3:1. This indicates that *bif2* and *ba1* genes segregate independently of each other. The data were pooled from four families. The four families were generated by the same F1 parents but the F2 was generated by selfed siblings. Chi-square analysis was performed in each individual family and the p values were all higher than 0.5. Therefore, we pooled these four families to show the data in the table. Because the data failed to reject the 9:3:3:1 segregation ratio, we conclude that *bif2* and *ba1* segregate independently.

3.4.2 *bif2;ba1* Double Mutants Mimic the Phenotype of *bif2* Single Mutants During Early Inflorescence Development

In *bif2* and *ba1* single mutants, branches, paired spikelets and single spikelets occasionally form in some of the weak phenotype plants. However, all *bif2;ba1* double mutants tassel do not have any branches and spikelets at all (Fig. 1a). Therefore, *bif2;ba1* mutants have a severe barren inflorescence phenotypes. In addition, no ear forms in the double mutants, which is similar to *ba1* mutants (Fig. 1a).

To further understand this severe phenotype, early inflorescence development was analyzed by Scanning Electron Microscopy (SEM) (Fig. 2). From the images, there were regular protrusions initiated along the *ba1* inflorescence (Fig. 2b, e). These protrusions are a unique phenotype of *ba1* mutants as they are outgrowths of bract primordia which are usually suppressed during normal inflorescence development (Ritter et al, 2002). However, in the *bif2* mutants, there were irregular rings along the smooth inflorescence surface (Fig. 2c, f). The irregular ring like bulges were observed both in *bif2* single mutants and *bif2;ba1* double mutants but not in *ba1* single mutants (Fig. 2e-g). Thus, in

early inflorescence development, the *bif2;ba1* double mutant mimics the phenotype of *bif2* single mutants.

3.4.3 *bif2* Interaction with *ba1* in Spikelet Formation

Spikelet number per tassel was counted from each category of plants, normal, *ba1* single mutants, *bif2* single mutants and *bif2;ba1* double mutants. Total spikelet number was analyzed for each category. The reduction in spikelet formation in the double mutants was more severe than either single mutant and the severity of phenotype was statistically significant ($P<0.05$, student t-test) (Fig. 1b). Therefore, *bif2* and *ba1* function in spikelet initiation is slightly additive.

To analyze this additive interaction in more detail, spikelets per tassel were counted in two addtional categories. These two categories were *bif2/bif2;ba1/+* and *bif2/+;ba1/ba1* mutants. Interestingly, we observed a slightly increase in spikelet initiation in *ba1/ba1;bif2/+* mutants compared with *+/+;ba1/ba1* and *bif2/bif2;+/+* single mutants (Fig. 1c). Although this increase in spikelet number in *ba1/ba1;bif2/+* is not statistically significant from *+/+;ba1/ba1* ($P=0.166$) and *bif2/bif2;+/+* ($P=0.108$) single mutants. In addition, *bif2/bif2;ba1/+* was more severe than *bif2/bif2;+/+* ($P=0.015$). However, we also notice that in some of our *bif2;ba1* double mutant families, there were weak *ba1* mutants segregating. We do not know whether this weak *ba1* phenotype is due to environmental cues or a genetic modifier, we have no clue yet. There is a possibility that there is a modifier in our plant population. In addition, we only identified this phenomenon in the field in 2007. Therefore, these results need to be confirmed by repeating the experiments.

3.4.4 Plant Height in *bif2;ba1* Double Mutants

Plant height was slightly reduced in *ba1* single mutants and more reduced in *bif2* and *bif2;ba1* mutants ($P<0.05$, student t-test) (Fig. 3a). however, there was not a significant reduction in plant height between *bif2* single mutants and *bif2;ba1* double mutants ($P=0.141$ student t-test). Thus, for the plant height phenotype, the *bif2* and *ba1* interaction is additive.

3.4.5 Leaf Initiation is Reduced in *bif2;ba1* Double Mutants

Leaf numbers per plant were counted by cutting the leaf blade with scissors every fifth leaf during development. There was no significant difference in total leaf initiation between the wild type and *ba1* mutants (Fig. 3b) (P=0.432, student t-test). However, there were statistically significant differences in total leaf initiation between *bif2* single mutants, *bif2;ba1* double mutants and the wild type plants (Fig. 3b) (P<0.05, student t-test). Furthermore, there were fewer leaves in *bif2;ba1* double mutants compared with *bif2* single mutants (P<0.05, student t-test). Although *ba1* alone does not influence leaf initiation and is not expressed in leaves, it may function together with *bif2* to influence leaf primordia initiation. Therefore, *ba1* may act nonautonomously during maize vegetative development.

3.4.6 *ba1* Expression is Suppressed in *bif2* Mutants

Real time RT-PCR analysis showed that the expression of *ba1* was reduced in *bif2* mutants (Fig. 4a,b). *ba1* expression reduced in *bif2/+* heterozygous plants and even lower in *bif2/bif2* homozygous plants (Fig. 4a). Although there was a slight threshold expression of *ba1* in *bif2* mutants, the same threshold expression is also detected in *ba1* mutants and it was lower than 0.1 at the relative expression level. Therefore, it is reasonable to conclude that *ba1* is not expressed in *bif2* mutants.

3.4.7 *bif2* is Still Expressed in *ba1* Mutants

Real time RT-PCR showed that *bif2* expression was reduced 4 fold in *ba1* mutants (Fig. 4c, d). Although the reduction of *bif2* expression is obvious, *bif2* expression is still detected due to expression of *bif2* in vasculature. Therefore, *bif2* may function upstream of *ba1*. In addition, there is no *bif2* expression difference between the wild type and *ba1* heterozygous plants (Fig. 4d). Therefore, *bif2* expression was not affected by *ba1*.

3.4.8 Chi-square Analysis Shows that Segregation Ratio of *bif2* and *ba1* with *kn1* Is 9:4:3

Since *bif2*, *ba1* and *kn1* are recessive alleles, the segregation ratio of their double mutants in the F2 generation would be normal*:bif2/ba1: kn1* = 9:4:3 for epistatic interactions. The chi-square analysis is shown in Table 1.

Since the P value are all higher than 0.5, this indicates the failure to reject the segregation ratio of 9:4:3. For *ba1;kn1-R1* double mutant chi-square analysis, four families with the same F1 and F2 parents were pooled to do the analysis. For *bif2;kn1-R1* double mutant chi-square analysis, the data were pooled from three families. The three families were generated by the same F1 parents but the F2 is generated by self pollinated siblings. Chi-square analysis was performed in each individual family and the p values were all higher than 0.5. Therefore, we pooled these three families to show the data in the table. Plants were genotyped to make sure their genotype. The genotyped data showed similar segregation ration. Therefore, it is supported from the chi-square analysis that both *bif2* and *ba1* are epistatic to *kn1*.

3.5 Discussion

Based on the analysis above, a model is proposed to explain the relationship between *bif2*, polar auxin transport (PAT) and *ba1* in spikelet initiation in maize inflorescence development (Fig. 5). Interactions that there is good evidence for are depicted as solid lines. Interactions that are not as certain are shown with dotted lines.

The main central pathway of *bif2* and *ba1* interaction is supported from the experimental results. First, auxin response elements (AuxRE: TGTCTC) are found in the promoter region of both *bif2* (two AuxRE loci at -1333 and -2203) and *ba1* (one AuxRE locus at -1423). ARF proteins can bind AuxRE cis-elements and regulate the gene at the transcriptional level (suppression or activation) during early auxin responses (Guilfoyle and Hagen, 2007). Although there is no direct evidence that ARF proteins bind to the *bif2* and *ba1* promoter, it is reasonable to deduce that ARF proteins may regulate *bif2* and *ba1* expression early in the signal transduction pathway. Therefore, both of the genes may be involved in auxin signaling in axillary meristem initiation. Second, RNA *in situ* hybridization analysis shows that *bif2* is still expressed in NPA treated meristems while *ba1* is not expressed (Wu and McSteen, 2007). This result puts *bif2* upstream of PAT and *ba1* downstream of PAT (Fig. 5a). In addition, blocking polar auxin transport can phenocopy the *bif2* mutant phenotype suggesting that *bif2* may positively regulate PAT in inflorescence development (McSteen et al., 2007; Wu and McSteen, 2007). Furthermore, research from other groups has shown that phosphorylation of PIN1 by PID regulates PIN1 localization and may direct auxin flow during axillary meristem initiation in Arabidopsis (Friml et al., 2004). Therefore, *bif2* may function upstream to regulate PAT during inflorescence development in maize. Moreover, we could draw the conclusion that PAT activates *ba1* transcription since *ba1* expression is absent in NPA treated inflorescence meristems. *bif2* is epistatic to *ba1* indicating that *bif2* is upstream of *ba1* Therefore, the main pathway of *bif2* and *ba1* interaction based on the evidence above is that *bif2* actively regulates PAT to activate *ba1* during initiation of all axillary meristems in maize inflorescence development.

How does the genetic interaction between *bif2* and *ba1* fit into this model? In addition to the main pathway above, we propose that both *bif2* and *ba1* may have separate functions in axillary meristem initiation although these additional functions are

considerately weaker than the main pathway (Fig. 5b, c). Firstly, in *ba1* single mutants, some spikelets are still made. Thus, *bif2* may regulate spikelet initiation by an alternative factor other than *ba1*. Secondly, in *bif2* single mutants, some spikelet formation is observed. This indicates that *ba1* may be somehow activated to initiate spikelets in *bif2* mutants. Thirdly, in the *bif2;ba1* double mutants, there is no spikelet initiation at all. This phenotype is consistent with this model since by knocking out both *bif2* and *ba1*, the main pathway and the alternative pathways are blocked, and thus, the tassels of the double mutants have a completely barren phenotype. However, an alternative explanation for the severe phenotype of *bif2;ba1* double mutants is that *bif2* and *ba1* genes act in the same pathway (Martienssen and Irish, 1999). Since there are duplicate genes for both *bif2* and *ba1* in the genome, redundancy of the duplicate genes causes the less severe phenotype in the single mutants compared with the double mutant phenotype.

It is plausible that *bif2*, as a kinase, may have multiple targets in regulating spikelet initiation so that there are other genes that are redundant with *ba1* function, although this redundancy is weak compared with the *ba1* pathway. In our lab, Andrea Skirpan has shown that BIF2 can physically interact with BA1 and phosphorylate BA1 in vitro. She also showed using yeast two hybrid experiments that BIF2 physically interacts with other transcription factors. These data strongly support the argument that there are genes controlled by *bif2* in addition to *ba1* in axillary meristem initiation. This also indicates that *bif2* may have a broader role than *ba1* in spikelet meristem initiation. A broader role of *bif2* in spikelet meristem initiation is also supported by the following evidence. First, RNA *in situ* hybridization analysis shows that the expression of *bif2* overlaps with *ba1* but is in a larger area before SPMs and SMs initiate (Gallavotti et al., 2004; McSteen et al., 2007). Second, cell biology experiments in heterologous systems show that BIF2::GFP signal is detected in both nucleus and cell periphery but BA1::GFP signal is only detected in the nucleus (Skirpan et al., 2008). Therefore, *bif2* and *ba1* functions are only partially overlapping as proposed in the model.

However, whether there are genes other than *bif2* controlling *ba1* is questionable. Why? In *bif2* mutants, *ba1* expression is suppressed. Interestingly, *ba1* expression is even suppressed in *bif2*/+ heterozygous mutants (Fig. 4a). Real time RT-PCR analysis shows that there is no significant difference in the residual expression of *ba1* in *bif2* mutants

compared with *ba1* mutants (Fig. 4a, b). If there are genes activating *ba1* other than *bif2*, we would expect that *ba1* expression would be higher in *bif2* mutants than in *ba1* null mutants. Since this is not what we observed, we propose that there may not be any other factors to activate *ba1* transcription besides *bif2* in spikelet meristem initiation. Although there is the possibility that the putative other factors may activate *ba1* at the posttranscriptional and/or translational level. If there was an additional pathway to activate *ba1*, we would expect more spikelet initiation in *ba1* mutants than in *bif2* mutants. However, statistical analysis shows there is no significant difference in spikelet initiation between *ba1* and *bif2* single mutants (Fig. 1c, P=0.363). Therefore, it is reasonable to propose that *ba1* is activated at the transcription level by *bif2*.

The next question is the phosphorylation of BA1 by BIF2. Since *bif2* is a protein kinase, transcription level regulation of *ba1* may not be direct. So, although *bif2* is required for *ba1* transcription, the activation of BA1 may require BIF2. For example, phosporylation of BA1 by BIF2 may cause a conformational change of the BA1 protein that activates BA1 for efficient transcription of the downstream genes. Thus, finding the direct target of *ba1* and using the interaction network to do further analysis would provide more evidence to understand *bif2* and *ba1* interaction. There are still other possibilities for phosphorylation of BA1 by BIF2 such as BIF2 may promote BA1 DNA binding ability, promote its dimerization ability or stabilize BA1 proteins. Therefore, to understand the role of the interaction of BIF2 and BA1 in vivo, we need further experimental evidence to rule out some of the possibilities.

How to coordinate all the facts that *bif2* regulates *ba1* at both transcription level and protein level? One hypothesis is that *ba1* activates its own transcription. This may lead to the deduction that BA1 may regulate its own transcription after it is activated by BIF2 phosphorylation. This fits with the result that *ba1* expression is down regulated in *bif2*/+ heterozygous mutants (Fig. 4a). Thus, transcription of *ba1* is sensitive to the *bif2* copy number. The reducting of *bif2* copy number in the *bif2*/+ heterozygous plants leads to decreased BA1 and less *ba1* is expressed as a result. Since we have only repeated this experiment twice, more experimental support is needed to finally draw a conclusion based on this. However, it is reasonable to propose that BA1 is activated at the protein level by BIF2 and at the transcription level by itself.

Based on the argument above, we propose the hypothesis that *ba1* is activated by itself at the transcription level when enough BIF2 is present. However, based on the hypothesis that *bif2* is responsible to activate *ba1* at the transcriptional level, we can not explain why there is some ear formation in *bif2* mutants but not *ba1* mutants. Therefore, *bif2* and *ba1* interaction in axillary meristem initiation may differ between the tassel and the ear. There are many examples in maize in which the same gene has different functions in tassel and ear development such as *zag1* and *zag2* (Schmidt et al., 1993; Mena et al, 1996). An alternative hypothesis to explain the different functions of *bif2* and *ba1* in male and female maize inflorescence development is that there are genes redundant with *bif2* and *ba1*. As mentioned previously, it is known that *bif2* and *ba1* each have a duplicate gene in the maize genome. These duplicate genes may play a redundant role to their homologs, *bif2* and *ba1*, when *bif2* and *ba1* are absent.

We also analyzed additional genotypes: *bif2/+;ba1/ba1*, *bif2/bif2;ba1/+* and *bif2/bif2;ba1/ba1*. Most of the analysis in Figure 1c is consistent with the model we proposed. We observed more spikelets in *bif2/+;ba1/ba1* and *bif2/bif2;ba1/+* mutants compared with *bif2/bif2;ba1/ba1* mutants. Both observed differences are statistically significant ($P<0.05$). Therefore, one copy of wild type *bif2* or *ba1* could maintain the alternative pathways and therefore some spikelet initiation, which is consistent with knocking down both *bif2* and *ba1* functions causing no spikelet initiation. In addition, there were more spikelets in *bif2/+;ba1/ba1* mutants compared with *bif2/bif2;ba1/+* mutants which was statistically significant ($P<0.05$). This is consistent with the model also. First, in *bif2/bif2;+/+* mutant, the *ba1* transcripts are the same as *ba1/ba1;+/+* mutants. Thus, the residual *ba1* transcript in *bif2/bif2;ba1/+* mutants should be around half that of *+/+;ba1/ba1* mutants. Therefore, there should be more spikelet formation in *+/+;ba1/ba1* mutants than in *bif2/bif2;ba1/+* mutants.

However, we can't explain the increased number of spikelets in *bif2/+;ba1/ba1* mutants compared with *bif2/bif2;+/+* and *+/+;ba1/ba1* mutants with the model (Fig. 1c). However, the difference in spikelet number increase in *bif2/+;ba1/ba1* mutants compared with *bif2/bif2;+/+* and *+/+;ba1/ba1* mutants was not statistically significant ($P=0.108$ & $P=0.166$). Therefore, whether this is true or not still needs to be confirmed by future analysis of more individuals.

As for vegetative development, leaf number is not different in *ba1* mutants compared with wild type plants (Fig. 3b). However, the plant height is reduced in *ba1* mutants compared with wild type. This could be explained by the measurement of the above ground plant height, which means from the ground to the tip of the tassel. Since the tassel of *ba1* mutants is shorter than the wild type tassel, the difference in plant height might be due to the tassel size difference. Second, as *ba1* is downstream of polar auxin transport and may be an auxin response gene (AuxRE TGTCTC detected in the promoter region), the mutant plants may have some defects in auxin response causing them to become shorter compared than the wild type plants.

In *bif2* mutant plants, leaf number is reduced and the plant height is shorter than the normal plants. Since *bif2* has a broader role than *ba1* in auxin transport and axillary meristem initiation, the *bif2* mutant plants are shorter than *ba1* mutants due to the initiation of fewer leaves. Moreover, the leaf number and the plant height is reduced further in the *bif2;ba1* double mutants compared with either of the single mutants. This indicates that both *bif2* and *ba1* have a role in vegetative development. This is supported by double mutant analysis of *bif2;tb1* and *ba1;tb1*(McSteen and Hake, 2007, Ritter et al, 2002). *ba1* is completely epistatic to *tb1* and inhibits tiller formation in the double mutant and *bif2* partially inhibits *tb1* in tiller formation in the double mutants. These analyses suggest that both *ba1* and *bif2* may play a role in vegetative axillary meristem formation. Although we do not fully understand the role of *bif2* and *ba1* in leaf initiation and plant height, it reminds us that *bif2* and *ba1* may have multiple roles and their functions are in multiple organs. Furthermore, these roles may probably involve auxin transport and auxin responses. Since *ba1* is not expressed in leaves, it must have a non autonomous effect in maize vegetative development.

Of course, we can not explain everything only based on genetic interaction analysis. However, from the analysis above, the interaction between *bif2* and *ba1* is more complicated than we expected from the beginning. Both *bif2* and *ba1* have partially overlapping effects in vegetative and inflorescence development. *bif2* regulates *ba1* function by activating its expression at the transcription level and phosphorylation at the protein level. More research is needed to understand the basis of the interaction between *bif2* and *ba1* in the future.

Acknowledgement

We thank Deb Grove of the Huck Institutes Nucleic Acid Facility for conducting the real time RT PCR experiments, Missy Hazen of the Huck Institutes EM Facility for training on the SEM, and Matt Davis and Chris Hudson for help with *bif2* and *ba1* genotyping. We thank Chris Cook and Jeff Buterbaugh for help with plant height measurement and leaf counting. We thank Tony Omeis and Scott Harkom for plant care in the greenhouse and the field.

Figure 3.1 Quantification of total spikelet number in *bif2;ba1* double mutants

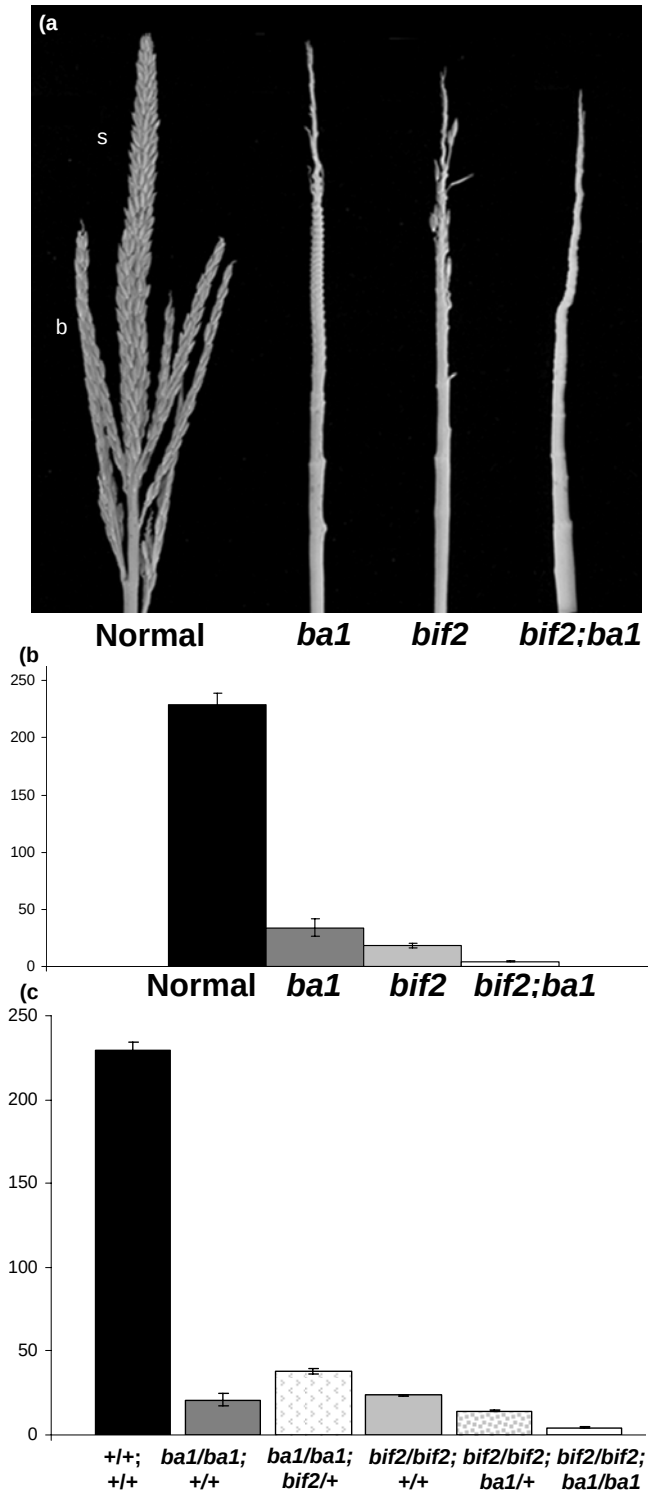

Figure 3.1 Maize inflorescence phenotype of *bif2;ba1* double mutants

(a) Mature tassel inflorescence phenotype. Normal tassel with branches (br) at the base and short branches called spikelet pairs (sp) covering the main spike and the branches. *ba1* tassel with no branches or spikelets. *bif2* tassel with no branches and few spikelets. *bif2; ba1* double mutant tassel with no branches or spikelets. (b) Quantification of total spikelet number in the mature tassel of four genotype categories (sample size: Normal: *bif2: ba1: bif2;ba1* =4:34:29:17). (c) Total spikelet number counted in the mature tassel of six genotype categories (sample size: Normal: *ba1/ba1;+/+: ba1/ba1;bif2/+: bif2/bif2;+/+: bif2/bif2;ba1/+: bif2/bif2;ba1/ba1* = 4:7:22:15:19:17)

Figure 3.2 SEM analysis of *bif2;ba1* double mutants

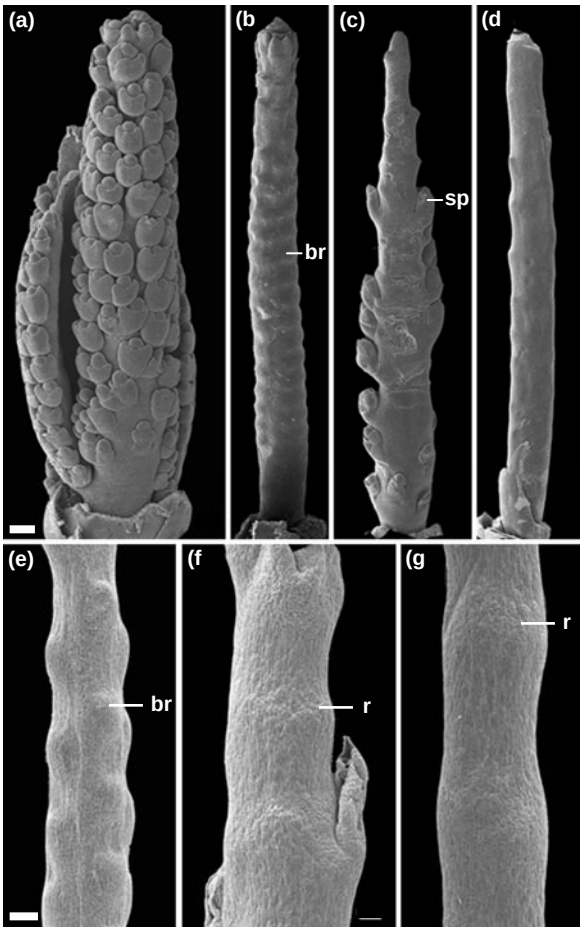

Figure 3.2 SEM analysis of *bif2; ba1* double mutants

(a–d) SEM view of the tassel, (a) Normal inflorescence, (b) *ba1* inflorescence with no spikelets and regular bract primordia (br) visible on the surface of the rachis, (c) *bif2* inflorescence with few spikelets (sp), (d) *bif2; ba1* inflorescence with no spikelets, (e-g) Close-up of surface of inflorescence rachis, (e) *ba1* rachis illustrating regular bract primordia (br) on the surface, (f) *bif2* rachis indicating ridges (r) which surround the rachis, (g) *bif2; ba1* rachis showing ridges (r) similar to those seen in *bif2*. Scale bars: (a-d) 200µm, (e-g) 100µm.

Figure 3.3 Phenotypic analysis of *bif2;ba1* double mutant

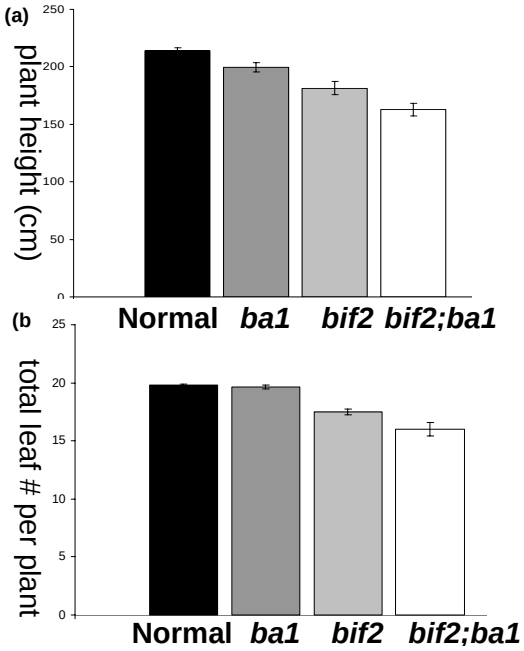

Figure 3.3 Phenotypic analysis of *bif2;ba1* double mutants

(a) Plant height was measured in centimeters and (b) leaf numbers were counted in normal, *ba1, bif2* and *bif2;ba1* plants (sample size: Normal: *bif2: ba1: bif2;ba1* = 60:17:15:5).

Figure 3.4 Real time RT-PCR analysis of *bif2* and *ba1* expression in *bif2* and *ba1* single mutants

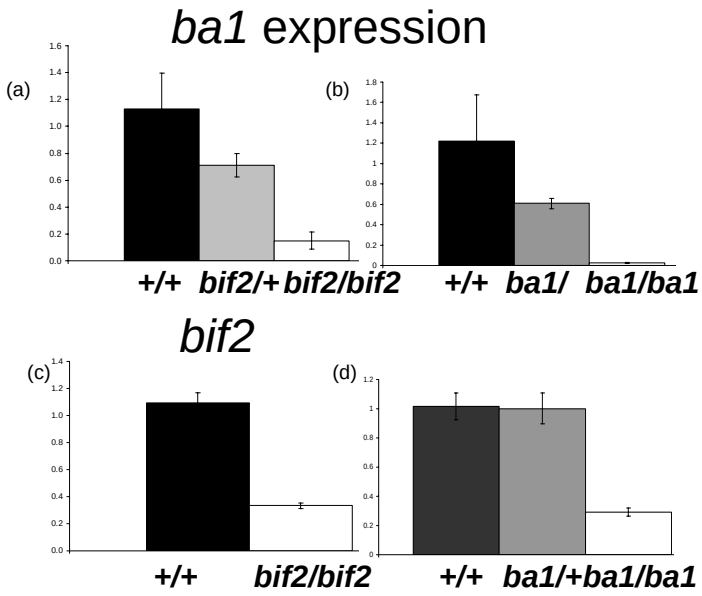

Figure 3.4 Real time RT-PCR analysis of *bif2* and *ba1* expression in *bif2* and *ba1* mutants

(a-b) *ba1* expression in normal siblings compared with *bif2* mutants (a) and *ba1* mutants (b). (c-d) *bif2* expression in normal siblings compared with *bif2* mutants (c) and *ba1/ba1* mutants (d).

Figure 3.5 Model for *bif2* and *ba1* interaction

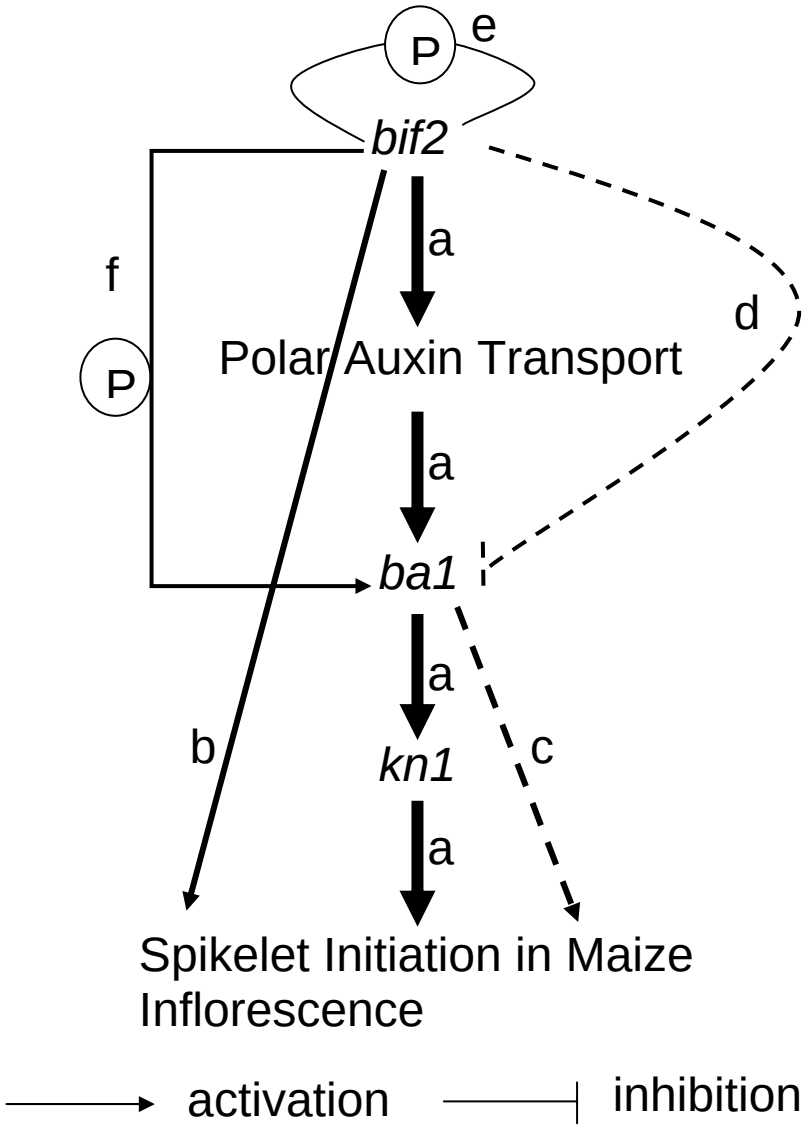

Figure 3.5 Model for *bif2* and *ba1* interaction

a) The cental pathway is the main pathway which shows that *bif2* is upstream of polar auxin transport to activate *ba1* in spikelet initiation during maize inflorescence development.

b) This pathway indicates that *bif2* may activate other factors to initiate spikelets.

c) The dotted arrow shows that *ba1* may have an alternative pathway to regulate spikelet initiation independent of *bif2*.

d) The dotted pathway is putative pathway suggested but not strongly supported by the data.

e-f) It is also not clear that how *bif2* auto phosphorylation (e) and phosphorylation on *ba1* (f) may be involved in the function and interaction of *bif2* and *ba1*.

Notes: P in the figure stands for phosphorylation

Table 3.S1 Chi-square analysis of double mutants

Family A;B	Total plants	Normal O	Normal E	gene*a* O	gene*a* E	gene*b* O	gene*b* E	*a;b* O	*a;b* E	X^2 P value
ba1;R1[1]	117	68	65.813	29	29.25	20	21.938	--	--	>0.5
bif2;R1[2]	86	45	48.375	26	21.5	15	16.125	--	--	>0.5
bif2;ba1[3]	183	98	102.938	33	34.313	37	34.313	15	11.438	>0.5

[1:] in *ba1;R1* double mutants, the expected segregation ratio is Normal: *ba1*: *R1* = 9:4:3
[2:] in *bif2;R1* double mutants, the expected segregation ratio is Normal: *bif2*: *R1* = 9:4:3
[3:] in *bif2;ba1* double mutants, the expected segregation ratio is Normal: *bif2*: *ba1*: *bif2;ba1* = 9:3:3:1

References

Barazesh, S., and McSteen, P. (2008). *Barren inflorescence1* functions in organogenesis during vegetative and inflorescence development in maize. *Genetics* **179,** 389-401.

Friml, J., Yang, X., Michniewicz, M., Weijers, D., Quint, A., Tietz, O., Benjamins, R., Ouwerkerk, P.B., Ljung, K., Sandberg, G., Hooykaas, P.J., Palme, K., and Offringa, R. (2004). A PINOID-dependent binary switch in apical-basal PIN polar targeting directs auxin efflux. *Science* **306,** 862-865.

Gallavotti, A., Zhao, Q., Kyozuka, J., Meeley, R.B., Ritter, M.K., Doebley, J.F., Pe, M.E., and Schmidt, R.J. (2004). The role of *barren stalk1* in the architecture of maize. Nature **432,** 630-635.

Guilfoyle, T.J., and Hagen, G. (2007). Auxin response factors. Curr Opin Plant Biol **10,** 453-460.

Jackson, D., Veit, B., and Hake, S. (1994). Expression of maize *KNOTTED1* related homeobox genes in the shoot apical meristem predicts patterns of morphogenesis in the vegetative shoot. *Development* **120,** 405-413.

Kerstetter, R.A., Laudencia-Chingcuanco, D., Smith, L.G., and Hake, S. (1997). Loss-of-function mutations in the maize homeobox gene, *knotted1*, are defective in shoot meristem maintenance. *Development* **124,** 3045-3054.

Martienssen R. and Irish V. (1999). Copying out our ABCs: the role of gene redundancy in interpreting genetic hierarchies. *Trends Genet* **15,** 435-437

Mena, M., Ambrose, B. A., Meeley, R. B., Briggs, S. P., Yanofsky, M. F. and Schmidt, R. J. (1996). Diversification of C-function activity in maize flower development. *Science* **274,** 1537-1540

McSteen, P., and Hake, S. (2001). barren inflorescence2 regulates axillary meristem development in the maize inflorescence. Development **128,** 2881-2891.

McSteen, P., and Leyser, O. (2005). Shoot branching. *Annual Review of Plant Biology* **56,** 353-374.

McSteen, P., Malcomber, S., Skirpan, A., Lunde, C., Wu, X., Kellogg, E., and Hake, S. (2007). *barren inflorescence2* encodes a co-ortholog of the *PINOID* serine/threonine protein kinase and is required for organogenesis during inflorescence and vegetative development in maize. *Plant Physiol* **144,** 1000-1011.

Ritter, M.K., Padilla, C. M. and Schmidt, R. J. (2002). The Maize Mutant BARREN STALK1 Is Defective in Axillary Meristem Development. Am J Bot **89,** 203-210.

Schmidt, R.J., Veit, B., Mandel, M.A., Mena, M., Hake, S., and Yanofsky, M.F. (1993). Identification and molecular characterization of *ZAG1*, the maize homolog of the Arabidopsis floral homeotic gene *AGAMOUS*. *Plant Cell* **5,** 729-737.

Skirpan, A., Wu, X., and McSteen, P. (2008). Genetic and physical interaction suggest that BARREN STALK1 is a target of BARREN INFLORESCENCE2 in maize inflorescence development. *Plant J* PMID: 18466309.

Wu, X., and McSteen, P. (2007). The role of auxin transport during inflorescence development in maize (*Zea mays, Poaceae*). *Am J Bot* **94,** 1745-1755.

CHAPTER FOUR

Suppressor of sessile spikelets1(Sos1) functions in the *ramosa* pathway controlling meristem determinacy in maize

This chapter has been written and submitted to *Plant Physiology* in June 20th, 2008.

4.1 Abstract

The spikelet, which is a short branch bearing the florets, is the fundamental unit of grass inflorescence architecture. In most grasses, spikelets are borne singly on the inflorescence. However, paired spikelets are characteristic of the Andropogoneae, a tribe of 1000 species including maize (*Zea mays*). The *Suppressor of sessile spikelets1* (*Sos1*) mutant of maize produces single instead of paired spikelets in the inflorescence. Therefore, the *sos1* gene may have been involved in the evolution of paired spikelets in the Andropogoneae. In this paper, we show that *Sos1* is a semi-dominant, antimorph mutation. *Sos1* mutants have fewer branches and spikelets because fewer spikelet pair meristems (SPM) are produced and because the SPM that are produced make one instead of two spikelet meristems (SM). The interaction of *Sos1* with the *ramosa* mutants, which produce more branches and spikelets, was investigated. The results show that *Sos1* has an epistatic interaction with *ramosa1* (*ra1*) and a synergistic interaction with *ramosa2* (*ra2).* Moreover, *ra1* mRNA levels are reduced in *Sos1* mutants while *ra2* levels are unaffected. Based on these genetic and expression studies, we propose that *sos1* functions in the *ra1* branch of the *ramosa* pathway controlling meristem determinacy.

4.2 Introduction

Organogenesis in plants is controlled by meristems (Steeves and Sussex 1989). Organs are produced in the peripheral zone of the meristem while the central zone retains a pool of cells that do not differentiate enabling the meristem to maintain itself. Meristems are defined by their determinacy, identity and position (McSteen et al. 2000). Determinate meristems produce a limited number of structures before terminating while indeterminate meristems have the potential to continue producing organs indefinitely (Bortiri and Hake 2007, Sablowski 2007). Apical meristems are indeterminate in many species. The shoot apical meristem gives rise to the vegetative shoot while the inflorescence apical meristem gives rise to the flowering shoot. Axillary meristems, which form in the axils of leaf primordia, can be indeterminate and give rise to branches or can be determinate and give rise to flowers.

In maize (*Zea mays*) inflorescence development, there are multiple types of axillary meristems which differ in their determinacy, resulting in a highly branched inflorescence (Irish 1997a, Bortiri and Hake 2007). The mature male inflorescence consists of a main spike and several long lateral branches, which are covered by short branches called spikelet pairs (Fig. 1A) (Kiesselbach 1949). The spikelet is defined as a short branch with two leaf like glumes enclosing the florets (Clifford 1987). During inflorescence development, the apical inflorescence meristem (IM) produces axillary meristems called branch meristems (BM) which are indeterminate and produce the branches. After several branches are made the IM switches abruptly to producing spikelet pair meristems (SPM) which are determinate because they produce two spikelets. Spikelet meristems (SM) are determinate as they produce two floral meristems (FM) which then produce the floral organs. Although maize has separate male and female inflorescences, called the tassel and ear respectively, early development is similar except that ears do not produce branches.

Two models had been proposed to understand how the SPM produces two SM and the SM produces two FM (Irish 1997a, Chuck et al. 1998, Irish 1998, Kaplinsky and Freeling 2003). In the lateral branching model, the SPM produces two SM by lateral branching and a residual meristem remains between the two SM (Chuck et al. 1998). In the conversion model, the SPM initiates an SM and then the remaining SPM converts to a

SM (Irish 1997a, 1998). Strong support for the conversion model was recently provided by experiments in which normal maize plants were treated with auxin transport inhibitors which inhibited SM initiation but did not inhibit the conversion of the SPM to a SM resulting in the formation of single spikelets (Wu and McSteen 2007).

The *Suppressor of sessile spikelet (Sos1)* mutant produces single instead of paired spikelets in the inflorescence and hence is more determinate than normal (Doebley et al. 1995). In normal plants, one spikelet is attached to the inflorescence rachis by a pedicel and is called the pedicellate spikelet, while the other spikelet, which has no pedicel, is called the sessile spikelet. In *Sos1* mutants, the sessile spikelet does not form resulting in single pedicellate spikelets. Single pedicellate spikelets are also characteristic of mutations affecting auxin transport. For example, *Barren inflorescence1 (Bif1)* and *barren inflorescence2 (bif2)* mutants, which are defective in auxin transport produce single spikelets (McSteen and Hake 2001, McSteen et al. 2007, Barazesh and McSteen 2008). *barren stalk 1 (ba1)*, which is proposed to act both upstream and downstream of auxin transport, also produces single spikelets when mutated (Ritter et al. 2002, Gallavotti et al. 2004, Wu and McSteen 2007, Gallavotti et al. 2008, Skirpan et al. 2008).

The determinacy of the SPM is positively regulated by the *ramosa* pathway (McSteen 2006, Kellogg 2007). *ramosa1* (*ra1*) encodes a zinc finger transcription factor expressed at the base of the SPM (Vollbrecht et al. 2005). In *ra1* mutants, the tassel and ear are highly branched because SPM become indeterminate and grow out to produce extra spikelets (Gernart 1912, Vollbrecht et al. 2005). *ra1* acts downstream of *ra2*, which encodes a LOB domain transcription factor expressed in the anlagen of BMs, SPMs and SMs (Bortiri et al. 2006a). *ra1* also acts downstream of *ramosa3 (ra3)* which encodes a trehalose-6-phosphate phosphatase (Satoh-Nagasawa et al. 2006). Interestingly, although *ra2* and *ra3*-like genes are present in other grasses such as rice, *ra1* has been identified only in the Andropogoneae, the clade to which maize belongs.

In the vast majority of grasses including rice, bamboo, barley and wheat, spikelets are produced singly (Clifford 1987). The production of paired spikelets is characteristic of the Andropogoneae, a tribe of 1000 species including maize, *Miscanthus*, sugarcane and sorghum (Kellogg 2000, G.P.W.G. 2001, Kellogg 2001). In the Paniceae tribe, which is sister to the Andropogoneae, spikelets are paired with bristles which are

modified spikelets (Doust and Kellogg 2002). Hence, the paired spikelet is a derived trait that arose at the base of the Panicoideae subfamily. It has been suggested that *ra1* may have been recruited for the evolution of the paired spikelet trait (Vollbrecht et al. 2005, McSteen 2006). As *Sos1* mutants produce single instead of paired spikelets, we propose that the *sos1* gene may also have been involved in the evolution of the paired spikelet in the Andropogoneae.

In this paper, we use quantitative analysis, scanning electron microscopy (SEM) and histology to show that the *Sos1* mutation causes defects in SPM and SM development in both the tassel and ear. We use dosage analysis to show that *Sos1* is an antimorph, i.e., a dominant negative mutation. Genetic interaction studies show that *bif2* and *ba1* function upstream of *sos1*. Moreover, genetic and expression analyses provide evidence that the *sos1* gene acts in the *ra1* branch of the *ramosa* pathway controlling meristem determinacy.

4.3 Materials and Methods

4.3.1 Plant Growth and Mature Phenotype Characterization

The S*os1-Reference* allele was obtained from the Maize Genetics Cooperation Stock Center (stock 427I) and backcrossed six times into the B73 genetic background of maize (*Zea mays*). Analysis of mature phenotype was carried out on plants grown at Rock Springs, PA during the summer. The plants were genotyped as *Sos1* heterozygotes or homozygotes using SSR marker *umc1294*, which is the closest genetic marker identified so far (umc1294F: 5'-GCC GTC AAC GGG CTT AAA CT-3' and umc1294R: 5'-GCC TCC ACG TCT CTC GTC TCT T-3'). For phenotype characterization, tassels and ears were collected at maturity from normal, *Sos1/+* and *Sos1/Sos1* plants from segregating families. Branch number and the number of paired versus single spikelets on the main spike were counted on the tassels after anthesis. The sample size was 28 normal, 35 *Sos1/+* and 33 *Sos1/Sos1* in the data presented in Fig. 1B,C. Kernel number was counted on open pollinated ears. The sample size was 10 normal, 13 *Sos1/+* and 15 *Sos1/Sos1* in the data presented in Fig. 1E,F.

4.3.2 SEM and Histology

Immature ears (5-20 mm) were collected from plants grown for eight weeks during the summer at Rock Springs, PA. Immature tassels (3-6 mm) were obtained from five week old plants grown in the spring in the greenhouse with supplemental lighting. Both tassels and ears were fixed and prepared for SEM as described (Wu and McSteen 2007). In addition, tassels and ears were embedded in wax and sectioned for TBO staining as described (Wu and McSteen 2007).

4.3.3 Dosage Analysis

Dosage analysis was conducted by crossing known hyperploids of the B-A translocation line, TB-4Sa (marked with *sugary1*, Coop stock 421D) as males to normal plants or plants heterozygous for *Sos1*. TB-4Sa is a reciprocal translocation of the short arm of chromosome 4 with the supernumery B chromosome, which due to a very high rate of non-disjunction during the second mitotic division of pollen development gives rise to pollen with either two or zero copies of chromosome 4S (Roman 1947, Beckett 1978, 1994). The ploidy of the F1 progeny can be determined by the rate of pollen abortion (Roman 1947, Carlson 1994). Pollen abortion was scored using a pocket microscope on four consecutive mornings as the anthers started to shed fresh pollen (Phillips 1994). As had been observed previously for TB4Sa, there was 50% pollen abortion in hypoploid plants and 2-10% pollen abortion in hyperploid plants (Carlson 1994) (D. Auger, South Dakota State University, personal communication). The tassels and ears of hypoploids and hyperploids were collected at maturity for phenotype analysis. The percentage of paired and single spikelets were counted on a 15 cm region of the tassel main spike after anthesis. For the analysis shown in Figure 4 the samples sizes were 13 Sos1/+/+ , 6 Sos1/-, 8 +/+/+ and 4 +/-.

4.3.4 Double Mutant Analysis

All double mutant segregating families were planted during the summer at Rock Springs, PA for two field seasons. At least 360 plants were planted for each double mutant combination each year. All plants were genotyped for *Sos1* with the SSR marker

umc1294 as described above. Each double mutant family was scored and chi-square analysis failed to reject the segregation ratio expected (data not shown).

Families segregating for *Sos1; bif2* and *Sos1; ba1* were genotyped for the *bif2* and *ba1* mutations as described (Skirpan et al. 2008). At maturity, tassel branch and spikelet number on the main spike was counted. For the analysis shown in Fig. 5B, the sample size was 2 normal, 4 *Sos1/+*, 11 *Sos1/Sos1*, 17 *bif2/bif2*, 13 *Sos1/+;bif2/bif2* and 13 *Sos1/Sos1; bif2/bif2*. For the analysis shown in Fig. 5D, the sample size was 2 normal, 5 *Sos1/+*, 7 *Sos1/Sos1*, 11 *ba1/ba1*, 11 *Sos1/+ ;ba1/ba1* and 8 *Sos1/Sos1; ba1/ba1*.

Families segregating *Sos1; ra1* and *Sos1; ra2* were scored and the tassel and ear phenotype analyzed at maturity (9 weeks old). Branches were removed from the tassels and classified according to (Vollbrecht et al. 2005, Bortiri et al. 2006a). For the analysis shown in Fig. 6B, the sample size was 4 normal, 9 *Sos1/+*, 4 *Sos1/Sos1*, 3 *ra1/ra1*, 10 *Sos1/+; ra1/ra1* and 10 *Sos1/Sos1; ra1/ra1*. For the analysis shown in Fig. 7B, the sample size was 4 normal, 6 *Sos1/+*, 4 *Sos1/Sos1*, 6 *ra2/ra2*, 8 *Sos1/+; ra2/ra2* and 9 *Sos1/Sos1; ra2/ra2*.

All graphs depict mean plus or minus standard error of the mean (s.e.). Probability values were determined from Student's two tailed *t* tests performed in Microsoft Excel 2003.

4.3.5 Real Time RT-PCR

Total RNA was extracted from 3-5 mm tassels from normal, *Sos1/+* and *Sos1/Sos1* plants with the NucleoSpin® RNA Plant kit (Macherey-Nagel GmbH & Co. KG, Germany). Four to six samples from each class were used as biological replicates. Three technical replicates for each biological replicate were performed. Synthesis of cDNA, real time RT-PCR and analysis was performed as described (Barazesh and McSteen 2008). To detect *ra1* expression, the Taqman® probe was (FAM-5'-ATC CAC AGG CTG GAC AGG GCC A-3'-BHQ) and the RT-PCR primers were ra1F (5'- GCT GGG AGG CCA CAT GAA-3') and ra1R (5'- GTG AAG TGT ACT GTT GGT GGA TCA G-3'). To detect *ra2* expression, the Taqman® probe was (FAM-5'-TCG TCA TTA GTA GCT CCC CAG GCG C-3'-BHQ) and the RT-PCR primers were ra2F (5'- TGC TAC TTC ATG CGG AAC CA -3') and ra2R (5'- TTA GCC ACG GAA GCG

TAA GG -3'). The internal control for amplification was *ubiquitin* (*ubq*). To detect *ubq* expression, the Taqman® probe was (5' FAM-AAA TCC ACC CGT CGG CAC CTC C-3' BHQ) and the RT-PCR primers were ubqF (5'-CTC TTT CCC CAA CCT CGT GTT-3') and ubqR (5'-ACG AGC GGC GTA CCT TGA-3').

4.4 Results

The *Sos1-Reference* allele arose spontaneously (Doebley et al. 1995). Seeds were obtained from the Maize Genetics Coop and backcrossed six times to B73. The mutant had previously been reported to map to the short arm of chromosome 4 (Doebley et al. 1995). To generate a mapping population, *Sos1* (in the B73 background) was crossed to the Mo17 genetic background and backcrossed to Mo17. SSR markers were used to further define the location of *Sos1* to within 4 cM of *umc1294* in bin 4.02. Since the *umc1294* marker was polymorphic between B73 and the original background in which *Sos1* arose, this marker was used for genotyping *Sos1* in the B73 background. Genotyping combined with analysis of the phenotype determined that the *Sos1* mutation was semi-dominant rather than dominant as previously reported (Fig. 1) (Doebley et al. 1995).

4.4.1 *Sos1* Mutants Produce Fewer Branches and Spikelets

Sos1 mutants have defects in both the tassel and ear. In the tassel, *Sos1* mutant plants produced fewer branches and spikelets (Fig. 1A-C). Families segregating for *Sos1* were genotyped and the number of branches and spikelets were counted in normal siblings compared to plants heterozygous and homozygous for *Sos1*. These results showed that *Sos1*/+ and *Sos1/Sos1* mutants produced fewer branches than normal (Fig. 1B). To analyze the spikelet defects, the number of paired versus single spikelets was counted separately. While normal plants had paired spikelets, *Sos1*/+ and *Sos1*/*Sos1* mutants had more single than paired spikelets in the tassel (Fig. 1C).

The *Sos1* mutation also affected the ear. Normal ears are not branched but they produce spikelets pairs (Kiesselbach 1949). Each spikelet produces one floret (the lower floret aborts) which, when pollinated, gives rise to a single kernel (Cheng et al. 1983). The spikelets in the ear are sessile so the pairing is not obvious, but it leads to an even

number of rows of kernels in the mature ear. In *Sos1* mutants, there were fewer kernels in the ear (Fig. 1D). Quantification showed that the total number of kernels was reduced in *Sos1/+* and *Sos1/Sos1* mutants relative to normal ears (Fig. 1E). There was also a reduction in the number of rows of kernels with *Sos1/+* mutants producing a variable number of rows and *Sos1* mutants producing less than half the number of rows of normal siblings (Fig. 1F).

To determine the developmental basis for the production of fewer branches and spikelets in *Sos1* mutants, SEM analysis was performed on developing tassels and ears. In normal inflorescences, SPM are produced from the IM at the tip of the inflorescence (Fig. 2A). The SPM then produces two SMs (Fig. 2A,D). The identity of the meristem as a SM is indicated by the production of glumes, protective leaf-like organs, which are the first organs produced by the SM (Cheng et al. 1983). The outer glume (og) is produced on the abaxial side of the SM and the inner glume (ig) forms internal to the outer glume on the adaxial side of the SM (Fig. 2D). Early in ear development, *Sos1/+* and *Sos1/Sos1* mutants produced SPM as normal except that there appeared to be fewer rows (Fig. 2B,C). Later in ear development when paired SMs were visible in normal ears, *Sos/Sos1* mutants had single SMs and *Sos1/+* mutants had a mixture of single and paired SMs (Fig. 2D-F). Similarly, in the tassel, SPM of normal plants produced two SMs (Fig. 2G), while *Sos/Sos1* mutants produced single SMs (Fig. 2I) and *Sos1*/+ mutants produced either one or two SMs (Fig. 2H). Hence, in *Sos1* mutants, SPMs produce one instead of two SMs and therefore are more determinate than normal.

If the only defect in *Sos1* mutants was the production of single instead of paired spikelets then we would expect the mutants to produce half the number of rows of kernels as normal ears. However, *Sos1/Sos1* mutants produced less than half the normal number of kernel rows (Fig. 1F) (Doebley et al. 1995). This is indicative of an additional defect in SPM initiation. To analyze the defects in SPM initiation, inflorescences were embedded in wax, sectioned and stained with Toludine Blue O (TBO). Early in development, SPMs initiated in a ring around the circumference of the inflorescence. In cross section, normal ears initiated nine SPMs (Fig. 3A), heterozygous ears initiated eight SPMs (Fig. 3B) and homozygous ears initiated six SPMs (Fig. 3C). Therefore, cross sectional analysis clearly showed that *Sos1* mutants initiate fewer SPMs. Later, when

normal SPMs initiate two SMs (Fig. 3D), some of the SPMs in *Sos1/+* mutants initiated two SMs (Fig. 3E), while very few of the SPMs in *Sos1/Sos1* mutants initiated two SMs (Fig. 3F). Instead, SPMs converted directly to an SM as evidenced by the production of glumes (Fig. 3F).

Therefore, histological and SEM analyses show that *Sos1* mutants produce fewer spikelets for two reasons, (1) There are fewer rows of SPMs and (2) The SPMs convert directly to an SM without initiating a second SM, resulting in the formation of single instead of paired spikelets.

4.4.2 The *Sos1* Mutation is An Antimorph

Analysis of the *Sos1* phenotype showed that plants homozygous for the *Sos1* mutation had a more severe phenotype than plants heterozygous for *Sos1*, and hence the mutation is semi-dominant. Four types of dominant mutations have been defined (Muller 1932). The two types of gain of function mutations are, neomorph mutations, which confer a new function, and hypermorph mutations, which cause increased expression of the gene. Two types of loss of function mutations are hypomorph and antimorph. Hypomorph mutations are also called haplo-insufficient or dosage sensitive mutations because one wild type copy of the gene is not sufficient for function. In antimorphs, which are also called dominant negative mutations, the mutant copy of the gene interferes with the wild type gene function (Veitia 2007).

To distinguish between these types of mutations, dosage analysis is used to vary the dose of the wild type copy of the gene in the mutant background (Greene and Hake 1994). In a neomorph, there would be no effect of varying dose (Freeling and Hake 1985, Poethig 1988) while in a hypermorph, increasing the number of wild type copies would cause the phenotype to be more severe (Kessler et al. 2002). On the other hand, in hypo- and antimorphs, adding wild type copies would cause the phenotype to be weaker (Poethig 1988, Nelson et al. 2002). A hypomorph can be distinguished from an antimorph by looking at the effect of varying the wild type copy number of the gene in the wild type background. Removing one wild type copy of the gene would cause a visible phenotype if the gene was haplo-insufficient and the mutation was a hypomorph but not if the mutation was an antimorph.

To determine the phenotypic effect of varying the wild type dose of *sos1*, pollen from hyperploids of the B-A translocation line, TB-4Sa, was crossed onto normal plants or plants heterozygous for *Sos1*. The F1 of the cross was analyzed for ploidy level (by scoring pollen abortion, see Materials and Methods) and for severity of phenotype (by counting the percentage of single spikelets in the tassel and the number of kernels in the ear). These results showed that *Sos1* plants with an extra copy of the short arm of chromosome 4 (*Sos*/+/+, hyperploid) had a weaker phenotype than plants that were missing a normal copy of the short arm of chromosome 4 (*Sos*/-, hypoploid) as they had a higher percentage of paired spikelets (Fig. 4A). Similar results were also observed in the ear (data not shown). These results show that *Sos1* is not a neomorph, as there was an effect of varying gene dosage and not a hypermorph, as the hyperploid was not more severe than the hypoploid.

To distinguish if *Sos1* was a hypomorph or an antimorph mutation, we generated a dosage series for chromosome 4S in a wild type genetic background. Normal plants missing one copy of the short arm of chromosome 4 did not have an *Sos1* phenotype. There were mostly paired spikelets in both the hypoploid (+/-) and the hyperploid (+/+/+) (Fig. 4B). This result indicates that the wild type *sos1* gene is not haplo-insufficient and therefore that the *Sos1* mutation is not a hypomorph. Thus, the *Sos1* mutation is likely an antimorph or dominant negative mutation.

4.4.3 *bif2* and *ba1* Act Upstream of *sos1*

bif2 and *ba1* are required for initiation of all axillary meristems during vegetative and reproductive development, with *bif2* proposed to act upstream of *ba1* (McSteen and Hake 2001, Ritter et al. 2002, Gallavotti et al. 2004, McSteen et al. 2007, Wu and McSteen 2007, Skirpan et al. 2008). *bif2* and *ba1* mutants produce fewer branches and fewer spikelets (McSteen and Hake 2001, Ritter et al. 2002). Furthermore, a characteristic of both mutations is the production of single spikelets (McSteen and Hake 2001, Gallavotti et al. 2004). Therefore, we investigated the genetic interaction between *sos1* and *bif2* or *ba1*.

To determine if *sos1* acted in the same pathway as *bif2*, double mutants were constructed. The F2 families were genotyped for both *bif2* and *Sos1* and the total number

of spikelets on the main spike were counted. Plants that were *Sos1*/+; *bif2/bif2* or *Sos1*/*Sos1*; *bif2/bif2* were indistinguishable from *bif2* single mutants (Fig. 5A). Quantification of spikelet number showed that there was no enhancement in severity of the double mutant phenotype compared with the *bif2* single mutant (Fig. 5B, P=0.55 for *Sos/+; bif2/bif2* and P=0.59 for *Sos1*/*Sos1*; *bif2/bif2*). Since the phenotype of the double mutant is similar to *bif2,* we conclude that *bif2* is upstream of *sos1*. This is in agreement with the earlier developmental defects reported in *bif2* mutants (McSteen and Hake 2001).

Similarly, *Sos1;ba1* double mutants resembled *ba1* single mutants with a barren tassel and no ears (Fig. 5C). Quantification of the spikelet number defects showed no enhancement of the severity of the double mutant phenotype compared to *ba1* single mutants (Fig. 5D, P=0.17 for *Sos1*/+; *ba1/ba1* and P=0.20 for *Sos1*/*Sos1*; *ba1/ba1*). Hence, *ba1* is upstream of *sos1* in agreement with its role in the *bif2* pathway (Ritter et al. 2002, Gallavotti et al. 2004, Wu and McSteen 2007, Skirpan et al. 2008).

4.4.4 *Sos1* Suppresses the *ra1* Mutant Phenotype

Sos1 mutants have single instead of paired spikelets because SPMs produce one instead of two SM. Hence, the SPM is more determinate than normal in *Sos1* mutants. Therefore, the *sos1* gene could be considered a negative regulator of the determinacy of the SPM. In *ra1* mutants, the SPM are indeterminate resulting in the production of highly branched tassels and ears (Fig. 6A,C) (Gernart 1912, Vollbrecht et al. 2005). The *ra1* gene is interpreted as a positive regulator of SPM determinacy (Vollbrecht et al. 2005). Because *Sos1* and *ra1* mutants have opposite effects on SPM determinacy, we tested if the corresponding genes acted in the same pathway by constructing double mutants.

In the tassel, *Sos1*/*Sos1*; *ra1/ra1* double mutants were less branched than *ra1* single mutants (Fig. 6A). To quantify the effects of both mutations, the branches on the tassels were removed, classified and counted using a scheme similar to that used to analyze *ra1* (Fig. 6B) (Vollbrecht et al. 2005). Normal plants produce branches before switching abruptly to producing spikelet pairs. *ra1* mutants produce several intermediates between branches and spikelet pairs (Vollbrecht et al. 2005). These intermediates include “mixed branches” which are branches with a mixture of single and

paired spikelets, “spikelet multimers” which are branches with single spikelets, and “triple spikelets”. Our analysis confirmed that, similar to the previous report (Vollbrecht et al. 2005), *ra1* mutants had a gradation in phenotype from branches through to spikelet pairs with a delayed switch to SPM identity compared to normal (Fig. 6B). The branches in *Sos1* mutants were found to be mixed branches rather than true branches (Fig. 6B). *Sos1* mutants produced fewer branch types overall, and therefore had an earlier switch to SPM identity than normal. In the *Sos1*/*Sos1*; *ra1/ra1* double mutants, there was a suppression of the *ra1* phenotype. Branches were replaced by mixed branches, and there were fewer of all branch types compared to *ra1* single mutants (Fig. 6B).

The reduction in the number of branch types in *Sos1*/*Sos1*; *ra1/ra1* double mutants could potentially be explained by the fact that *Sos1* mutants produce fewer SPM. So, we also estimated the percentage of branch types compared to the total number of axillary structures produced by the tassel. In this case, the *Sos1* mutation still had a suppressive effect on the *ra1* phenotype, as the percentage of all branch types was reduced from 41.8% in *ra1* single mutants to 18.7% in *Sos1*/*Sos1*; *ra1/ra1* double mutants. Therefore, even taking into account the production of fewer SPM by *Sos1* mutants, branching in the double mutant tassel was suppressed.

The suppression of the *ra1* phenotype by *Sos1* was even more obvious in the ear than in the tassel. Ears of plants that were *Sos1*/+; *ra1/ra1* were less branched than *ra1* and even initiated some viable kernels which happens very rarely in *ra1* single mutants. Furthermore, in the *Sos1*/*Sos1*; *ra1/ra1* double mutant ear, branching was almost completely suppressed. In the most extreme examples, the ears looked like *Sos1* except that they were smaller and more barren (Fig. 6C).

To investigate the developmental basis for the suppression of *ra1* by *Sos1*, SEM analysis was performed on the ears of families segregating for both mutations. In normal ears, SPM produce two SM (Fig. 6D) while in *ra1* ears, each SPM becomes indeterminate and branches to continuously produce SM in a reiterative manner (Fig. 6E). *Sos1*/+; *ra1/ra1* ears were suppressed compared to *ra1* (Fig. 6E,F). The tip resembled *Sos1*, but at the base of the ear SPM branched to produce multiple SM, although not as many as in the *ra1* mutants (Fig. 6F). In severe cases, *Sos1*/*Sos1*; *ra1/ra1* produced ears that resembled *Sos1* (Fig. 6G). Furthermore, there was sometimes a barren patch along

the side of the ear in the double mutants (arrow, Fig. 6G), a phenotype which was not seen in either single mutant. This barren phenotype was also visible in the mature ear (Fig. 6C). Therefore, the *Sos1* mutation suppressed the phenotype of the *ra1* mutation in the ear.

4.4.5 *sos1; ra2* Double Mutants Have a Synergistic Phenotype

ra2 also functions in SPM determinacy. In *ra2* mutants, the SPM becomes indeterminate and produces extra branches and spikelets in the tassel (Fig. 7A) (Kempton 1923, Nickerson and Dale 1955, Bortiri et al. 2006a). However, the ear is only mildly affected with irregular rowing and occasional extra branches (Fig. 7E). *ra2* also plays unique roles in inflorescence development as, unlike *ra1*, tassel branches are upright and spikelet pedicels are elongated in *ra2* mutants (Bortiri et al. 2006a). *ra2* is proposed to act upstream of *ra1* (Vollbrecht et al. 2005, Bortiri et al. 2006a).

To test if *sos1* acted in the same pathway as *ra2*, double mutants were constructed. Surprisingly, *Sos1* had a synergistic interaction with *ra2* in both the tassel and the ear (Fig. 7). To determine the effect of the *Sos1* mutation on the *ra2* phenotype in the tassel, the branches were removed, classified and quantified using the same classification system used previously for *ra1* and *ra2* (Vollbrecht et al. 2005, Bortiri et al. 2006a). *ra2* mutants, like *ra1*, produced intermediates between branches and spikelets along the main spike except the phenotype was weaker than *ra1* (Fig. 7B) (Vollbrecht et al. 2005, Bortiri et al. 2006a). Both *Sos1* and *ra2* single mutants had a small effect on the total number of axillary structures produced by the tassel (Fig. 7B) (Bortiri et al. 2006a). Strikingly, there was a massive decrease (over three fold) in the total number of axillary structures produced by *Sos1/Sos1; ra2/ra2* double mutants compared to either single mutant (Fig. 7B). Both *Sos1* and *ra2* single mutants produce a small number of rudimentary spikelets with 1-2 glumes and no florets (called aborted spikelets). The axillary structures that were produced in the *Sos1/Sos1; ra2/ra2* double mutants consisted almost entirely of aborted spikelets (Fig. 7B,D). We interpret these phenotypes as a synergistic enhancement of the *ra2* defects.

In the *Sos1; ra2* double mutant ear, an enhancement of the phenotype of *ra2* was also apparent. The ears of *ra2* mutants only occasionally produce branches (Vollbrecht et

al. 2005, Bortiri et al. 2006a). However, *Sos1*/+; *ra2*/*ra2* and *Sos1*/*Sos1*; *ra2*/*ra2* ears were much more highly branched than *ra2* ears (Fig. 7E). *Sos1*/+; *ra2*/*ra2* produced branches with a few kernels on them while *Sos1*/*Sos1*; *ra2*/*ra2* branches were long and barren (Fig. 7F).

To understand the developmental basis for the enhanced branching and sterility of *Sos1; ra2* double mutant ears, SEM analysis was performed on developing ears. In normal ears, SPMs produced two SM (Fig. 7G) while in the *ra2* mutant, the SPM produced more than two SM and there were occasional branches (Fig. 7H). The *Sos1*/+; *ra2*/*ra2* mutants were more highly branched than *ra2* with each SPM branching multiple times (Fig. 7I). The branches were more elongated than *ra2* and produced few SM (Fig. 7H,I). In the *Sos1*/*Sos1*; *ra2*/*ra2* double mutant, the phenotype was further enhanced with elongated branches in place of SPM and even fewer SM (Fig. 7J). Therefore, *Sos1* enhanced the phenotype of the *ra2* mutant in both the tassel and ear implying that the corresponding genes function in parallel pathways in inflorescence development.

4.4.6 Expression of *ra1* and *ra2* in *Sos1* Mutants

To further test the role of *sos1* in the *ramosa* pathway, the relative mRNA expression level of *ra1* and *ra2* was tested in *Sos1* mutants using quantitative real time RT-PCR. The results showed that *ra1* mRNA levels were reduced in *Sos1/*+ and *Sos1/Sos1* mutants (Fig. 8A). The reduction was statistically significant (P= 0.029 *Sos/*+, 0.017 *Sos1/Sos1*). On the other hand, *ra2* mRNA levels were not statistically different from normal in either *Sos1/*+ or *Sos1/Sos1* mutants (Fig. 8B,P =0.20 *Sos/*+, 0.66 *Sos1/Sos1*). Therefore, in addition to having a different genetic interaction with *ra1* and *ra2*, *Sos1* mutations also had a different effect on *ra1* and *ra2* expression.

4.5 Disscusion

The most striking defect in *Sos1* mutants is that the SPM initiates one instead of two SMs. In addition, *Sos1* mutants have defects in SPM initiation. *Sos1* mutants also produce fewer branches. However, the branches that are produced are not normal branches but are “mixed branches” which are more determinate than normal. Once SMs are produced in *Sos1* mutants, they usually produce two florets. However, a small

percentage of aborted spikelets (spikelets with no florets) are apparent later in development. Rudimentary spikelets were also reported by (Doebley et al. 1995). Therefore, the *Sos1* mutation affects the initiation and determinacy of all meristems produced during inflorescence development.

4.5.1 The Role of *sos1* in the *ramosa* Pathway for Meristem Determinacy

ra1 and *ra2* mutants are highly branched because the SPM are indeterminate. Therefore, the role of the *ra1* and *ra2* genes is to impose determinacy on the SPM (Vollbrecht et al. 2005, Bortiri et al. 2006a), represented by an arrow in the model shown in Figure 8C. *ra2* is proposed to act upstream of *ra1* because *ra1* mRNA levels are reduced in *ra2* mutants, and double mutants between *ra2* and a weak allele of *ra1* have an enhanced phenotype (Vollbrecht et al. 2005, Bortiri et al. 2006a, Satoh-Nagasawa et al. 2006). Furthermore, *ra2* is proposed to have additional roles, independent of *ra1* (Bortiri et al. 2006a).

In *Sos1* mutants, the SPM are more determinate than normal producing one instead of two SM. The *Sos1* mutation is an antimorph, which is a type of dominant loss of function mutation (more correctly an antagonist of wild type function). Therefore, in *Sos1* mutants, the absence of the normal function of the *sos1* gene causes an increase in determinacy. One interpretation of the wild type function of the *sos1* gene is to oppose SPM determinacy, represented as a bar in Figure 8C. Another way of describing this is that the *sos1* gene confers indeterminacy on the SPM, but as the SPM is normally determinate we propose that *sos1* inhibits determinacy. As the *sos1* gene inhibits SPM determinacy, while the *ramosa* genes promote SPM determinacy, double mutants were constructed to test the genetic interaction between *sos1* and the *ramosa* genes. Surprisingly, we found a difference in the interaction between *sos1* and *ra1* or *ra2*.

We propose the model shown in Figure 8C to account for all of the genetic interaction and expression data. *Sos1*; *ra1* double mutants resemble *Sos1* single mutants. As the *Sos1* and *ra1* single mutants have opposite phenotypes, we interpret the double mutant result to mean that the wild type *sos1* gene functions downstream of *ra1* (Fig. 8C) (Avery and Wasserman 1992). Therefore, *ra1* could confer SPM determinacy by negatively regulating the *sos1* gene. Unexpectedly, *Sos1*; *ra2* double mutants had an

enhanced phenotype compared to *ra2* single mutants. The *Sos1*; *ra2* double mutant looks strikingly similar to the double mutant between *ra2* and a weak allele of *ra1* (Vollbrecht et al. 2005). One hypothesis to account for the enhancement of the *ra2* phenotype by the *Sos1* mutation would be if the *sos1* gene positively regulated the *ra1* gene. In support of this hypothesis, *ra1* mRNA levels are reduced in *Sos1* mutants. Therefore, we propose that *sos1* acts in the *ra1* branch of the *ramosa* pathway, providing a feedback loop to control SPM determinacy (Fig. 8C).

The *Sos1* mutation had a more suppressive effect on the *ra1* phenotype in the ear than the tassel. An alternative interpretation of the *Sos1;ra1* tassel phenotype would be that the *Sos1* and *ra1* mutations have an additive effect indicating that *Sos1* acts independently of the *ra1* pathway. However, the reduction of expression of *ra1* in *Sos1* mutants does not support an independent interaction. Furthermore, as there is a complete suppression of the *ra1* phenotype in the *Sos1; ra1* ear, we favor the hypothesis that the difference between the tassel and ear double mutant phenotypes is due to differences in modifying factors between the tassel and the ear. Differences in severity of tassel versus ear phenotypes are common in maize inflorescence determinacy mutants (Irish 1997a, b, Laudencia-Chingcuanco and Hake 2002, Kaplinsky and Freeling 2003, Bortiri et al. 2006a). One explanation is that the tassel forms in an apical position and the ear forms in an axillary position so their hormonal environments likely differ. Furthermore, sub-functionalization of duplicate genes between tassel and ear has been demonstrated (Mena et al. 1996). Moreover, the extent of branching is affected by environmental conditions indicating that additional modifying factors influence branching.

The *Sos1; ra2* double mutant had a synergistic effect on branching in the ear. An alternative interpretation is that the *Sos1; ra2* double mutant phenotype could be considered additive. For example, if the *ra2* mutation caused the SPM to become indeterminate but the SPM were unable to initiate sessile SMs due to the *Sos1* mutation. However, as the SPMs in the *Sos1; ra2* double mutant are more indeterminate than *ra2* single mutants, we conclude that the interaction between *Sos1* and *ra2* is not additive in the ear. Furthermore, the effect of the *Sos1* mutation on the *ra2* phenotype in the tassel is not additive.

Therefore, although other interpretations can be envisioned, we favor the model presented in Figure 8C because it explains all of the single and double mutant phenotypes as well as the expression studies. Dominant negative mutations can be caused by mutations in transcription factors that, for example, can dimerize but not bind DNA or can bind DNA but not activate transcription (Veitia 2007). Based on the *Sos1* mutant phenotype, genetic interaction with *ra1* and *ra2* and the decrease in *ra1* expression in *Sos1* mutants, we hypothesize that *sos1* may encode a transcription factor that interacts with *ra1*.

4.5.2 Additional Roles of *sos1, ra1* and *ra2* in Inflorescence Development

Besides the effect on determinacy of the SPM, the *Sos1; ra1* and *Sos; ra2* double mutants had additional defects in inflorescence development. This implies that the corresponding genes play additional roles in development that had not previously been discovered. *Sos1; ra1* double mutants produced barren patches in the ear which were not seen in either single mutant. This synergistic interaction could be explained by the function of both genes in the SPM. We infer that as the genes have opposing functions in the SPM, that in their absence the SPM sometimes fails to initiate. This effect was also seen in the tassel as there was an overall reduction in the number of axillary structures produced in the *Sos1; ra1* double mutant. In *Sos1*; *ra2* double mutants there was an even more severe reduction in the number of axillary structures produced in the tassel. These results indicate that the *sos1*, *ra1* and *ra2* genes play overlapping roles in the production of SPM in both the tassel and ear.

In the single *Sos1*, *ra1* and *ra2* mutants, a small number of aborted spikelets were produced in the tassel with *ra2* mutants having the strongest effect. In *Sos1; ra1* double mutants there was a somewhat additive increase in the number of aborted spikelets in the tassel compared to either single mutant. However, in *Sos1; ra2* double mutants, there was a synergistic increase in the number of aborted spikelets. In fact, almost all of the spikelets produced in the double mutant tassel were aborted. Therefore, we propose that *sos, ra1* and *ra2* also function in SMs.

4.5.3 Interaction of *sos1* with *bif2* and *ba1*

bif2 is proposed to regulate auxin transport while *ba1* has been interpreted to act either upstream or downstream of auxin transport (McSteen et al. 2007, Wu and McSteen 2007, Gallavotti et al. 2008). These mutants and others that affect auxin transport produce single spikelets (McSteen and Hake 2001, Gallavotti et al. 2004, Barazesh and McSteen 2008). Furthermore, treatment of normal maize inflorescences with auxin transport inhibitors later in development results in the production of single spikelets (Wu and McSteen 2007). Therefore, auxin transport is required for sessile spikelet initiation. Genetic analysis shows that there is no enhancement of the *bif2* and *ba1* phenotype by the *Sos1* mutation indicating that *sos1* acts in the same pathway as *bif2* and *ba1*. Thus, *Sos1* mutants may have a defect in enabling auxin, directly or indirectly, to initiate the sessile SM.

However, unlike *Sos1* mutants, *bif2* and *ba1* mutants have barren regions with no SPMs initiated in the inflorescence (McSteen and Hake 2001, Ritter et al. 2002). In addition, treatment of maize inflorescences with auxin transport inhibitors earlier in development results in the production of a barren inflorescence with no SPM (Wu and McSteen 2007). Although *Sos1* mutants produce fewer SPM than normal, the phyllotaxy of SPM initiation is not affected and no barren patches are visible in the single mutant. Therefore, *Sos1* mutants do not have a general defect in auxin transport, but rather, a specific defect in the sessile spikelet. Interestingly, *Sos1* mutants produce barren patches in the ear when in double mutant combination with *ra1*, indicating that *sos1* and *ra1* together play a broader role in SPM initiation.

We are currently fine mapping *Sos1* to identify the gene using positional cloning (Bortiri et al. 2006b). Cloning the *sos1* gene will elucidate the molecular basis for its interaction with *ra1*. Furthermore, the cloning of *sos1* will provide insight into its predicted role in the evolution of the paired spikelet in the Andropogoneae. Since *ra1* has only been identified in the Andropogoneae, it would be interesting to determine if *sos1* was co-opted at the same timepoint during the diversification of the grasses.

Acknowledgement

We thank Erik Vollbrecht for pointing out the similarity between *Sos1*; *ra2* and *ra1*; *ra2* double mutants and David Barnes and Sarah Hake for first discovering the *Sos1; ra2* interaction. We thank Deb Grove of the Huck Institutes Nucleic Acid Facility for conducting the real time RT-PCR experiments, Missy Hazen of the Huck Institutes Electron Microscopy Facility for training on the SEM, and Jeffrey Buterbaugh, Jason Hoar, Chris Cook, Kim Phillips, Matt Davis and Chris Hudson for help in the field and with *Sos1* genotyping. We thank the Maize Coop for *Sos1* seed, Frank Baker for seed of TB4Sa hyperploids and Don Auger for advice on TB dosage analysis. We thank Tony Omeis and Scott Harkcom for plant care. We thank members of the McSteen and Braun labs for discussion and comments on the manuscript.

Figure 4.1 *Sos1* tassel and ear phenotype

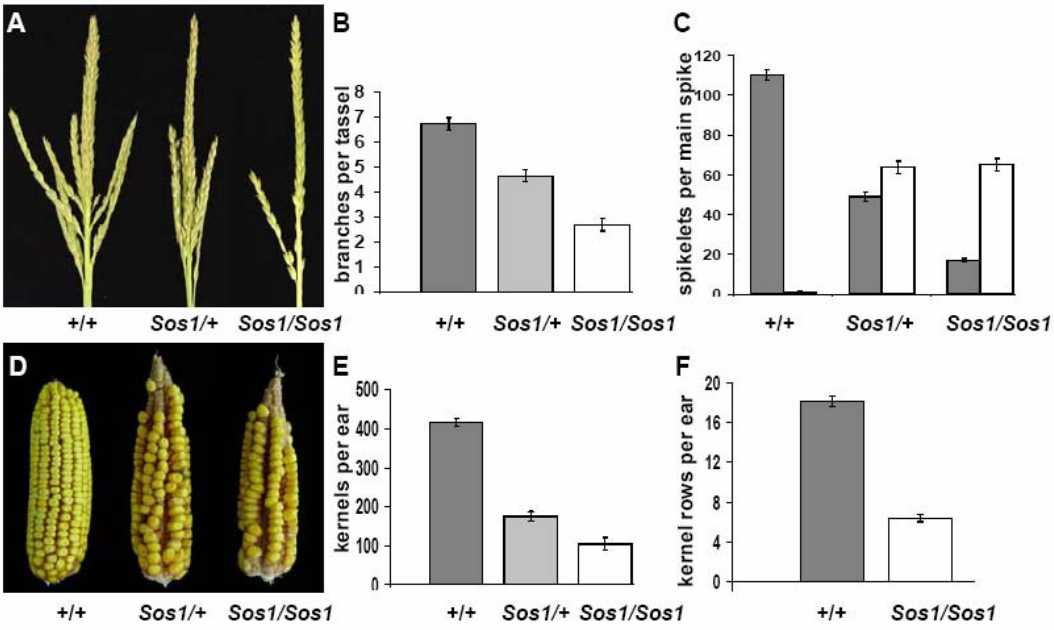

Figure 4.1 *Sos1* tassel and ear phenotype

(A) Photograph of mature tassels before anthesis. Normal tassels have long branches at the base of a main spike. Spikelet pairs cover the branches and the main spike. *Sos1*/+ mutants have a sparse appearance due to the production of fewer branches and spikelets. *Sos1/Sos1* mutants have very few branches and single spikelets. (B) Quantification of branch number in the tassel. (C) Quantification of the number of paired (grey bar) versus single (white) spikelets on the tassel main spike. (D) Photograph of mature ears after open pollination. Normal ears have paired rows of kernels. *Sos1*/+ and *Sos1/Sos1* ears have fewer rows of kernels in the ear. (E) Quantification of the number of kernels per ear. (F) Quantification of the number of kernel rows per ear. *Sos1/Sos1* ears have fewer than half the number of rows compared to normal siblings. All graphs are mean plus or minus s.e.

Figure 4.2. Scanning electron microscopy of *Sos1* inflorescences

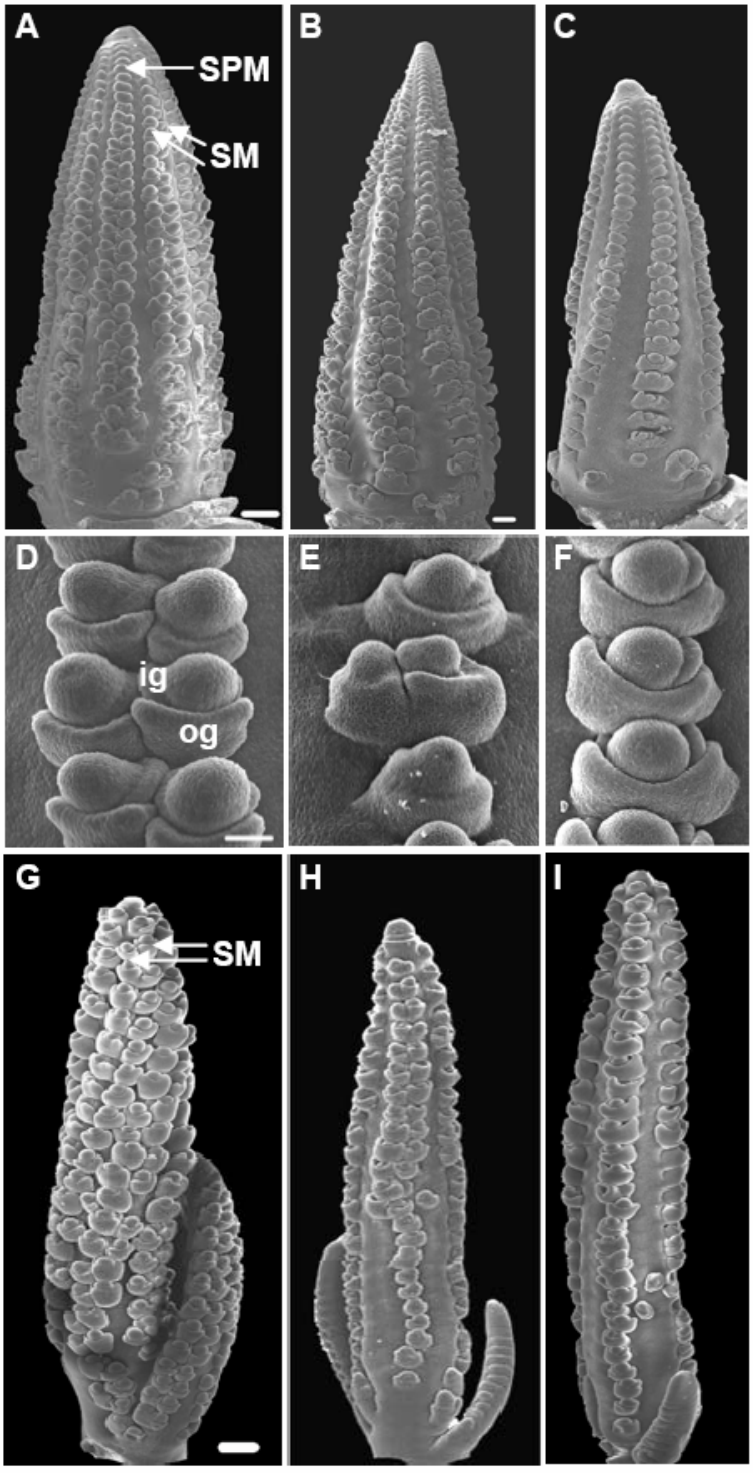

Figure 4.2 Scanning electron microscopy of *Sos1* inflorescences
(A-C) SEM of 8 week old ears. (A) Normal ear producing rows of SPM at the tip of the ear that transition to producing paired SM below the tip. (B) *Sos1/+* ear producing either single or paired SM. (C) *Sos1/Sos1* ear producing single SM. (D-F) Higher magnification of developing SM in the ear. (D) Normal ear with paired SM. The outer glume (og) and inner glume (ig) are the first organs to be produced by the SM. (E) *Sos1/+* ear producing either single or paired SM. (F) *Sos1/Sos1* ear with single SM. (G) Normal tassel producing paired SM. (H) *Sos1/+* tassel producing paired SM at the top and single SM at the base. (I) *Sos1/Sos1* tassel producing rows of single SM. Scale bar = 100 um in A-C and G-I and 50um in D-F.

Figure 4.3 Cross sections of *Sos1* ears stained with TBO

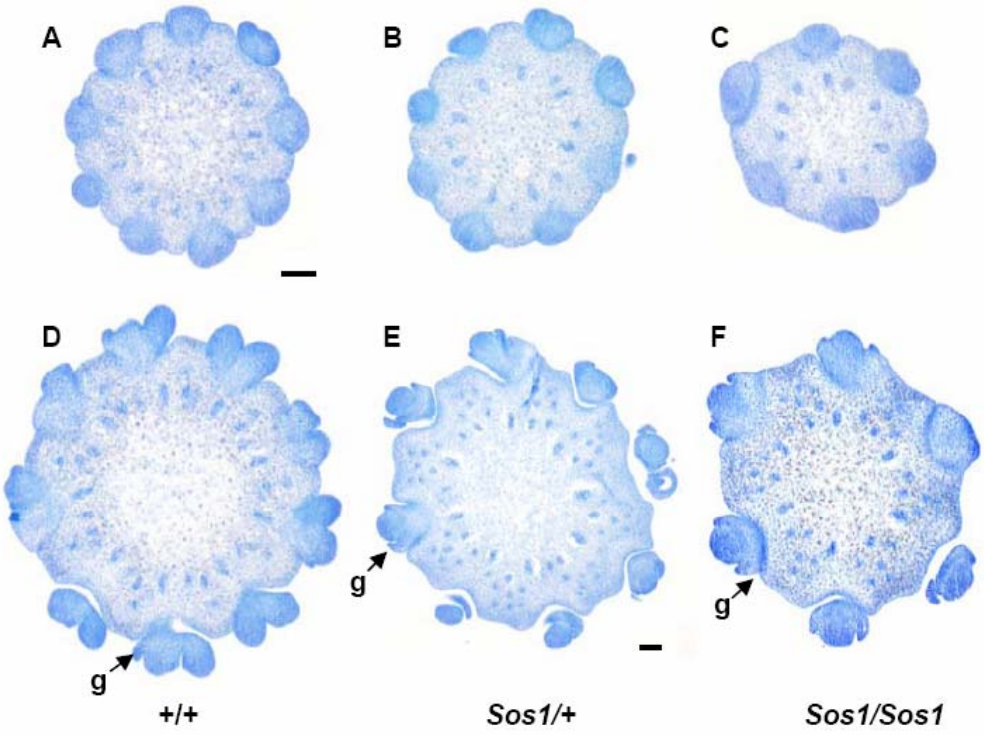

Figure 4.3 Cross sections of *Sos1* ears stained with TBO
(A-C) Cross sections of ears near the tip of the ear at the stage when SPM are being produced. (A) Normal ear showing nine SPM some of which are just beginning to form SM. (B) *Sos1/+* ear showing eight SPM. (C) *Sos1/Sos1* ears showing six SPM. (D-F) Cross sections later in development when normal ears have produced paired SMs. (D) Normal ear showing nine pairs of SMs. Note that the outer glume (g) is visible on some of the SMs. (E) *Sos1/+* ear in which two out of eight SPM are producing two SM. (F) *Sos1/Sos1* ear in which six single SMs are visible. All SM are producing glumes (g). Scale bar = 100 um.

Figure 4.4 Dosage analysis

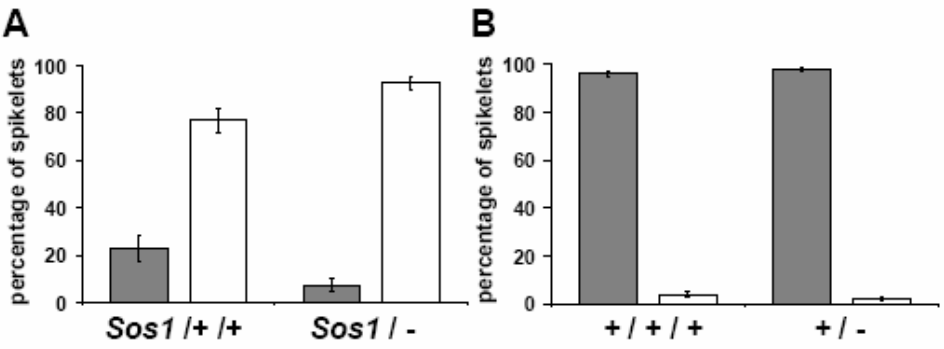

Figure 4.4 Dosage analysis
(A) The percentage of paired (grey bar) versus single (white) spikelets in *Sos1* plants containing two copies of wild type chromosome 4S (hyperploid) or missing the short arm of chromosome 4 (hypoploid). (B) The percentage of paired (grey) versus single (white) spikelets in normal plants containing three wild type copies of chromosome 4S (hyperploid) or one wildtype copy of chromosome 4S (hypoploid).

Figure 4.5 Genetic interaction of *Sos1* with *bif2* or *ba1*

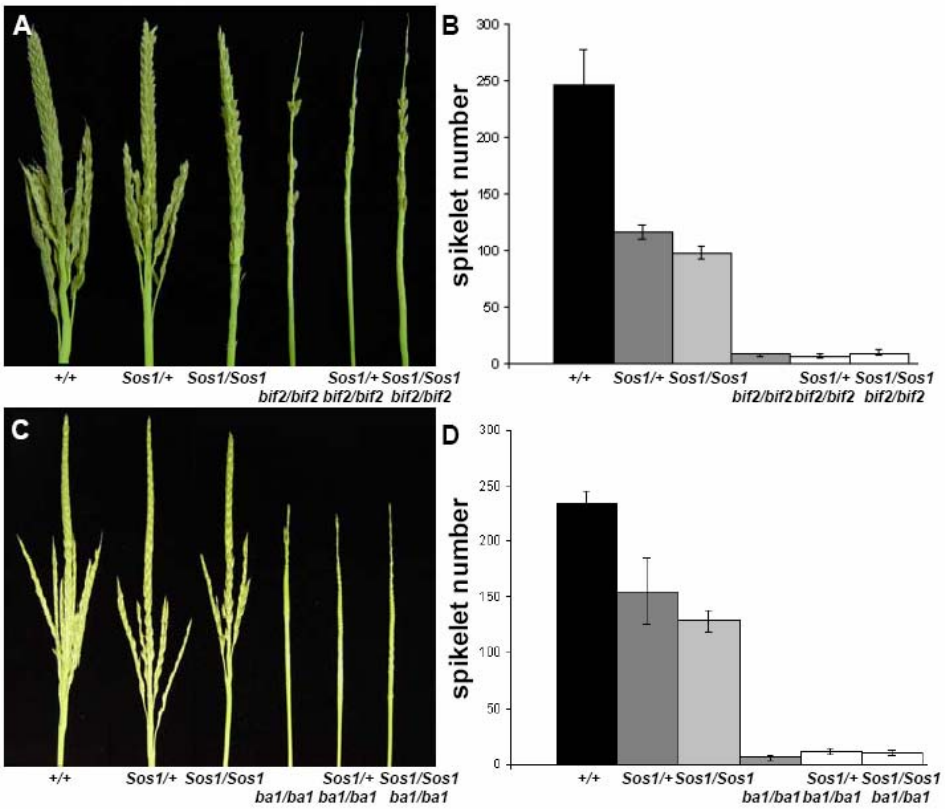

Figure 4.5 Genetic interaction of *Sos1* with *bif2* or *ba1*
(A) Photograph of the mature tassels of all genetic classes of an F2 family segregating for *Sos1* and *bif2*. (B) Quantification of spikelet number on the main spike of the tassel in *Sos1*; *bif2* double mutant family. (C) Photograph of the mature tassels of all genetic classes of an F2 family segregating for *Sos1* and *ba1*. (D) Quantification of spikelet number on the main spike of the tassel in *Sos1*; *ba1* double mutant family.

Figure 4.6 Genetic interaction between *Sos1* and *ra1*

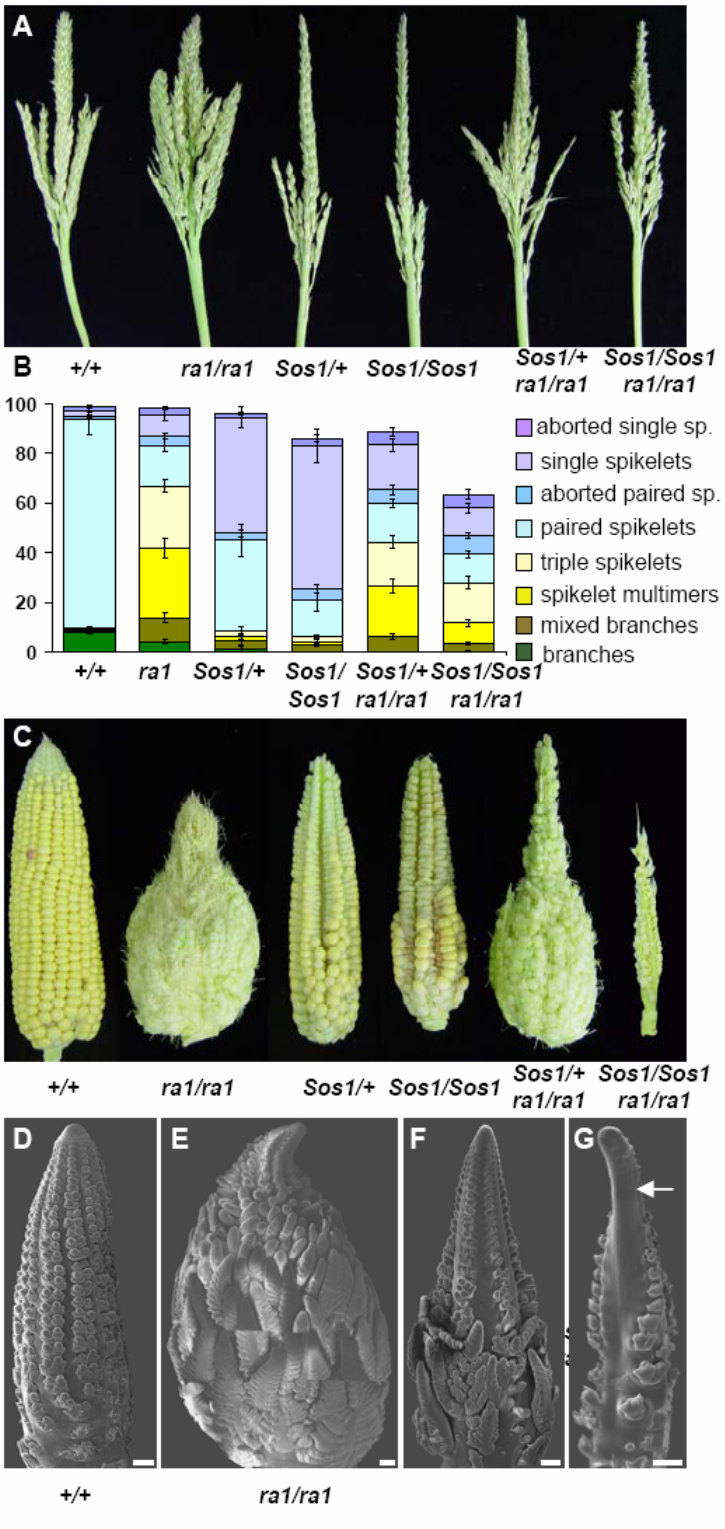

Figure 4.6 Genetic interaction between *Sos1* and *ra1*
(A) Photograph of the mature tassel of all genetic classes of an F2 family segregating for *Sos1* and *ra1*. (B) Classification of the number of different types of axillary structures produced by the tassel. (C) Photograph of mature ears of all genetic classes of an F2 family segregating for *Sos1* and *ra1*. (D-G) SEM of ear inflorescence. (D) Normal ear showing rows of paired SM. (E) *ra1* ear which is highly branched as all SPM are converted to branches. (F) *Sos1/+; ra1*/*ra1* ear in which SPM produce extra SM but not as many as *ra1*. (G) *Sos1/Sos1; ra1/ra1* ear in which SPM mainly produce single spikelets. One side of the tip is bare with no SPMs (arrow). Scale bar = 100 um.

Figure 4.7 Genetic interaction between *Sos1* and *ra2*

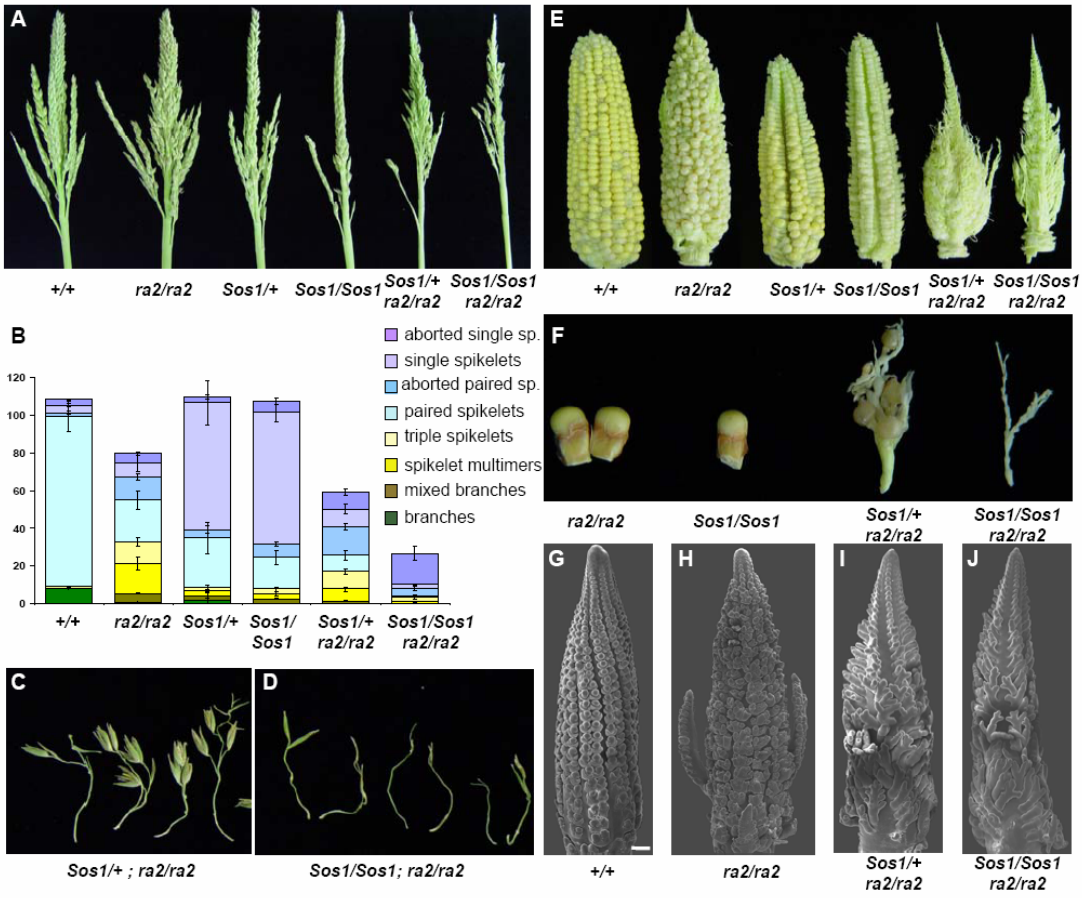

Figure 4.8 Expression of *ra1* and *ra2* in *Sos1* mutants and model for genetic interaction

(A, B) Real time RT-PCR experiments showing the relative expression level of *ra1* (A) and *ra2* (B) in *Sos/+* and *Sos/Sos1* mutants. (C) Model for the interaction between *Sos1* and *ra1*/*ra2*. *ra1* and *ra2* are both required to promote SPM determinacy. We propose that *Sos1* is a negative regulator of SPM determinacy. *ra2* acts upstream of *ra1* as well as having roles independent of *ra1*. As *Sos1*; *ra1* double mutants resemble *Sos1* single mutants, *sos1* is placed downstream of *ra1*. As *Sos1; ra2* double mutants have an enhanced phenotype similar to *ra1*; *ra2* double mutants, *sos1* is proposed to positively regulate *ra1*. The model is supported by the expression studies showing that *ra1* is reduced, and *ra2* is unchanged in *Sos1* mutants.

Figure 4.8 Expression of *ra1* and *ra2* in *Sos1* mutants and model for genetic interaction

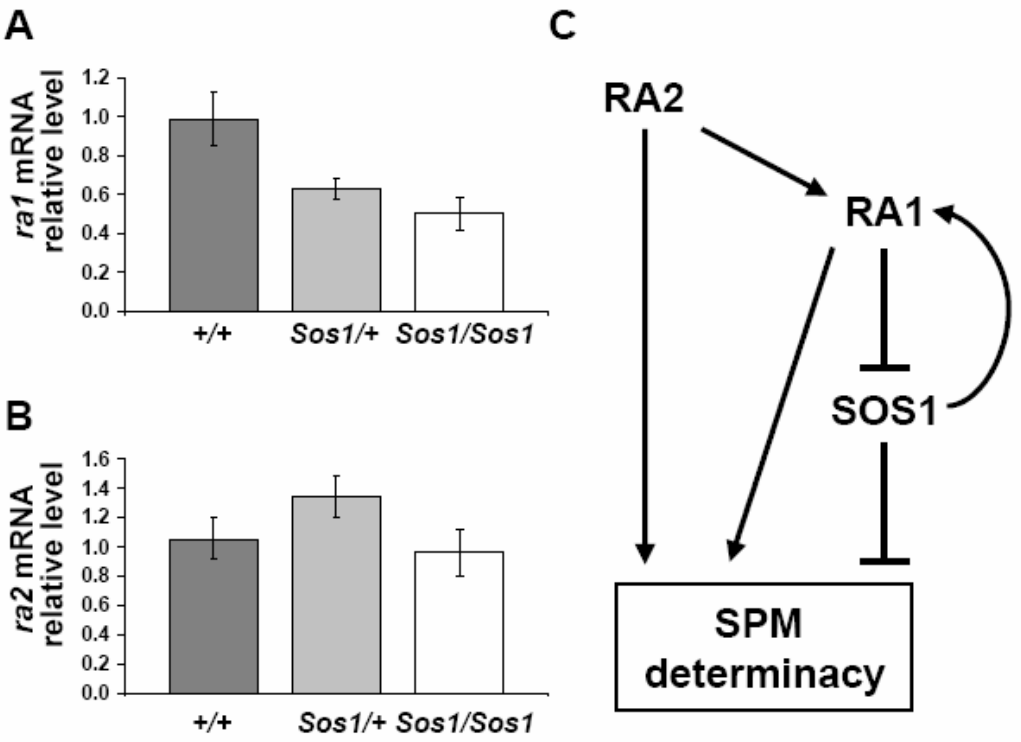

Figure 4.8 Expression of *ra1* and *ra2* in *Sos1* mutants and model for genetic interaction

(A, B) Real time RT-PCR experiments showing the relative expression level of *ra1* (A) and *ra2* (B) in *Sos/+* and *Sos/Sos1* mutants. (C) Model for the interaction between *Sos1* and *ra1*/*ra2*. *ra1* and *ra2* are both required to promote SPM determinacy. We propose that *Sos1* is a negative regulator of SPM determinacy. *ra2* acts upstream of *ra1* as well as having roles independent of *ra1*. As *Sos1*; *ra1* double mutants resemble *Sos1* single mutants, *sos1* is placed downstream of *ra1*. As *Sos1; ra2* double mutants have an enhanced phenotype similar to *ra1*; *ra2* double mutants, *sos1* is proposed to positively regulate *ra1*. The model is supported by the expression studies showing that *ra1* is reduced, and *ra2* is unchanged in *Sos1* mutants.

Table 4.S1 Chi-square analysis of double mutants

Family A;B	Total plants	Normal O	Normal E	gene*a* O	gene*a* E	gene*b* O	gene*b* E	*a;b* O	*a;b* E	X^2 P value
Sos1;tb1[1]	40	4	2.5	28	22.5	2	7.5	6	7.5	>0.05
Sos1;bif2[2]	97	29	24.5	23	24.5	45	48.5	--	---	>0.5
Sos1;ba1[3]	58	9	10.875	33	32.625	16	14.5	--	---	>0.5
Sos1;ra1[4]	57	13	10.688	23	32.063	11	3.5625	10	10.688	<0.05
Sos1;ra2[5]	69	15	12.938	35	38.813	6	4.313	15	12.938	>0.5

[1]: in *Sos1;tb1* double mutants, the expected segregation ratio is Normal: *Sos1*: *tb1:Sos1;tb1* = 1:9:3:3
[2]: in *Sos1;bif2* double mutants, the expected segregation ratio is Normal: *Sos1*:*bif2* =3:9:4
[3]: in *Sos1;ba1* double mutants, the expected segregation ratio is Normal: *Sos1:ba1*=3:9:4
[4]: in *Sos1;ra1* double mutants, the expected segregation ratio is Normal: *Sos1*: *ra1:Sos1;ra1* = 1:9:3:3
[5]: in *Sos1;ra2* double mutants, the expected segregation ratio is Normal: *Sos1*: r*a2:Sos1;ra2* = 1:9:3:3

References

Avery, L., and Wasserman, S. (1992). Ordering gene function: the interpretation of epistasis in regulatory hierarchies. *Trends in Genetics* **8,** 312-316.

Barazesh, S., and McSteen, P. (2008). *barren inflorescence1* functions in organogenesis during vegetative and inflorescence development in maize. *Genetics* **179,** 389-401.

Bortiri, E., and Hake, S. (2007). Flowering and determinacy in maize. *Journal of Experimental Botany* **58,** 909-916.

Bortiri, E., Chuck, G., Vollbrecht, E., Rocheford, T., Martienssen, R., and Hake, S. (2006). *ramosa2* encodes a LATERAL ORGAN BOUNDARY domain protein that determines the fate of stem cells in branch meristems of maize. *Plant Cell* **18,** 574-585.

Chuck, G., Meeley, R.B., and Hake, S. (1998). The control of maize spikelet meristem fate by the *APETALA2*- like gene *indeterminate spikelet1*. *Genes & Development* **12,** 1145-1154.

Chuck, G., Muszynski, M., Kellogg, E., Hake, S., and Schmidt, R.J. (2002). The control of spikelet meristem identity by the *branched silkless1* gene in maize. *Science* **298,** 1238-1241.

Colombo, L., Marziani, G., Masiero, S., Wittich, P.E., Schmidt, R.J., Gorla, M.S., and Pe, M.E. (1998). *branched silkless* mediates the transition from spikelet to floral meristem during *Zea mays* ear development. *Plant Journal* **16,** 355-363.

Doebley, J., Stec, A., and Kent, B. (1995). *Suppressor of sessile spikelets1* (*Sos1*) - a dominant mutant affecting inflorescence development in maize. *American Journal of Botany* **82,** 571-577.

Doebley, J., Stec, A., and Hubbard, L. (1997). The evolution of apical dominance in maize. *Nature* **386,** 485-488.

Doust, A.N., and Kellogg, E.A. (2002). Inflorescence diversification in the panicoid "bristle grass" clade (Paniceae, Poaceae): evidence from molecular phylogenies and developmental morphology. *American Journal of Botany* **89,** 1203-1222.

G.P.W.G. (2001). Phylogeny and subfamilial classification of the grasses (*Poaceae*). *Annals of the Missouri Botanical Garden* **88,** 373-457.

Gallavotti, A., Zhao, Q., Kyozuka, J., Meeley, R.B., Ritter, M., Doebley, J.F., Pe, M.E., and Schmidt, R.J. (2004). The role of *barren stalk1* in the architecture of maize. *Nature* **432,** 630-635.

Gernart, W. (1912). A new subspecies of *Zea mays* L. American Naturalist **46,** 616-622.

Greene, B., and Hake, S. (1994). Use of segmental aneuploids for mutant analysis. In The Maize Handbook, M. Freeling and V. Walbot, eds (New York: Springer), pp. 270-273.

Irish, E.E. (1997). Class II *tassel seed* mutations provide evidence for multiple types of inflorescence meristems in maize (Poaceae). *American Journal of Botany* **84,** 1502-1515.

Irish, E.E. (1998). Grass spikelets: a thorny problem. Bioessays **20,** 789-793.

Kellogg, E.A. (2000). The grasses: A case study in macroevolution. *Annual Review of Ecology and Systematics* **31,** 217-238.

Kempton, J.H. (1923). Heritable characters of maize XIV - Branched ears. *Journal of Heredity* **14,** 243-252.

Kiesselbach, T.A. (1949). The structure and reproduction of corn. (Cold Spring Harbor, New York: Cold Spring Harbor Press).

McSteen, P. (2006). Branching out: The *ramosa* pathway and the evolution of grass inflorescence morphology. *Plant Cell* **18,** 518-522.

McSteen, P., and Hake, S. (2001). *barren inflorescence2* regulates axillary meristem development in the maize inflorescence. *Development* **128,** 2881-2891.

McSteen, P., Malcomber, S., Skirpan, A., Lunde, C., Wu, X., Kellogg, E., and Hake, S. (2007). *barren inflorescence2* encodes a co-ortholog of the *PINOID* serine/threonine kinase and is required for organogenesis during inflorescence and vegetative development in maize. *Plant Physiology* **144,** 1000-1011.

Mena, M., Ambrose, B.A., Meeley, R.B., Briggs, S.P., Yanofsky, M.F., and Schmidt, R.J. (1996). Diversification of C-Function Activity in Maize Flower Development. *Science* **274,** 1537-1540.

Muller, H.J. (1932). Further studies on the nature and causes of gene mutations. In Proceedings of the Sixth International Congress of Genetics, D.F. Jones and W.I. Menasha, eds (Brooklyn Botanical Gardens), pp. 213-255.

Nickerson, N.H., and Dale, E.E. (1955). Tassel modifications in *Zea mays*. *Annals of the Missouri Botanical Garden* **42,** 195-211.

Ritter, M.K., Padilla, C.M., and Schmidt, R.J. (2002). The maize mutant *barren stalk1* is defective in axillary meristem development. *American Journal of Botany* **89,** 203-210.

Sablowski, R. (2007). Flowering and determinacy in Arabidopsis. *Journal of Experimental Botany* **58,** 899-907.

Satoh-Nagasawa, N., Nagasawa, N., Malcomber, S., Sakai, H., and Jackson, D. (2006). A trehalose metabolic enzyme controls inflorescence architecture in maize. *Nature* **441,** 227-230.

Skirpan, A., Wu, X., and McSteen, P. (2008). Genetic and physical interaction suggest that *barren stalk1* is a direct target of *barren inflorescence2* in maize inflorescence development. *The Plant Journal* PMID 18466309

Smith, L.G., Greene, B., Veit, B., and Hake, S. (1992). A Dominant Mutation in the Maize Homeobox Gene, Knotted-1, Causes Its Ectopic Expression in Leaf-Cells with Altered Fates. *Development* **116,** 21-&.

Steeves, T., and Sussex, I. (1989). Patterns in plant development. (Cambridge, UK: Cambridge University Press).

Vollbrecht, E., Springer, P.S., Goh, L., Buckler IV, E.S., and Martienssen, R. (2005). Architecture of floral branch systems in maize and related grasses. *Nature* **436,** 1119-1126.

Wu, X., and McSteen, P. (2007). The role of auxin transport during inflorescence development in maize, *Zea mays* (Poaceae). *American Journal of Botany* **11,** 1745-1755.

CHAPTER FIVE
General Discussion

5.1. General Discussion of *bif2* and *ba1*

In chapter two, it was shown that polar auxin transport (PAT) is required for initiation of all axillary meristems in maize tassel development. In addition, RNA *in situ* hybridization analysis showed that *barren inflorescence2 (bif2)* is expressed upstream of PAT while *barren stalk1 (ba1)* is expressed downstream of PAT. In addition, genetic analysis of *bif2;ba1* double mutants shown in chapter three provided more support that *bif2* acts upstream of *ba1*. However, this is just the beginning to understand how the plant integrates auxin signaling with inflorescence development. There are still many questions remaining to be answered. These questions will be discussed one by one in each of the following paragraphs.

5.1.1 How Is *bif2* Regulated?

The first question is how is *bif2* regulated? RNA *in situ* hybridization analysis shows that *bif2* is expressed specifically in all axillary meristems including branch meristem (BM), spikelet pair meristem (SPM), spikelet meristem (SM) and floral meristem (FM) (McSteen et al., 2007). This indicates that *bif2* expression is regulated coordinately with its function in axillary meristem initiation. Therefore, understanding *bif2* regulation is critical to understand how *bif2* functions. To answer this question, at least two levels of regulation need to be tested: the transcription level and the protein level. At the transcription level, we could do promoter analysis of the *bif2* gene. As mentioned in chapter 3 discussion, there are auxin response elements (AuREs) in the promoter of *bif2*. It is necessary to test whether *bif2* expression is auxin induced or not. *BIF2::GUS* transgenic plants could be treated with auxin to test whether *bif2* is auxin induced in vivo. cDNA libraries made from both tassel and ear are available in our lab, therefore it would be possible to use the *bif2* promoter region to do yeast-one-hybrid to screen these libraries to find proteins which bind to the *bif2* promoter to either activate or suppress *bif2* transcription. This method will help to find genes upstream of *bif2*. Thus,

factors which specify *bif2* expression in the region where axillary meristems initiation would be found. Identifing these factors would fill the gap between *bif2* regulation and its function downstream.

On the other hand, there must be protein level modification and regulation of BIF2. In Arabidopsis, 3-Phophoinositide-Dependant Kinase (PDK1) has been shown to activate PINOID (PID), which is an ortholog of BIF2 (Zegzouti et al., 2006, McSteen et al., 2007). PDK1 binds to PID and promotes PID autophosporylation and transphosporylation efficiency in Arabidopsis protoplasts (Zegzouti et al., 2006). It is required to confirm whether maize *PDK1* has similar function as it in Arabidopsis to regulate *bif2*. PDK1 is also a membrane associated protein, this indicates that PDK1 may react to the early signals at the membrane to activate downstream responses including the *bif2* pathway. Auxin seems to be one of these signals. Are there other signals regulating PDK1 to regulate PID/BIF2? Are these signals some other hormones or light or even sugar? If signals other than auxin activate/suppress the PDK1 pathway to promote/suppress PID/BIF2 function downstream, this would help to identify cross talk between different signaling pathways. This would provide clues to understand how meristems coordinate environmental and hormonal cues to regulate axillary meristem initiation during inflorescence development.

In addition, another two calcium related proteins, which have been identified that physically interact with PID, are TOUCH3 (TCH3) and PID-BINDING PROTEIN1 (PBP1) (Benjamins et al., 2003). PID transphosporylation (Zegzouti et al., 2006) of Myelin Basic Protein (MBP) is suppressed by calcium but promoted by magnesium. How do these biochemical signals coordinate with PID/BIF2 in meristem initiation? In addition, the proton pump has been shown to be involved in controlling auxin flow (Li et al., 2005). Is calcium/magnesium flow in/out of the cell coordinated with proton pumps in regulating electron physiology changes across the cell membrane? How do these electron physiology changes integrate with *bif2* signal transduction to initiate axillary meristems? Protein interaction domain analysis and functional analysis of PID/BIF2 with these proteins would provide some clues to understand how plants combine both external and internal cell signals to specify meristem development. Thus, detailed protein

interaction and functional analysis of these known players and/or identification of more players upstream of PID/BIF2 are all very important to understand PID/BIF2 function.

Therefore, by the analysis of both the transcription and protein level, more information would be added into understanding the regulation of *bif2* such as how early environmental and hormonal cues are integrated into the signal transduction pathway, received by BIF2 and connected to the downstream responses in axillary meristem initiation. This would improve our understanding of the role of *bif2* in maize inflorescence development.

5.1.2 How Does Phosphorylation of PIN1 by PID/BIF2 Direct Polar Auxin Flow?

Although PIN1 is a direct phosphorylation target of PID, the process by which the phosporylation of PIN1 by PID regulates PAT is still not clear. We know that the apical localization of PIN1 in the cells of the inflorescence meristem is switched to basal in *pid* mutants (Friml et al., 2004). However, there are unknown factors to be identified to fill in the gap between PIN1 phosporylation and PIN1 polar localization. In maize, we assume that BIF2 may have similar function as PID in Arabidopsis to phosphorylate ZmPIN1. However, direct in vitro kinase assay of BIF2 on ZmPIN1 is still necessary to confirm this hypothesis. Otherwise, to test whether PID::BIF2 could rescue the *pid* phenotype in Arabidopsis is an alternative way to show that *bif2* has a similar function as *PID* in polar auxin transport regulation. This is important because BIF2::GFP is localized in the cell periphery as well as the nucleus, which is not reported in Arabidopsis. This indicates that *bif2* may have additional roles in maize.

Since *bif2* may have some additional regulatory pathways compared to *PID*, it is necessary to screen for other downstream targets of BIF2 and/or modifiers of ZmPIN1. Some maize specific factors would be found as the inflorescence development in maize is more complex than in Arabidopsis. Yeast two hybrid analysis could help to find direct PID/BIF2 targets. Moreover, transcriptome changes in *bif2* mutants compared with *pid* mutant microarray data could help to find these maize specific factors in the BIF2 regulatory network. Furthermore, genome wide proteomics analysis would help to identify some of these maize specific factors regulated by BIF2 at the protein level. Maize inflorescence development is a unique system: four types of axillary meristem

initiation and the larger size of meristem are advantages for protein level analysis. Thus, adding more players to the *bif2* regulatory network and exploring their relationship with *bif2* in axillary meristem initiation would provide a clearer picture of how *bif2* functions in maize inflorescence development.

5.1.3 What Are the Downstream Gene Responses to PAT?

The third question we could ask is what are the down stream gene responses after PAT? In my work, I found that *ba1* is one of the downstream genes of PAT. However, we need to prove first that the absence of *ba1* expression in the NPA treated meristem is due to PAT rather than the absence of meristem initiation. This question could be answered by testing whether *ba1* is an auxin induced gene. There is an AuRE in the *ba1* promoter. We could test if BA1::GFP signal is auxin induced in transgenic maize plant. Furthermore, since PAT is required for axillary meristem initiation, auxin induced transcriptome analysis during maize inflorescence development would also provide some information to fill the gap between PAT and PAT responses in axillary meristem initiation.

5.1.4 How is *ba1* Regulated?

Since *ba1* plays an important role in axillary meristem initiation in maize inflorescence development, understanding *ba1* regulation is also very important. RNA *in situ* hybridization analysis shows that *ba1* expression is detected in all axillary meristems where they are initiated but in a smaller adaxial region compared with the *bif2* expression pattern (Gallavotti et al., 2004; McSteen et al., 2007). Real time RT-PCR analysis also shows that *ba1* expression is down regulated in *bif2* mutants. Since *bif2* is a kinase, its effects on *ba1* expression may not be direct. PAT effects on *ba1* expression may not be direct, either. Therefore, what is the direct activator of *ba1*? The transcription activator could be found by screening a maize library by yeast-one-hybrid analysis. However, as BA1 has been shown to be a direct target of BIF2, what is the function of phosphorylation of BA1? *ba1* is a transcription factor, phosphorylation would stimulate BA1 transcription ability such as DNA binding ability or transcription efficiency. To address these questions, we need to search for direct targets of *ba1*. First, we need to do

transcriptome analysis in *ba1* mutants. Then, we could use Systematic Evolution of Ligands by EXponential enrichment (SELEX) method to screen for the *ba1* binding cis-element. Finally, we can screen the cis-element in the promoter region of genes whose expression pattern is changed in the microarray. Those genes will be good candidates for targets of *ba1*. A gel-shift analysis to test direct *ba1* binding ability of these candidate genes will provide evidence for which one is the direct target of *ba1*. It is possible that ba1 is self activated, although this need to be tested to be sure. Once the direct target of *ba1* is defined, we can test whether phosphorylation of BA1 by BIF2 would improve BA1 binding ability to its target. If BA1 binding ability is not changed by phosphorylation, we would test whether BIF2 phosphorylation effect is on the transcription efficiency of BA1.

Interestingly, BA1 activates its own transcription in yeast (Andrea Skirpan personal observation, data not shown). If BA1 is self activated, why does BIF2 still phosphorylate and activate it? One possibility is that BA1 phosphorylation increase its binding efficiency. However,it could be also explained as *ba1* functions are so important in maize inflorescence development that many factors are involved in regulating it including itself. The function of *ba1* in axillary meristem initiation is a balance by all its regulators. Decrease or increase of either of the regulators would cause this balance to be broken. Thus, axillary meristem initiation is affected as the phenotype shows. Therefore, we need to search for the BA1 transcription/interaction complex. Yeast two hybrid analysis could be used to screen for proteins that bind BA1 which may provide clues to the BA1 transcription complex and/or interaction complex. To find more factors involved in regulation or interaction of BA1, more clues would be provided to understand the role of *ba1* in coordinating auxin signals to developmental changes in maize inflorescence development.

5.1.5 How is BIF2 and BA1 Function Inactivated?

Finally, the question of interest to ask is how BIF2 and BA1 functions are deactivated. It has been shown that PP2A dephosporylates PIN and hence antagonizes PID (Michniewicz et al., 2007). Therefore, this provides some clues on deactivation of BIF2 function. This is important since a complete signaling transduction pathway should

include both on and off mechanisms for subtle regulation. Is BA1 dephosporylated by PP2A also? How does BIF2 kinase activity shut down? To address these questions, we need to do detailed protein domain and protein structure analysis to locate the regulatory sites on these proteins. In addition, genetic modifier screening such as identifying suppressors or enhancers of *bif2* and *ba1* would provide clues to these questions, also.

5.2 General Discussion of *Sos1*

In chapter 4, we first described the genetic interaction between *Sos1* and the *ramosa* pathway in spikelet pair meristem determinacy. To further understand *Sos1* function and its interaction with *ra1* and *ra2* proteins, cloning of this gene is essential. To identify and prove the cloning of *Sos1*, there are mainly two steps. First, we need to generate more markers to narrow down the region and find the candidate genes. Furthermore, we can use the available resources such as comparison with the sorghum genome and the rice genome database to search for candidate genes in the region. In addition, we can collaborate with Erik Vollbrecht's lab to use their *ra1* microarray data to help us narrow down the candidate gene. Second, we need to generate more mutant alleles of *Sos1* so we can prove we have cloned the gene. We need to generate a mutant population by EMS mutagenesis of the wild type pollen and use the mutated pollen to cross to *Sos1* plants to generate the F1 population. Then, we will screen for severe *Sos1* mutants phenotype among the population. The newly mutated allele of *Sos1* will segregate in the F2 generation. Thus, we can use the mutant allele to further prove we have cloned the right gene.

Transcription factors often have both a protein-DNA binding domain and a protein-protein interaction domain. Dominant negative mutations in transcription factors cause one of these two functional domains to be affected leaving the remaining functional domain unaffected (Veitia, 2007). Thus, the mutated protein either still can bind the promoter region of the target gene but fail to transcribe it or it can still dimerize with another protein but fail to bind DNA. *Sos1* is a dominant negative mutation, which means that the protein is still made but part of its normal function has been changed in the mutants. I speculate that *Sos1* encodes a transcription factor. Since it shows such a tight interaction with *ra1*, it is possible it would be another zinc finger protein which can form

a heterodimer with *ra1*. It could possibly be another LOB domain transcription factor similar to *ra2* which regulates *ra1*. If *sos1* encodes a transcription factor as I expect, it is possible that SOS1 loses its DNA binding ability. As a result, *ra1* expression is down regulated in the *Sos1* mutants. However, the protein-protein interaction domain of SOS1 may still functional. It may form a heterodimer with RA1 to promote RA1 functions which positively regulates spikelet pair meristem determinacy. On the other hand, SOS1 may form a homodimer with itself to block its own function to negatively regulate spikelet pair meristem determinacy. Therefore, the spikelet pair meristems are more determinate in *Sos1* mutants.

References

Benjamins, R., Ampudia, C.S., Hooykaas, P.J., and Offringa, R. (2003). PINOID-mediated signaling involves calcium-binding proteins. *Plant Physiol* **132,** 1623-1630.

Friml, J., Yang, X., Michniewicz, M., Weijers, D., Quint, A., Tietz, O., Benjamins, R., Ouwerkerk, P.B., Ljung, K., Sandberg, G., Hooykaas, P.J., Palme, K., and Offringa, R. (2004). A PINOID-dependent binary switch in apical-basal PIN polar targeting directs auxin efflux. *Science* **306,** 862-865.

Gallavotti, A., Zhao, Q., Kyozuka, J., Meeley, R.B., Ritter, M.K., Doebley, J.F., Pe, M.E., and Schmidt, R.J. (2004). The role of *barren stalk1* in the architecture of maize. *Nature* **432,** 630-635.

Li, J., Yang, H., Peer, W.A., Richter, G., Blakeslee, J., Bandyopadhyay, A., Titapiwantakun, B., Undurraga, S., Khodakovskaya, M., Richards, E.L., Krizek, B., Murphy, A.S., Gilroy, S., and Gaxiola, R. (2005). Arabidopsis H+-PPase AVP1 regulates auxin-mediated organ development. *Science* **310,** 121-125.

McSteen, P., Laudencia-Chingcuanco, D., and Colasanti, J. (2000). A floret by any other name: control of meristem identity in maize. *Trends Plant Sci* **5,** 61-66.

McSteen, P., Malcomber, S., Skirpan, A., Lunde, C., Wu, X., Kellogg, E., and Hake, S. (2007). *barren inflorescence2* Encodes a co-ortholog of the PINOID serine/threonine kinase and is required for organogenesis during inflorescence and vegetative development in maize. *Plant Physiol* **144,** 1000-1011.

Michniewicz, M., Zago, M.K., Abas, L., Weijers, D., Schweighofer, A., Meskiene, I., Heisler, M.G., Ohno, C., Zhang, J., Huang, F., Schwab, R., Weigel, D., Meyerowitz, E.M., Luschnig, C., Offringa, R., and Friml, J. (2007). Antagonistic regulation of PIN phosphorylation by PP2A and PINOID directs auxin flux. *Cell* **130,** 1044-1056.

Veitia, R.A. (2007). Exploring the molecular etiology of dominant-negative mutations. *Plant Cell* **19,** 3843-3851.

Zegzouti, H., Anthony, R.G., Jahchan, N., Bogre, L., and Christensen, S.K. (2006). Phosphorylation and activation of PINOID by the phospholipid signaling kinase 3-phosphoinositide-dependent protein kinase 1 (PDK1) in Arabidopsis. *Proc Natl Acad Sci U S A* **103,** 6404-6409.

APPENDIX A

Cloning of *Suppressor of sessile spikelet1 (Sos1)*

A.1 Abstract

Efforts to understand the function of *Sos1* in inflorescence development are just beginning. Cloning of the *sos1* gene is the next necessary step. A map-based chromosome walking strategy is being used to clone the *sos1* gene. *Sos1* in the B73 background was crossed into the Mo17 inbred background, and then backcrossed to Mo17 to generate the mapping population. This population was then screened for recombinants with Simple Sequence Repeats (SSRs) markers. The closest marker found so far on either side of the *Sos1* locus is IDP2484 (3.02cM) and pumc1757 (2.83cM). More markers are needed to further narrow down the region.

Once the sequence information of the *sos1* region is known, other *Sos1* mutant alleles will be needed to prove that the correct gene has been cloned. Several *Sos1* like mutants have been isolated. Unfortunately, the F2 allelism analysis of these genes with *Sos1* shows that none of these mutants are allelic to *Sos1*. Therefore, more mutant alleles will need to be generated by EMS.

A.2 Map Based Cloning of *Sos1*

Sos1 was first identified as a spontaneous mutation by Hepperly in 1949 (Hepperly, 1949). It has been mapped to the short arm of chromosome 4 (Doebley et al., 1995) and shown by segregation ratio that *Sos1* is a semi-dominant mutant. The *Sos1* mutant allele has been crossed to several different inbred lines to find good molecular markers to map the *Sos1* locus.

Four *Sos1* like mutants have been identified. They are *Sos1-ref* (spontaneous mutation), *Sos-tls, Sos-up* and *Sos-mum1* (isolated from a transposon tagging experiment). *Sos1-ref* is the original mutant identified by Hepperly. Among the four alleles, only *Sos-mum1* is transposon tagged, therefore, it would be easier to clone *Sos-mum1* than *Sos1-ref*. We tested if *Sos-mum1* was allelic to *Sos1-ref*. The strategy was to cross *Sos1-ref/+* with *Sos-mum1/+* and plant all F1 seeds to self all *Sos1* phenotype plants. If these two alleles

are allelic to each other, we would expect that none of the F2 plants would segregate wildtype plants. However, if they are not allelic to each other, we should observe that 1/16 of the F2 plants would segregate wildtype plants. In addition, not all of our self crossed F1 plants contain both *Sos-mum1* and *Sos1-ref* mutant copies. As a result, some of the self crossed F2 family should segregate 1/4 wildtype plants. Thus, if these two alleles were not allelic to each other, we should observe a variation of wildtype segregation of 1/16 or 1/4 among the families in the F2. We scored 11 families and observed the wildtype versus *Sos1* phenotype segregation ratio to be 9/33, 12/44, 12/49, 6/39, 1/13, 2/19, 8/43, 14/49, 17/48, 14/46 and 13/47. This data showed that wildtype segregation was either 1/16 or 1/4. Therefore, *Sos1-ref* is not allelic to *Sos-mum1*. F2 allelism testing between either *Sos-tls, Sos-up* with *Sos1-ref* has also shown that they are not allelic (data not shown).

Since it is time consuming to clone *Sos1-ref* by chromosome walking and *Sos-mum1* shows a similar *Sos* phenotype, we decided to attempt to clone *Sos-mum1* first. Enzyme-digested genomic DNA of both *Sos-mum1* mutants and wildtype plants was screened with different *Mu* probes (*Mu1, 3, 4, 5, 6, 8* and *MuDR*) using Southern Blotting analysis. Unfortunately, none of these probes cosegregated with the *Sos-mum1* mutants phenotype. This means that we could not clone *Sos-mum1* by the transposon tagging strategy. Therefore, we proceeded with the map-based chromosome walking strategy using molecular markers to map *Sos1-ref*. We generated a mapping population with this allele in the B73 background crossed to the wild type Mo17 background.

Since *Sos1* has already been mapped to the short arm of chromosome 4, all of the SSR markers in the 4.02 bin were identified from the maize genome database (http://www.maizegdb.org/). A small population of 70 plants was screened first with these markers to determine which markers contained polymorphisms, and then the markers which showed polymorphisms in our mapping population were used for further screening. A mapping population of 662 plants was planted and screened during the summer of 2006 in Rocksprings, PA. All of the screened recombinant DNA samples were recollected and rechecked. In addition, all of the identified recombinant plants were self crossed and the F1 seeds were replanted in 2007 to double check that they were true

recombinants. The markers and their genetic distance from the *Sos1* locus are shown in Figure 1.

By searching the maize genome database, the marker pumc1757 is located in contig156 and the marker pumc1294 is located in contig157 (http://www.maizesequence.org/Zea_mays/mapview?chr=4). The rice genome database was used to identify the synteny between the rice genome and the maize genome. However, the two closest markers were not found in the rice genome. Two other markers that were found in the rice genome were IDP483 and *inra2*. These two markers are located on rice chromosome 11 between 2201200 to 24698600. *inra2* is closer to the *Sos1* locus than pumc1294. The total genetic distance according to our mapping data is around 17cM. The sequence from this rice chromosome region was downloaded (http://www.tigr.org/tdb/e2k1/osa1/data_download.shtml) and the predicted genes in this region in rice totaled 352 genes. If the two closest markers can be located within this region, the estimate of the number of genes between the two closest markers is about 120 genes. Thus, more markers are clearly required to further narrow down this region before identifying the candidate genes. However, since *ra1* is absent in the rice genome but present in the sorghum genome (Vollbrecht et al., 2005), *Sos1* may also be present in sorghum but absent in rice. Therefore, when we further narrow down the cloning region, we could select our candidate gene by comparison between the rice genome and the sorghum genome. Furthermore, we could collaborate with Erik Vollbrecht's lab to use their *ra1* microarray data to help choose the candidate genes since we are expecting that *Sos1* expression would be increased in *ra1* mutants.

Once we define the *Sos1* gene, we could generate more *Sos1* alleles by EMS or by *Mutator* transponson tagging and use the sequence information to prove that mutations are present in the gene. Thus, we could draw the conclusion that we have cloned *Sos1* at that time.

Figure A.1 Iillustration of map based cloning of *Sos1*

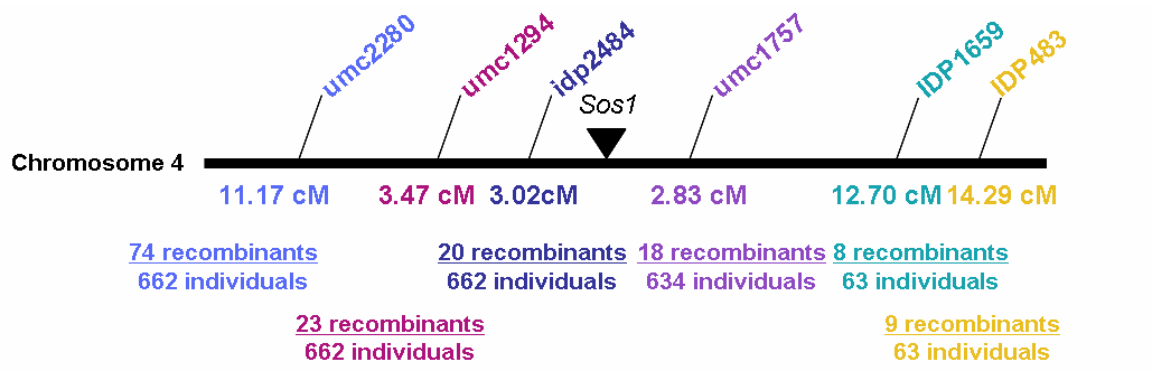

Figure A.1 Iillustration of map based cloning of *Sos1*

Markers and their distance from the *Sos1* locus are illustrated. The data for number of recombinants for each marker is listed below the marker with the same color.

References

Doebley, J., Adrian, S., and Kent, B. (1995). *Suppressor of Sessile spikelets 1 (Sos1)*: A Dominant Mutant Affecting Inflorescence Development in Maize. *American Journal of Botany* **82,** 571-577.

Hepperly, I.W. (1949). A corn with odd-rowed ears. *Journal of Heredity* **40,** 63-64.

Vollbrecht, E., Springer, P.S., Goh, L., Buckler, E.S.t., and Martienssen, R. (2005). Architecture of floral branch systems in maize and related grasses. *Nature* **436,** 1119-1126.

VITA

Xianting Wu

Education

2002-present	Ph.D. student in Biology Department, the Pennsylvania State University, final GAP is 3.92/4.00
2002-2003	Ph.D. students in Plant Biology Department, Rutgers, the State University of New Jersey, final GPA is 3.70/4.00
1998-2001	M.S. in Genetics, Capital Normal Univeristy, Beijing, China
1994-1998	B.S. in Biology, Capital Normal University, Beijing, China

Awards

09/2007	Award by the Biology Department, the Braddock Award for spring 2008
05/2007	Award by the Biology Department, the Henry W. Popp Fellowship for the 2007/2008 academic year
06/2004	Award by the Biology Department, J. Ben and Helen D. Hill Memorial Fund

Publications

Xianting Wu and Paula McSteen. *Suppressor of sessile spikelets1(Sos1)* functions in the *ramosa* pathway controlling meristem determinacy in maize. To submit to *PlantPhysiology* in May 2008

Andrea Skirpan, **Xianting Wu** and Paula McSteen.(2008) Genetic and physical interaction of *barren inflorescence2* and *barren stalk1* in maize inflorescence development. *Plant Journal* accepted Feb-19-2008, Manuscript No. TPJ-01099-2007

Xianting Wu and Paula McSteen. The role of auxin transport during inflorescence development in Maize (*Zea mays*, Poaceae). *American Journal of Botany* (2007),94(11): 1745-1755

Paula McSteen, Simon Malcomber , Andrea Skirpan , China Lunde , **Xianting Wu**,Elizabeth Kellogg, and Sarah Hake. *Barren inflorescence2* encodes a co-ortholog of the *PINOID* serine/threonine kinase and is required for organogenesis duringinflorescence and vegetative development in maize. *Plant Physiology* (2007),144(2):1000-11

Xianting Wu, Yuying Luo (2000) Application of Diphtheria Toxin and TOX gene in molecular biology in *Arabidopsis* and *Nicotiana tabacum.* *CNU Journal* 56:35-41